UNIVERSITY OF OKLAHOMA

GRADUATE COLLEGE

RESPONSES OF TERRESTRIAL BIOGEOCHEMICAL CYCLES TO GLOBAL CHANGE – SYNTHESES AND DATA-MODEL INTEGRATION

A DISSERTATION

SUBMITTED TO THE GRADUATE FACULTY

in partial fulfillment of the requirements for the

Degree of

DOCTOR OF PHILOSOPHY

By

JUNYI LIANG
Norman, Oklahoma
2016

RESPONSES OF TERRESTRIAL BIOGEOCHEMICAL CYCLES TO GLOBAL CHANGE – SYNTHESES AND DATA-MODEL INTEGRATION

A DISSERTATION APPROVED FOR THE
DEPARTMENT OF MICROBIOLOGY AND PLANT BIOLOGY

BY

_____
Dr. Yiqi Luo, Chair

_____
Dr. Ying Wang

_____
Dr. Heather McCarthy

_____
Dr. Lara Souza

_____
Dr. Xiangming Xiao

To my family who support me always

Acknowledgements

I am very grateful to my major professor, Dr. Yiqi Luo, whose guidance and support made it possible for me to finish my PhD program. Throughout my PhD study, he has been very encouraging, and helped me to be my best. This dissertation would not have been possible without his help. I would also like to thank my committee members, Drs. Lara Souza, Heather McCarthy, Xiangming Xiao, and Ying Wang, for their help and service over the last four years.

I wish to acknowledge colleagues and friends in Luo Ecolab, Drs. Lifen Jiang, Jianyang Xia, Zheng Shi, Dejun Li, Jianwei Li, Wenting Feng, Xinjie Lu, Jiang Jiang, Kevin Wilcox, and other lab members. I would also like to thank collaborators, Drs. Edward Schuur and Jizhong Zhou for their generous help.

Finally, thanks to my family. To my parents, who are always there for me. To my wife, Xiaoming, for all her understanding, support, and encouragement. To Ethan, who brightens up my life.

Table of Contents

List of Tables

List of Figures

Abstract

Global observations and model simulations show that atmospheric carbon dioxide (CO_2) concentrations and surface temperatures have been and will keep increasing. These environmental changes have significant influences on terrestrial biogeochemical cycles. On the other way, how changes in terrestrial biogeochemistry in response to the environmental changes can either amplify or alleviate climate change. Soils, the primary research subject of this dissertation, store more than twice as much carbon (C) as the atmosphere. As such, small changes in soil C may have large impacts on the magnitude of atmospheric CO_2 concentrations and therefore climate change. However, due to the huge storage and relatively long residence time, how soil C responds to increasing atmospheric CO_2 concentrations and surface temperatures is still unclear. The unclear response of soil C is one of the most important reasons for the uncertainties of the magnitude of global change in this century. In this dissertation, I attempted to study the responses of soil C and related biogeochemical processes to increased temperature and CO_2 concentrations, through syntheses and data-model integration.

In the first study, I estimated the responses of two critical soil C dynamic processes, replenishment and priming effect, to increased C input. With the responses of the two processes, I estimated the net change of soil organic C by increased C input. Results show that approximately 58% of newly added C is transferred into soil organic C (SOC) via replenishment, whereas the additional loss of old SOC due to priming effect only accounts for 8.4% of the added new C in the first year after a one-time new C input. As a result, the new C input leads to a net increase in SOC, ranging from 40% to 49% of

the added new C. The magnitude of the net increase in SOC is positively correlated with the nitrogen-to-C ratio of the added substrates. Furthermore, a 100-year modeling experiment confirms that an increase in new C input leads to significant SOC accumulation over time. The findings suggest that increasing plant productivity and the consequent increase in C input to soils likely promote SOC storage despite the enhanced decomposition of old C, potentially mitigating further climate change.

The first study evaluated impacts of C input on soil C dynamics. My second study evaluated how nitrogen (N) regulates C input under elevated CO_2. A popular hypothesis of the N constraint to the CO_2 fertilization effect is progressive N limitation (PNL), which postulates that the stimulation of plant growth by CO_2 enrichment results in more N sequestered in plant, litter and soil organic matter (SOM) so that, the N availability for plant growth progressively declines in soils over time. The reduced N availability then in turn constrains the further CO_2 fertilization effect on plant growth over longer time scales. Although extensive research has explored whether or not PNL occurs under CO_2 enrichment, a comprehensive assessment of the N processes that regulate PNL is still lacking. In the second study, I quantitatively synthesized the responses of all major processes and pools in the terrestrial N cycle with meta-analysis of CO_2 experimental data available in the literature. The results showed that CO_2 enrichment significantly increased N sequestration in the plant and litter pools but not in the soil pool, partially supporting one of the basic assumptions in the PNL hypothesis that elevated CO_2 results in more N sequestered in organic pools. However, CO_2 enrichment significantly increased the N influx via biological N fixation and the loss via nitrous oxide (N_2O) emission, but decreased the N efflux via leaching. In addition, no general diminution

was observed in effects of CO_2 fertilization on plant growth. Overall, the analyses suggest that the extra N supply by the increased biological N fixation and decreased leaching may potentially alleviate PNL under elevated CO_2 conditions in spite of the increases in plant N sequestration and N_2O emission. Moreover, the syntheses indicate that CO_2 enrichment increases soil ammonium (NH_4^+) to nitrate (NO_3^-) ratio. The changed NH_4^+/NO_3^- ratio and subsequent biological processes may result in changes in soil microenvironments, above-belowground community structures and associated interactions, which could potentially affect the terrestrial biogeochemical cycles. In addition, the data synthesis suggests that more long-term studies, especially in regions other than temperate ones, are needed for comprehensive assessments of the PNL hypothesis.

In the third study, I evaluated methods for estimating the temperature sensitivity (Q_{10}) of SOC decomposition since the Q_{10} estimate substantially depends on their specific assumptions. I compared several commonly used methods (i.e., one-pool (1P) model, two-discrete-pool (2P) model, three-discrete-pool (3P) model, and time-for-substrate (T4S) Q_{10} method) plus a new and more process-oriented approach for estimating Q_{10} of SOC decomposition from laboratory incubation data. The process-oriented approach is a three-transfer-pool (3PX) model that resembles the decomposition sub-model commonly used in Earth system models. The estimated Q_{10}s generally increased with the soil recalcitrance, but decreased with the incubation temperature increase. The results indicated that the 1P model did not adequately simulate the dynamics of SOC decomposition and thus was not adequate for the Q_{10} estimation. All the multi-pool models fitted the soil incubation data well. The Akaike

information criterion (*AIC*) analysis suggested that the 2P model is the most parsimonious. As the incubation progressed, Q_{10} estimated by the 3PX model was smaller than those by the 2P and 3P models because the continuous C transfers from the slow and passive pools to the active pool were included in the 3PX model. Although the T4S method could estimate the Q_{10} of labile carbon appropriately, the analyses showed that it overestimated that of recalcitrant SOM. The similar structure of 3PX model with the decomposition sub-model of Earth system models provides a possible approach, via the data assimilation techniques, to incorporate results from numerous incubation experiments into Earth system models.

In the fourth study, I studied how warming affect SOC storage in Alaskan tundra. By combining a process-based model and a unique field experiment, this study shows that warming reduced the base turnover rate of SOC, which is the representation of unresolved microbial community and activity on the resolved scale. The reduced base turnover rate of SOC suggests that microbial decomposers acclimate to warming in Alaskan tundra. Although warming still accelerates SOC loss, the acclimation counterbalances the SOC loss acceleration by 62%. Our study suggests that it is critical to incorporate changes in biological properties (as parameters) to improve the model performance in predicting C dynamics and its feedback to climate change.

This dissertation demonstrates that integrating data and model can advance our understanding of biogeochemical cycles in the context of global change. Future research is needed to study the integrated effect of global change factors on the responses and feedbacks of biogeochemical cycles to global change.

Keywords: acclimation, carbon cycling, carbon dioxide, climate change, data assimilation, meta-analysis, modeling, nitrogen fixation, permafrost, priming effect, progressive nitrogen limitation, replenishment, soil carbon storage, temperature sensitivity, warming

Chapter 1: Introduction

1.1 Introduction: Global change and terrestrial biogeochemical cycles

Human activities, such as fossil-fuel burning and deforestation, have led to substantial increase in atmospheric carbon dioxide (CO_2) concentrations and the Earth surface temperature (IPCC, 2013). How to control the climate change in a reasonable magnitude is one of the most critical issues for humans in the 21st century (IPCC, 2013). Terrestrial ecosystems contain around 5 times carbon (C) as the atmosphere does (Chapin III *et al.*, 2011). In addition, the two largest C fluxes, photosynthetic uptake of CO_2 and ecosystem CO_2 release via respiration, are sensitive to atmospheric CO_2 enrichment and climate warming (Rustad, 2006, Schwalm *et al.*, 2010). Therefore, terrestrial C and related biogeochemical cycles play critical roles in regulating climate change. However, there still huge uncertainties exist in simulating and predicting terrestrial C cycle under global change (IPCC, 2013, Jones *et al.*, 2013).

One of the most important uncertainties is how soil organic C (SOC) will change under increased new C input. Priming effect, which promotes microbial growth and liberates C from mineral associations, has been identified as a major mechanism that stimulates decomposition of old soil organic C (SOC) by the addition of new C to soils (Kuzyakov *et al.*, 2000, Fontaine *et al.*, 2004a, Dijkstra & Cheng, 2007, Heimann & Reichstein, 2008, Kuzyakov, 2010, Sayer *et al.*, 2011, Schmidt *et al.*, 2011, van Groenigen *et al.*, 2014, Keiluweit *et al.*, 2015). In the context of climate change, a major concern is that if priming effect is substantial and pervasive across ecosystems, enhanced plant production due to elevated CO_2 and thus increased C input to soils may limit or reduce SOC storage, leading to a positive feedback to climate change (Heimann & Reichstein, 2008, Sayer *et al.*, 2011, van Groenigen *et al.*, 2014). However, enhanced

SOC decomposition due to priming effect may be counter-balanced by replenishment of SOC due to increased C input through various mechanisms (Rubino *et al.*, 2010, Cotrufo *et al.*, 2013, Cotrufo *et al.*, 2015, Soong & Cotrufo, 2015). As a result, the direction and magnitude of SOC change in response to increased C input is determined by the net effect of priming and replenishment. Therefore, it is critical to quantify both priming effect and replenishment and thus the net SOC change caused by increasing C input.

The researches on the priming effect and replenishment are based on an important assumption that atmospheric CO_2 enrichment stimulate plant growth and the consequent C input to soil. Thus, a third important uncertainty is that whether the stimulated plant growth and the increased C input to soils by CO_2 fertilization sustains on longer temporal scales. An important reason is that the stimulated plant growth requires additional nitrogen (N), an essential element for molecular compounds of amino acids, proteins, ribonucleic acids (RNAs) and deoxyribonucleic acids (DNAs) in organisms (Oren *et al.*, 2001, Hungate *et al.*, 2003, Luo *et al.*, 2004, Thornton *et al.*, 2009, Norby *et al.*, 2010). Therefore, N limitation has the potential to constrain the CO_2 fertilization effect on terrestrial C sequestration (Rastetter *et al.*, 1997, Oren *et al.*, 2001, Luo *et al.*, 2004, Reich *et al.*, 2006, Norby *et al.*, 2010, Reich & Hobbie, 2013). The N limitation potential is dependent on the balance of N demand and supply (Luo *et al.*, 2004, Finzi *et al.*, 2006, Walker *et al.*, 2015). To date, no general pattern of N limitation under enriched CO_2 across ecosystems has yet been revealed. To reveal the general pattern, it is necessary to synthesize the response of multiple N cycling processes to CO_2 enrichment.

Another important uncertainty is the response of soil organic matter (SOM) decomposition to warming. SOM is the largest C pool in terrestrial ecosystems (Schlesinger, 1995). As a biochemical process, the decomposition of SOM is sensitive to increased temperature (Luo *et al.*, 2001, Fang *et al.*, 2005, Davidson & Janssens, 2006). Thus, it is important to accurately estimate the temperature sensitivity (expressed as Q_{10}, which measures the change in decay rates for a 10 K warming) of SOM decomposition. However, the Q_{10} estimation substantially relies on the methods used, which usually have their respective assumptions, leading to contradictory conclusions (Liski *et al.*, 1999, Fang *et al.*, 2005, Rey & Jarvis, 2006, Conant *et al.*, 2008). To better understand the warming impacts on SOM decomposition, it is important to evaluate these methods and the underlying assumptions.

In addition, one more question is whether the increased Earth surface temperature alters soil microbial community which may reduce (i.e., acclimation) or enhance the C release from terrestrial soils (Luo *et al.*, 2001, Bradford *et al.*, 2008, Hartley *et al.*, 2008, Karhu *et al.*, 2014). Although many warming studies in both fields and laboratories have been conducted, the microbial response to warming and the consequent effects on C cycle are still lacking in the permafrost soils, which store around twice as much C as the atmosphere does (Zimov *et al.*, 2006, Schuur *et al.*, 2008, Schuur *et al.*, 2009, Chapin III *et al.*, 2011, IPCC, 2013). In addition, in the permafrost regions, the SOM is relatively easy to be decomposed as long as temperature gets warmer (Schuur *et al.*, 2008, Schuur *et al.*, 2009). Therefore, the C dynamics in permafrost regions is potentially critical to climate change. Scientists are trying to incorporate the permafrost C dynamics into Earth system models (ESMs) (Koven *et al.*,

2011). However, lacking of accurate understanding of the possible nonlinear microbial responses to climate warming may lead to mislead the model prediction. Thus, a comprehensive study including both experimental evidence and model simulation is critically needed to understand the C dynamics in the permafrost regions and evaluate the current generation's ESMs.

1.2 Literature review

1.2.1 Effect of new C input on soil C storage.

The research on the effect of new C input on the dynamic of old SOM could be traced back to 1926 (Löhnis, 1926). Löhnis (1926) found that more nutrient released from old SOM after adding fresh detritus, which is called priming effect. The priming effect has attracted much attention again in the context of climate change because it may promote the decomposition of old SOM and consequently amplify climate change (Kuzyakov *et al.*, 2000, Fontaine *et al.*, 2004a, Dijkstra & Cheng, 2007, Kuzyakov, 2010, Cheng *et al.*, 2014, van Groenigen *et al.*, 2014). Recent researches have demonstrated that the priming effect includes both positive and negative (Kuzyakov *et al.*, 2000). When increased new C is added, microbial community would decompose more old SOM with positive priming effect, whereas it would decompose less old SOM with negative priming effect. The direction and magnitude of the priming effect could be affected by the amount of the new substrate added into the system, the chemical characters of added substrates and SOM (e.g, C/N ratio), and soil microbial community composition (Kuzyakov *et al.*, 2000, Guenet *et al.*, 2010a, Kuzyakov, 2010, Blagodatskaya *et al.*, 2011). Although the negative priming effect has been observed in

some studies (e.g., Guenet *et al.*, 2010a, Qiao *et al.*, 2014), new C addition usually leads to positive priming effect (Wu *et al.*, 1993, Kuzyakov *et al.*, 2000, Bell *et al.*, 2003, Perelo & Munch, 2005, Fontaine *et al.*, 2007, Kuzyakov, 2010, Guenet *et al.*, 2012, Qiao *et al.*, 2014, van Groenigen *et al.*, 2014). Because the SOM stores a huge amount of C, the priming effect may increase the CO_2 concentrations in the atmosphere, and consequently aggravate the positive feedback to climate change (Kuzyakov *et al.*, 2000, Fontaine *et al.*, 2004a, Dijkstra & Cheng, 2007, Fontaine *et al.*, 2007, Kuzyakov, 2010, van Groenigen *et al.*, 2014).

On the other hand, studies on soil aggregates and stabilization have suggested that labile C could be transferred to relatively resistant form to replenish SOC (Sollins *et al.*, 1996, Jastrow & Miller, 1997, Six *et al.*, 2002). The mechanisms for the replenishment include physical, chemical, and biochemical ones (Jastrow & Miller, 1997, Six *et al.*, 2002). In other words, not all the new C has been respired to CO_2 in the priming effect studies. Thus, to understand the SOC change by new C input, it is critical to quantify both the replenishment and priming effect, and consequently, the net effect.

1.2.2 Nitrogen limitation to plant growth under CO_2 enrichment.

Although the constraint of N to CO_2 fertilization effect has been studied widely, it is still controversial and no general pattern has been generated. Several proposed mechanisms on both negative and positive effects of CO_2 enrichment on the N availability for plant growth have been discussed during the past decades. On the one hand, progressive N limitation (PNL) hypothesis postulates that the stimulation of plant growth by CO_2 enrichment results in more N sequestered in plants, litter and soil

organic matter (SOM) so that, the N availability progressively declines in soils over time (Hungate *et al.*, 2003, Luo *et al.*, 2004). In addition, the growth dilution hypothesis posits that as the plants get larger under CO_2 enrichment, litter quality decreases due to lower tissue N concentration and greater C:N ratio (Justes *et al.*, 1994, Luo *et al.*, 2006). The low litter quality induced by the growth dilution could depress the litter mineralization and, in turn, the N release from litter to soil (Rastetter *et al.*, 1997). On the other hand, the stimulated fresh C input to soils by CO_2 enrichment has the potential to increase the N mineralization due to the enhanced microbial activities, as posited by the "priming effect" hypothesis (Löhnis, 1926, Kuzyakov *et al.*, 2000). In addition, the enhanced biological N fixation (Luscher *et al.*, 2000, Hoque *et al.*, 2001) and increased fine root production (Iversen, 2010, Iversen *et al.*, 2011) under CO_2 enrichment could partially alleviate the N limitation. Moreover, with the relatively constant resorption efficiency, the greater amount of N in plant tissues under enriched CO_2 could also provide more N for the next step's plant growth (Norby *et al.*, 2000, Norby *et al.*, 2001, Luo *et al.*, 2004). The diverse mechanisms of the CO_2 enrichment effects on available N in soils have constrained the accurate predictions of terrestrial C dynamics in Earth system models. Therefore, a synthesis of comprehensive data across ecosystems are needed to derive the general patterns of the N availability and plant growth in response to CO_2 enrichment.

1.2.3 Methods for estimating temperature sensitivity of SOM decomposition.

Temperature sensitivity of SOM decomposition has been estimated by using a variety of methods, such as seasonal soil respiration directly in field experiments (Luo

et al., 2001) and laboratory incubation (Fang *et al.*, 2005). Comparing to direct field measurements, laboratory incubation can better exclude influences of factors other than temperature on SOM decomposition. Thus, it has widely been used for estimating temperature sensitivity (i.e., Q_{10}). In the laboratory incubation experiments, direct calculation at specific incubation time has been used to estimate Q_{10} of SOM decomposition based on incubation data using the CO_2 emission rates at different incubation temperatures (Rey & Jarvis, 2006). The estimate is likely underestimates the temperature sensitivity because greater decomposition results in less substrate at high than low temperatures at the same point of incubation time. An improvement has been made recently by estimating the Q_{10} by comparing the times for respiring a given amount of C at different temperatures (Rey & Jarvis, 2006, Conant *et al.*, 2008). One important assumption of this method is that a given amount of respired CO_2 is from similar fractions of SOM when the substrates are at the same level at different temperatures (Conant *et al.*, 2008).

In addition to the direct calculations, C dynamic models have also been used to simulate laboratory incubation studies and estimate Q_{10} (Kätterer *et al.*, 1998, Rey & Jarvis, 2006). In these models, the soil is usually divided into discrete pools based on their turnover rates (Kätterer *et al.*, 1998, Rey & Jarvis, 2006). Through these models, the Q_{10} for each conceptual pool can be estimated (Rey & Jarvis, 2006). Generally, multi-pool models fit incubation data very well and are more popular for Q_{10} estimation (Kätterer *et al.*, 1998, Rey & Jarvis, 2006).

1.2.4 Effect of warming on soil C loss in permafrost regions.

Permafrost regions have experienced, and will likely experience faster climate warming than other regions (IPCC, 2013). SOC in the permafrost regions is huge in magnitude and has long been protected due to low temperatures. As climate gets warmer, SOC in these regions can become vulnerable to rising temperatures and could potentially lose a large amount of carbon (C) to the atmosphere, acting as an important C source (Schuur *et al.*, 2009, Koven *et al.*, 2011, MacDougall *et al.*, 2012, Schuur *et al.*, 2015, Hicks Pries *et al.*, 2016). However, it is still controversial that to what extent the C source will be.

Climate warming in the permafrost regions can lead to direct temperature rise and permafrost thaw. In addition, long-term warming may also affect soil microbial community composition, which may further change microbial activity, and consequently CO_2 emissions to the atmosphere (Manzoni *et al.*, 2012, Hultman *et al.*, 2015, Xue *et al.*, 2016). The changed microbial community and activity may lead to nonlinear response of soil C decomposition to warming (Luo *et al.*, 2001, Bradford *et al.*, 2008, Hartley *et al.*, 2008, Karhu *et al.*, 2014). One of the most common nonlinear responses is acclimation (Luo *et al.*, 2001; Bradford *et al.*, 2008). With acclimation, the accelerated SOC loss can be alleviated. Moreover, the altered microbial community and activity may also change C use efficiency (CUE) (Allison *et al.*, 2010, Li *et al.*, 2014). With higher CUE, microbes use more proportion of derived C to build up their body mass and community size, and consequently less proportion of C would be respired to the atmosphere via CO_2 emission, and vice versa (Luo *et al.*, 2001, Bradford *et al.*, 2008, Hartley *et al.*, 2008, Karhu *et al.*, 2014). Thus, how SOC change in the

permafrost regions is determined by all the magnitude of temperature rise, permafrost thaw, and possible changes in decomposers.

1.3 Studies conducted in the dissertation

Four studies were conducted in this dissertation to study the responses of soil carbon and related biogeochemical processes to increased temperature and carbon dioxide concentrations. In Chapter 2, I attempted to synthesize the effects of increasing carbon input on soil carbon replenishment and priming effect, and the consequent net soil organic carbon change. I first compiled 45 datasets from laboratory incubation experiments using isotope-labelled carbon to trace the origins of emitted carbon dioxide, which can provide information on carbon replenishment and priming effect. Second, against the collected dataset, I evaluated four soil dynamic models, including a conventional first-order kinetic model, an interactive model, a regular Michealis-Menten model, and reverse Michealis-Menten model. I selected the most parsimonious model (i.e., the interactive model). After that, using the interactive model, I synthesized short-term and long-term effects of increasing carbon input on soil carbon replenishment and priming effect, and the consequent net soil organic carbon change for the datasets spanning a diverse range of different soils and substrate quality.

In Chapter 3, I synthesized data published in the literature on the nitrogen limitation to plant growth under enriched carbon dioxide conditions. Two sets of data from the literature were collected. With the first dataset, I quantitatively examined the effects of carbon dioxide enrichment on all the major processes and pools in the nitrogen cycle using meta-analysis. These processes and pools included nitrogen sequestered in

organic components, biological nitrogen fixation, net mineralization, nitrification, denitrification, leaching, and total inorganic nitrogen, ammonium and nitrate contents in soils. The first dataset was also used to explore the responses of the nitrogen processes to short- vs. long-term carbon dioxide treatments. In addition, the responses of the nitrogen processes to carbon dioxide enrichment were compared between without and with nitrogen addition conditions. The second dataset was compiled for the plant growth in decadal free air carbon dioxide enrichment (FACE) experiments. With the dataset, I explored whether the carbon dioxide fertilization effect on plant growth diminishes or not over time.

In Chapter 4, I evaluated five methods for estimating the temperature sensitivity (Q_{10}) of soil organic carbon decomposition. A data set from a long-term laboratory soil incubation experiment was collected. Then I developed a new three-transfer-pool (3PX) model to resemble the model structure of soil carbon dynamics in Earth system models for estimating Q_{10} of SOM decomposition. I compared four widely used methods: one-pool (1P) model, two-discrete-pool (2P) model, three-discrete-pool (3P) model, and time-for-substrate (T4S) with the 3PX model for Q_{10} estimation using the same data set from a laboratory soil incubation experiment.

In Chapter 5, by integrating data from a unique long-term field manipulative experiment and a process-based model, I attempted to test the hypothesis that soil microbial community can acclimate to warming, and consequently alleviate the accelerated SOC loss.

Chapter 2: More replenishment than priming loss of soil organic carbon with additional carbon input

Abstract: An increase in carbon (C) input to soil under increasing atmospheric CO_2 can replenish soil organic C (SOC) through various stabilization mechanisms, and stimulate the decomposition of old SOC by priming effect. The net change in SOC under increased C input is a balance between those two effects, and remains controversial. Here I show, through data-model integration and synthesis, that approximately 58% of newly added C is transferred into SOC via replenishment, whereas the additional loss of old SOC due to priming effect only accounts for 8.4% of the added new C in the first year after a one-time new C input. As a result, the new C input leads to a net increase in SOC, ranging from 40% to 49% of the added new C. The magnitude of the net increase in SOC is positively correlated with the nitrogen-to-C ratio of the added substrates. Furthermore, a 100-year modeling experiment confirms that an increase in new C input leads to significant SOC accumulation over time. The findings suggest that increasing plant productivity and the consequent increase in C input to soils likely promote SOC storage despite the enhanced decomposition of old C, potentially mitigating further climate change.

2.1 Introduction

Soils store more than twice as much carbon (C) as the atmosphere (IPCC, 2013). As such, a small change in soil C content may have a large impact on the magnitude of atmospheric CO_2 concentrations and therefore climate change. Priming effect has been identified as a major mechanism that stimulates decomposition of old soil organic C (SOC) by the addition of new C to soils (Kuzyakov *et al.*, 2000, Fontaine *et al.*, 2004a, Dijkstra & Cheng, 2007, Heimann & Reichstein, 2008, Kuzyakov, 2010, Sayer *et al.*,

2011, Schmidt *et al.*, 2011, van Groenigen *et al.*, 2014, Keiluweit *et al.*, 2015). The latter promotes microbial growth and liberates C from mineral associations (Kuzyakov, 2010, Keiluweit *et al.*, 2015). In the context of climate change, a major concern is that if priming effect is substantial and pervasive across ecosystems, enhanced plant production due to elevated CO_2 and thus increased C input to soils may limit or reduce SOC storage, leading to a positive feedback to climate change (Heimann & Reichstein, 2008, Sayer *et al.*, 2011, van Groenigen *et al.*, 2014). However, enhanced SOC decomposition due to priming effect may be counter-balanced by replenishment of SOC due to increased C input through various mechanisms (Rubino *et al.*, 2010, Cotrufo *et al.*, 2013, Cotrufo *et al.*, 2015, Soong & Cotrufo, 2015). Therefore, it is critical to quantify the net effect of priming and replenishment on SOC balance as it determines the direction and magnitude of SOC changes caused by increasing C input as anticipated in the higher CO_2 world in the future.

We used a data-model synthesis to quantify both short-term and long-term replenishment and priming effect of new C input, and consequently the net SOC change. I compiled 45 datasets from laboratory incubation experiments using isotope-labelled C to trace the origins of emitted CO_2 (Table 2.1). Observations from those experiments provide information on C replenishment and priming. The 45 studies were divided into two data groups, one for model selection and parameter optimization (data group I with 40 datasets) and the other for model validation (data group II with 5 datasets) (Table 2.1).

Table 2.1 Summary of the collected studies. 40 studies were used for model selection and parameter optimization (data group I), and the other 5 were used for out-of-sample model validation (data group II).

Study	Ecosystem/Soil type	Added substrate	SOC (mg kg^{-1})	New C (mg kg^{-1})	Duration of Experiment (days)	Data group
1	Vertisol	Glucose	19000	1000	66	I
2	Vertisol	Starch	19000	1000	66	I
3	Vertisol	Legume leaves	19000	1000	66	I
4	Vertisol	Wheat leaves	19000	1000	66	I
5	Grass savannah	Cellulose	10500	495	70	I
6	Grassland	Cellulose	23300	1000	160	I
7	Cropland	Cellulose	5000	500	39	I
8	Cropland	Wheat straw	10400	3200	80	I
9	Cropland	Wheat straw	10400	2200	80	II
10	Cropland	Wheat straw	10400	1500	80	II
11	Barren	Glucose	26300	1000	97	I
12	Barren	Glucose	19100	1000	97	I
13	Barren	Glucose	15900	1000	97	I
14	Cropland	Ryegrass leaves	35000	424	100	I
15	Brown forest soil	Sucrose	39700	6000	32	I
16	Brown forest soil	Chopped leaves	39700	6000	32	I
17	Brown forest soil	Ground leaves	39700	6000	32	I
18	Cropland	Wheat straw	14700	5000	120	I
19	Cropland	Alfalfa leaves	14700	5000	120	I
20	Cropland	Glucose	17000	500	98	I
21	Cropland	Glucose	14000	500	98	I
22	Cropland	Mustard leaves	17000	500	98	I
23	Cropland	Mustard leaves	14000	500	98	I
24	Coniferous forest	*Pinus* leaves	17500	1430	120	I
25	Coniferous forest	*Michelia* leaves	17500	1430	120	I
26	Coniferous forest	*Pinus* leaves & N	17500	1430	120	I
27	Coniferous forest	*Pinus* leaves & P	17500	1430	120	I
28	Coniferous forest	*Michelia* leaves & N	17500	1430	120	I
29	Coniferous forest	*Michelia* leaves & P	17500	1430	120	I
30	Coniferous forest	*Pinus* leaves	4780	1430	120	I
31	Coniferous forest	*Pinus* leaves & N	4780	1430	120	I
32	Coniferous forest	*Michelia* leaves	4780	1430	120	I
33	Coniferous forest	*Michelia* leaves & N	4780	1430	120	I
34	Permanent grassland	Glucose	40900	5000	100	I
35	Permanent grassland	Glucose	40900	500	100	II
36	Permanent grassland	Ryegrass leaves	40900	5000	145	I
37	Permanent grassland	Ryegrass leaves	40900	500	145	II
38	Cropland	Wheat straw	8300	1540	31	I
39	Cropland	Wheat straw	8800	1540	31	I
40	Cropland	Wheat straw	9300	1540	31	I
41	Cropland	Wheat straw	9200	1540	31	I
42	Grassland	Glucose	24000	1000	54	I
43	Grassland	Glucose	24000	100	54	II
44	Subtropical forest	Glucose	138400	2768	168	I
45	Tropical forest	Glucose	27800	556	168	I

Before estimating the effects of increased C input on the net SOC balance, I evaluated four models, representing four different approaches to quantify replenishment and priming effect. The four models are: 1) a conventional (i.e., first-order kinetic) decomposition model, 2) an interactive two-pool model, 3) a regular Michaelis-Menten model, and 4) a reverse Michaelis-Menten model (Fig. 2.1). In the conventional and the

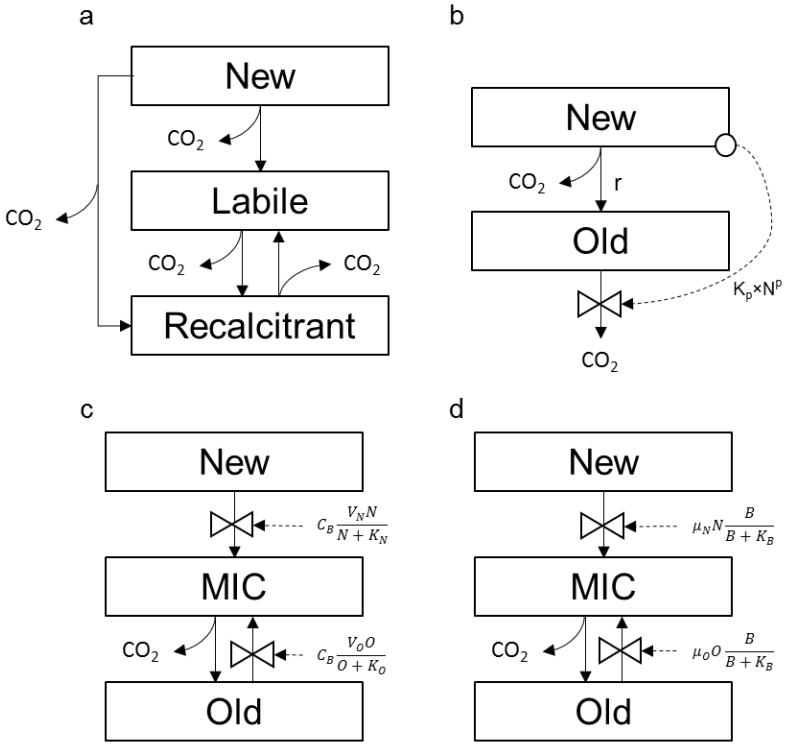

Figure 2.1 Models evaluated in the study. a, conventional model, in which C loss from each pool is only determined by pool size and its decay rate. b, interactive model, in which old C loss is affected by both new and old C pools. c, regular Michaelis-Menten model, in which C transfer rate has a linear relationship with microbial pool size (MIC) and a Michaelis-Menten relationship with substrates (i.e., new and old C). d, reverse Michaelis-Menten model, in which C transfer rate has a Michaelis-Menten dependence on MIC and a linear dependence on substrate.

interactive two-pool models, replenishment is represented by a transfer coefficient from the new C to the old soil C (Fig. 2.1a, b), while the regular and reverse Michaelis-Menten models transfer the new C to the old C through microbial uptake and turnover

(Fig. 2.1c, d). For the priming effect, it is represented by changing model parameters (e.g., increase of decay rates of C pools) in the conventional model, and by a nonlinear relationship between the decomposition rate of old C and the amount of the new C in the interactive model. The regular and reverse Michaelis-Menten models represent priming effect by including the dependence of old C decomposition on microbial biomass (linearly in the regular Michaelis-Menten model and nonlinearly in the reverse Michaelis-Menten model) and effects of new C input on microbial biomass (Fig. 2.1c, d).

2.2 Materials and Methods

2.2.1 Data collection.

Laboratory incubation experiments with isotope-labelled carbon (C) addition were chosen for this study. Since isotope measurements are necessary to trace the origins of the emitted CO_2, a comprehensive literature search with the terms of "isotope" and "soil incubation" was conducted using the online search connection *Web of Science* in Endnote. Studies meeting the following criteria were selected for further analyses: (i) both control and new C addition treatment were included; (ii) the added new C was isotope labelled to distinguish the origins of emitted CO_2; (iii) soil organic C (SOC) contents before incubation and the added new C amount were reported; (iv) CO_2 emissions from old SOC at both control and new C addition treatment, and from the added new C were reported or could be estimated; (v) multiple CO_2 emission measurements (> 2 time points) over the incubation period were conducted; (vi) experiments lasted at least one month. One month was chosen based on the tradeoff

between the number of studies I can synthesize vs. the information available for model optimization in each study. A total of 45 datasets from 16 publications were collected (Table 2.1) (Wu *et al.*, 1993, Chotte *et al.*, 1998, Magid *et al.*, 1999, Luna-Guido & Dendooven, 2001, Bell *et al.*, 2003, Fontaine *et al.*, 2004b, Perelo & Munch, 2005, Fontaine *et al.*, 2007, Nottingham *et al.*, 2009, Guenet *et al.*, 2010a, Guenet *et al.*, 2010b, Blagodatskaya *et al.*, 2011, Pascault *et al.*, 2013, Qiao *et al.*, 2014, Wang *et al.*, 2014a, Wang *et al.*, 2014b). In three publications, different amounts of new C were applied (Wu *et al.*, 1993, Guenet *et al.*, 2010a, Blagodatskaya *et al.*, 2011). In this case, one new C amount was used for model selection and parameter optimization (studies 8, 34, 36, 42 in Table 2.1), and the others were used for model validation (studies 9, 10, 35, 37, 43 in Table 2.1). Overall, there were 40 datasets for model selection and parameter optimization (data group I), and 5 for model validation (data group II). The studies were divided into three categories based on added substrate nitrogen-to-C (N:C) ratio: (i) without N, (ii) low N:C ratio (i.e., straw), and (iii) high N:C ratio (leaf materials), to investigate the influence of substrate N:C ratio on SOC storage change.

2.2.2 Models.

Four different types of models, including a conventional model, an interactive model, a regular Michaelis-Menten model, and a reverse Michaelis-Menten model, were used to represent soil C dynamics in this tudy. The conventional model used first-order equations which are commonly used in the current generation of Earth system models (Fig. 2.1a) (Liang *et al.*, 2015, Luo *et al.*, 2016). As new (N) C is added to the soil with

labile (L) and recalitrant (R) pools, the C dynamics among the three pools can be represented by the following equations:

$$\frac{dN}{dt} = I - K_N \times N$$

$$\frac{dL}{dt} = K_N \times N \times a_{L,N} + K_R \times R \times a_{L,R} - K_L \times L$$

$$\frac{dR}{dt} = K_N \times N \times a_{R,N} + K_L \times L \times a_{R,L} - K_R \times R$$

where I is new C input; K_N, K_L, and K_R are decay rates of new C, labile SOC, and recalcitrant SOC; $a_{L,N}$ and $a_{R,N}$ are transfer coefficients from new C to labile and recalcitrant SOC, respectively; $a_{R,L}$ is transfer coefficient from labile to recalcitrant SOC; $a_{L,R}$ is transfer coefficient from recalcitrant to labile SOC. The conventional model can represent nonlinear processes, such as priming effect, through changing parameters (van Groenigen *et al.*, 2014). Thus, the model had two sets of parameters, one for the control and the other for the new C addition treatment.

The interactive model was built based on the Introductory C Balance Model (ICBM) (Andrén & Kätterer, 1997). In the interactive model, the soil C dynamics are described by:

$$\frac{dN}{dt} = I - K_N \times N$$

$$\frac{dO}{dt} = K_N \times N \times r - (K_O + K_p \times N^p) \times O$$

where *N* and *O* are the pool sizes of new and old C, respectively; K_N and K_O are the base decay rates of new and old C, respectively; *r* is the transfer coefficient from new to old C (i.e., replenishment coefficient); K_p is the decay rate of old C due to priming effect; *p*

is a power factor that determines the magnitude of the effect of new C pool size on priming effect.

The third model is the regular Michaelis-Menten model (Allison *et al.*, 2010, Wieder *et al.*, 2013, Wang *et al.*, 2014c) (Fig. 2.1c) with the following equations

$$\frac{dN}{dt} = I - B \times \frac{V_N \times N}{N + K_N}$$

$$\frac{dO}{dt} = \mu_B \times B - B \times \frac{V_O \times O}{O + K_O}$$

$$\frac{dB}{dt} = -\mu_B \times B + \varepsilon \times B \times \left(\frac{V_N \times N}{N + K_N} + \frac{V_O \times O}{O + K_O}\right)$$

where *N*, *O*, and *B* are pool sizes of new C, old C, and microbial biomass; V_N and V_O are maximum substrate C (new or old C) assimilation rates; K_N and K_O are Michaelis-Menten constants; μ_B is turnover constant of microbial biomass; ε is microbial growth efficiency.

The fourth model is the reverse Michaelis-Menten model (Wutzler & Reichstein, 2013, Wang *et al.*, 2016) as,

$$\frac{dN}{dt} = I - \mu_N \times N \times \frac{B}{B + K_B}$$

$$\frac{dO}{dt} = \mu_B \times B - \mu_O \times O \times \frac{B}{B + K_B}$$

$$\frac{dB}{dt} = -\mu_B \times B + \varepsilon \times (\mu_N \times N + \mu_O \times O) \times \frac{B}{B + K_B}$$

where *N*, *O*, and *B* are pool sizes of new C, old C, and microbial biomass; μ_N, μ_O, μ_B are turnover constants of new C, old C, and microbial biomass; K_B is a constant for C consumption by microbes; ε is microbial growth efficiency.

2.2.3 Model optimization and selection.

The model optimization was based on Bayes' theorem:

$$P(\theta|Z) \propto P(Z|\theta)P(\theta)$$

in which the posterior probability density function (PDF) $P(\theta|Z)$ of model parameters (θ) was estimated from the prior PDF $P(\theta)$ and the data information represented by a likelihood function $P(Z|\theta)$. The prior PDFs were uniform distributions over specific parameter ranges. The likelihood function $P(Z|\theta)$ was calculated assuming that errors of observations were independent and followed a multivariate Gaussian distribution:

$$P(Z|\theta) \propto exp\left\{-\sum_{i=1}^{n}\sum_{t\in obs(Z_i)}\frac{[Z_i(t)-X_i(t)]^2}{2\sigma_i^2(t)}\right\}$$

where $Z_i(t)$ and $X_i(t)$ are the observed and modeled values, respectively. $\sigma_i(t)$ is the standard deviation of measurements.

For each study in data group I, the models were optimized by using the adaptive Metropolis-Hastings algorithm, a Markov Chain Monte Carlo (MCMC) technique (Metropolis *et al.*, 1953, Hastings, 1970). In the conventional model, it is necessary to change parameters to capture priming effect. Thus, there were two separate sets of parameters, one for the control and the other for the new C addition treatment. In the rest three models, one set of parameters for each study was derived using data from both the control and the new C addition treatment simultaneously. To derive the posterior PDFs of parameters, two steps were repeated (Xu *et al.*, 2006, Liang *et al.*, 2015): (i) a proposing step and (ii) a moving step (Xu *et al.*, 2006, Liang *et al.*, 2015). In the proposing step, a new point θ^{new} was generated based on the previously accepted point θ^{old}:

$$\theta^{new} = \theta^{old} + d(\theta_{max} - \theta_{min})/D$$

where θ_{max} and θ_{min} are the maximum and minimum values in the prior uniform distribution of the given parameter, d is a random value between -0.5 and 0.5, and D is used to control the proposing step size. In the moving step, the new point θ^{new} was tested against the Metropolis criterion to determine whether θ^{new} is accepted or rejected. The covariance from a test run was used for the first 4000 iterations. After that, the covariance was updated each iteration based on previously generated parameters. The first half of accepted samples were discarded, and only the rest were used for further analyses.

Deviance information criterion (DIC) (Spiegelhalter *et al.*, 2002) and likelihood of model (Burnham & Anderson, 2002) were used to evaluate the models given the data. For each study, DIC was calculated by

$$DIC = \bar{D} + p_D$$

where

$$\bar{D} = \frac{1}{S}\sum_{i=1}^{S}\left(-2log\left(P(Z|\theta^i)\right)\right)$$

and

$$p_D = \bar{D} + 2log(P(Z|\bar{\theta}))$$

where S is the number of the generated parameter sets, and $\bar{\theta}$ is the mean of the generated parameter sets. The weighted average DIC for all studies was calcuted by

$$DIC_w = \frac{\sum_{i=1}^{40} DIC_i N_i}{\sum_{i=1}^{40} N_i}$$

where N_i is the number of data points in the ith study. Smaller DIC means better model. The likelihood (L) of model given the data was calculated by

$$L = e^{-0.5(DIC - DIC_{min})}$$

where DIC_{min} is the minimum DIC value of the four models. In this study, 0.5 was used as a threshold for L to select model. Only the interactive model had a L value bigger than 0.5 (Fig. 2.2). Thus, the interactive model was used for further analyses.

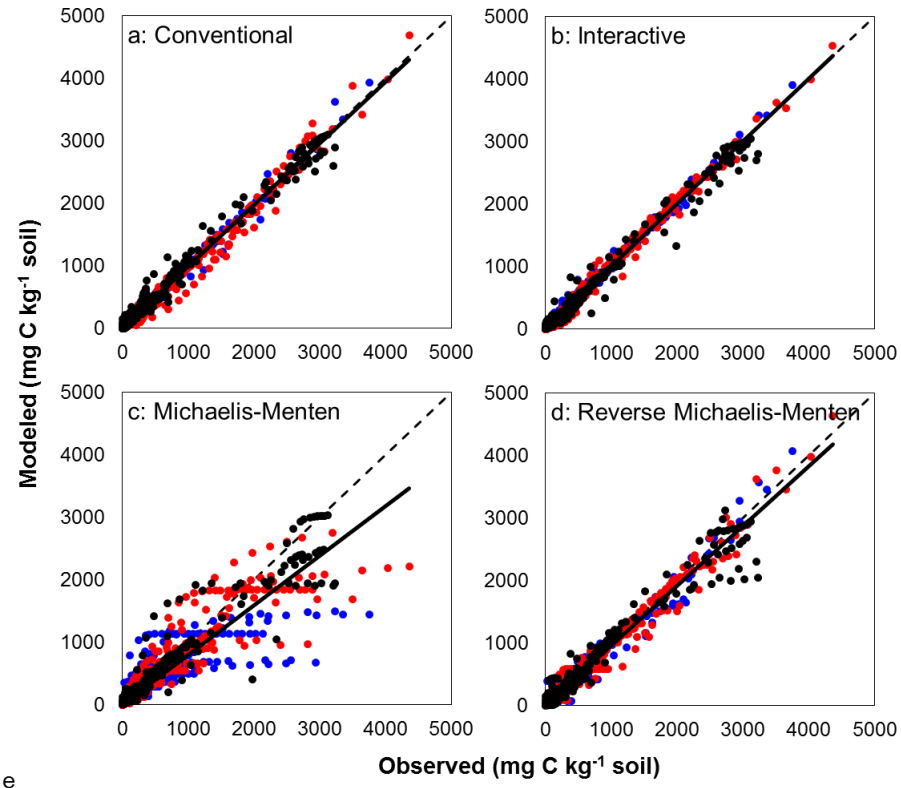

e

Model	Number of parameters	Slope	R^2	P	DIC	Likelihood of model
Conventional	12	0.99	0.99	< 0.01	15.5	0.02
Interactive	6	1.00	0.99	< 0.01	7.59	1.00
Michaelis-Menten	8	0.79	0.81	< 0.01	32.8	< 0.01
Reverse Michaelis-Menten	7	0.96	0.97	< 0.01	20.2	< 0.01

Figure 2.2 Within-sample model evaluation. a – d, comparison between observed and model simulated cumulative CO_2 emissions in data group I. a, conventional model; b, interactive model; c, regular Michaelis-Menten model; d, reverse Michaelis-Menten model. Blue, CO_2 emission from old C at control; Red, CO_2 emission from old C at new addition treatment; Black, CO_2 emission from added new C; Dashed line, 1:1 line; Solid line: linear regression line (slope, R^2, P values are shown in e). e, number of parameters, slope, R^2, P values, deviance information criterion (DIC), and likelihood of the models given the data. The number of parameters in the conventional model is 12 due to 6 parameters for each of control and new C addition treatment.

2.2.4 Model validation.

The interactive model was further validated against data group II (i.e., out-of-sample validation). For example, the optimized model in study 8 was used to estimate CO_2 emissions for studies 9 and 10, with their respective new C input amount. The model was run repeatedly with all the generated parameter sets from study 8. The procedule was repeated for study 35, 37, and 43 with parameters generated from study 34, 36, and 42, respectively. Then the mean values of the modeled CO_2 emissions were compared with the observed ones in data group II to reveal the performance of the model in SOC dynamic simulation. Through the validation, the predictive skill of the interactive model given the soil and substrate types could be revealed.

2.2.5 Short-term replenishment, priming and net SOC change.

For each study, short-term replenishment, priming and net SOC change, with their respective new C input at the beginning, were estimated using the optimized interactive model. I paid particular interest in the first year to estimate annual C balance. The annual replenishment is the C amount that is transferred from new to old pool and has not been decomposed within the first year. The annual priming loss is the cumulative stimulated C loss from old C pool due to priming effect during the same period. For each study, all the generated parameter sets were treated as replicates. Mean (*M*) and standard deviation (*SD*) of the replicates were calculated. For each variable and category, the weighted mean and 95% confidence interval (*CI*) were estimated by the

following two steps (Borenstein *et al.*, 2009). In the first step, the within-study variance was calculated by

$$V = \frac{SD^2}{n}$$

and the between-study variance T^2 was calculated by

$$T^2 = \frac{Q - df}{U}$$

where

$$Q = \sum_{j=1}^{k} W_j M_j^2 - \frac{\left(\sum_{j=1}^{k} W_j M_j\right)^2}{\sum_{j=1}^{k} W_j}$$

$$df = k - 1$$

$$U = \sum_{j=1}^{k} W_j - \frac{\sum_{j=1}^{k} W_j^2}{\sum_{j=1}^{k} W_j}$$

where k is the number of studies. M_j is the mean value of study j. W_j is the first-step weighting factor of each study, which is $1/V_j$. In the second step, the weighting factor of the random-effects model was calculated by

$$W_j^* = \frac{1}{V_j^*}$$

where V_j^* is the sum of the within-study variance for study j and the between-studies variance:

$$V_j^* = V_j + T^2$$

Then the weighted mean was calculated as

$$M_{weighted} = \frac{\sum_{j=1}^{k} W_j^* M_j}{\sum_{j=1}^{k} W_j^*}$$

with the variance as

$$V_{weighted} = \frac{1}{\sum_{j=1}^{k} W_j^*}$$

The 95% lower and upper limits ($LL_{weighted}$ and $UL_{weighted}$) for the weighted mean were computed as

$$LL_{weighted} = M_{weighted} - 1.96 \times \sqrt{V_{weighted}}$$

and

$$UL_{weighted} = M_{weighted} + 1.96 \times \sqrt{V_{weighted}}$$

The effect was considered statistically significant at $P < 0.05$ level if the 95% *CI* did not overlap with zero. The difference among categories were considered statistically significant at $P < 0.05$ level when their 95% *CI*s did not overlap. All the calculations were conducted in MetaWin 2.1 (Rosenberg *et al.*, 2000).

2.2.6 Long-term modeling experiment.

For each of the datasets spanning a diverse range of different soils and substrate quality, 100 sets of parameters were randomly sampled from the posterior PDFs. The sampled parameter sets, as replicates, were then used for the modeling experiment. Assuming global average C input to top soils (1m) is 378 g m^{-2} y^{-1} (Field *et al.*, 1998) and average soil bulk density is 1.3 g cm^{-3}, monthly C input is about 24 mg C kg^{-1} soil $month^{-1}$. For each study, the interactive model was spun up to steady state with monthly new C input by 24 mg C kg^{-1} soil $month^{-1}$. Then the model was run for 100 years in three C input scenarios. The first scenario was constant C input by 24 mg C kg^{-1} soil $month^{-1}$ (i.e., no increase in C input). The second scenario was constant C input by 26.4 mg C kg^{-1} soil $month^{-1}$ (i.e., a 10% step increase in C input). In the third scenario, the

increase in C input was linearly increased from 0.0475 mg C kg^{-1} soil $month^{-1}$ in the first year to 4.7525 mg C kg^{-1} soil $month^{-1}$ in the 100th year. The C was added every 30 days. Over the 100 years, the C input in the second and the third scenarios was 2880 mg C kg^{-1} soil greater than that in the first scenario. The weighted effect of increased C input and the 95% *CI* were estimated using the synthesis method described above.

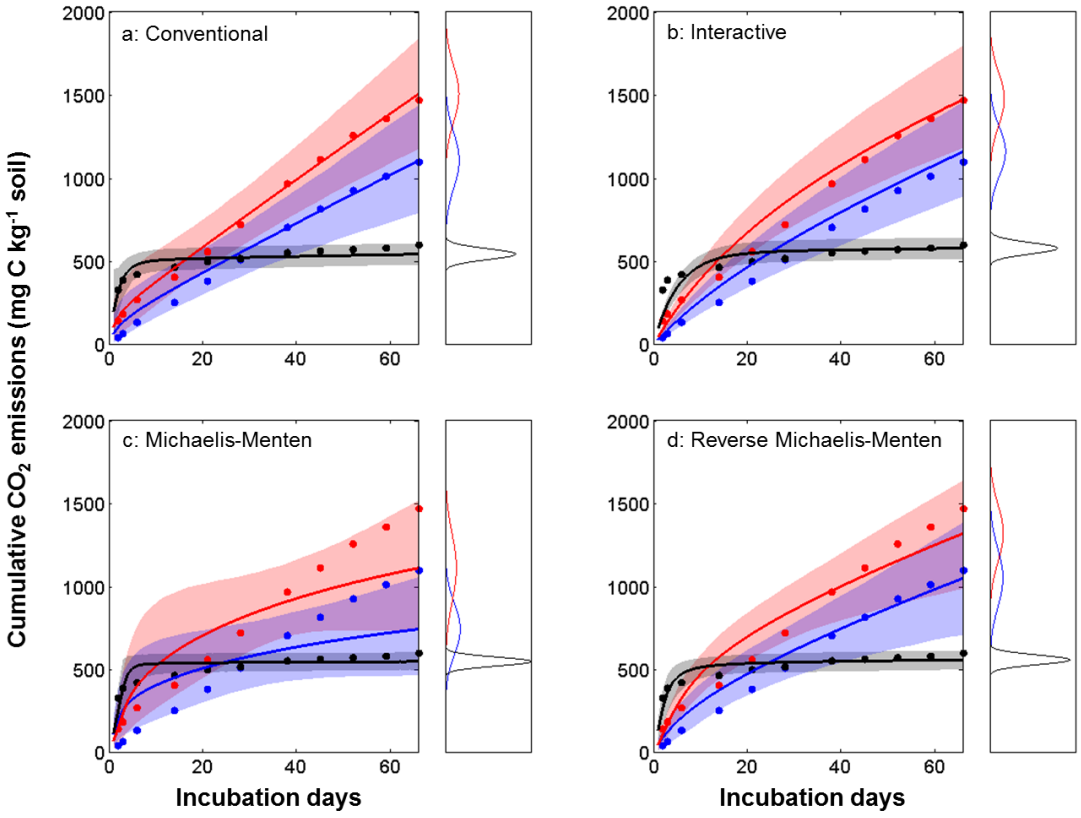

Figure 2.3 An example showing the comparison between observed (dots) and simulated (lines and shading areas) cumulative CO_2 emissions by the conventional (a), interactive (b), regular Michaelis-Menten (c), and reverse Michaelis-Menten (d) models during laboratory incubation. Lines are mean values of model simulations and shading areas are the ranges from 2.5th to 97.5th percentiles (i.e., 95% range). The box on the right of each panel shows the distributions of model simulated cumulative CO_2 emissions at the last day (i.e., day 66). Blue, CO_2 emission from old C at control; Red, CO_2 emission from old C at new C addition treatment; Black, CO_2 emission from added new C. The difference between red and blue is priming effect. a, in the conventional model, two sets of parameters, one for control and the other for new C addition treatment, were used to simulate priming effect.

2.3 Results

The model evaluation against data group I (i.e., within-sample evaluation) showed that the regular Michaelis-Menten model underestimated cumulative CO_2 emission from SOC as experiments proceed (Fig. 2.2c, e; Fig. 2.3). Although the conventional and the reverse Michaelis-Menten models well simulated the cumulative CO_2 emissions, neither demonstrated a high likelihood (<< 0.5) to represent replenishment and priming effect due to overfitting issues given the data (Fig. 2.2a, d, e). The interactive two-pool model was the most parsimonious model given the data (Fig. 2.2b, e). The interactive model was further validated by data group II (i.e., out-of-sample validation). The analysis indicates that the calibrated interactive two-pool model has a high predictive skill (Fig. 2.4).

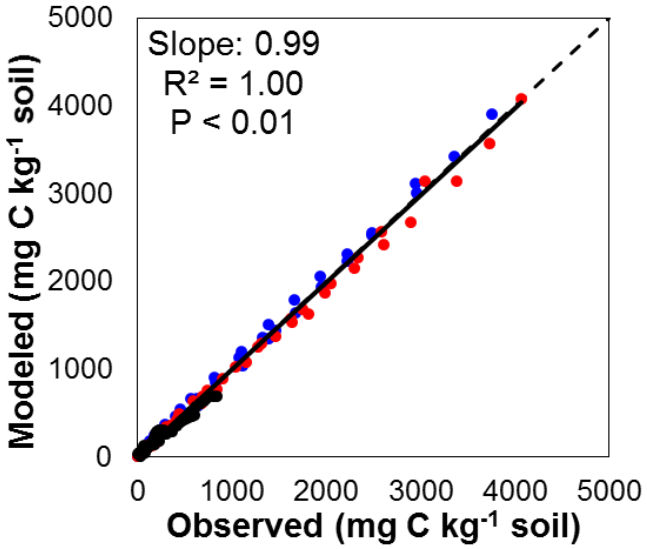

Figure 2.4 Out-of-sample validation of the interactive model against data group II. y-axis shows mean values of simulated CO_2 emissions for studies in data group II by the interactive model optimized against the corresponding studies in data group I. Blue, CO_2 emission from old SOC at control; Red, CO_2 emission from old SOC at new C addition treatment; Black, CO_2 emission from added new C. Dashed line: 1:1 line; Solid line: linear regression line.

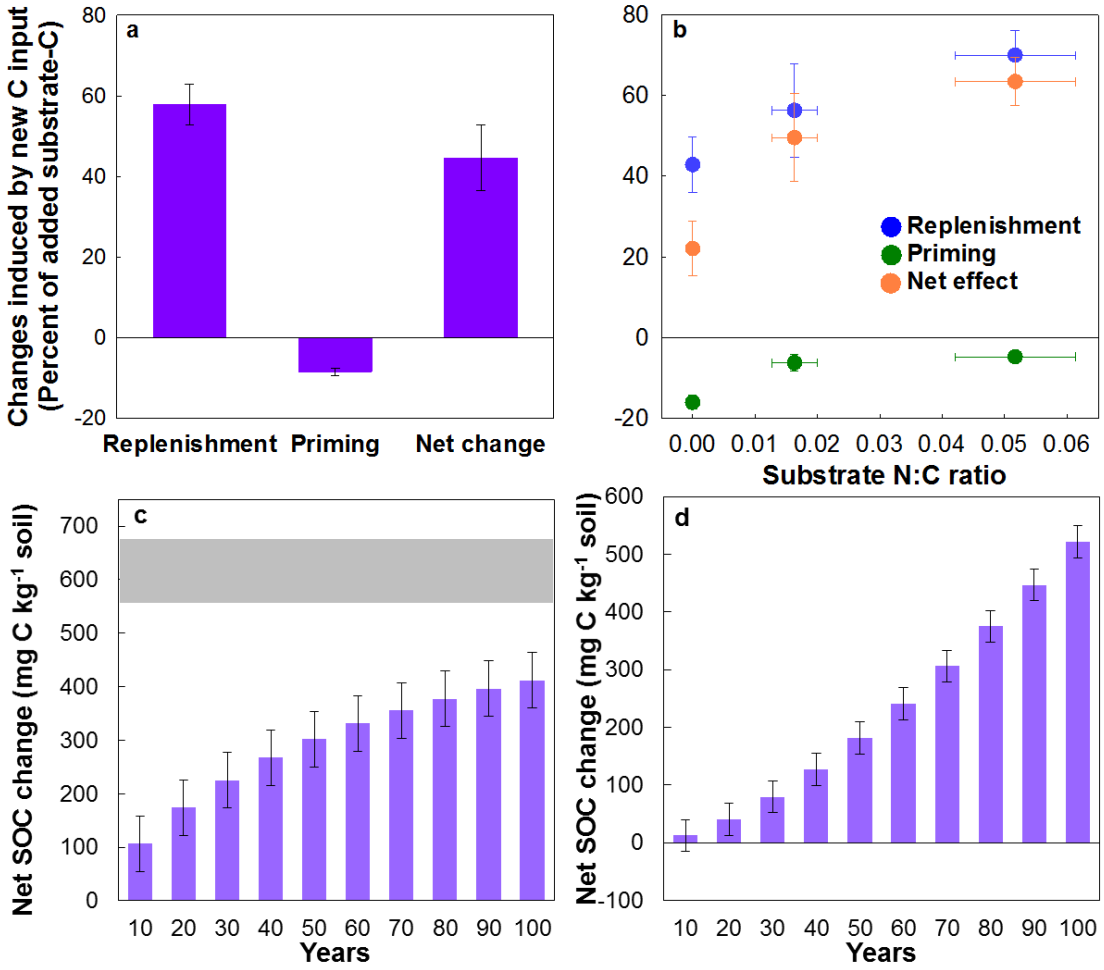

Figure 2.5 Syntheses of new C input induced replenishment, priming, and net SOC change and their dependence on substrate N:C ratio (Mean ± 95% confidence interval). a – b, annual replenishment, priming and net SOC change (a) and their dependence on substrate N:C ratio (b) with a one-time new C addition at the beginning. c – d, long-term modeling experiment showing net SOC increase by additional C input. c, predicted net SOC change by a 10% step increase in C input (24.0 vs. 26.4 mg C kg^{-1} soil $month^{-1}$) for 100 years. Gray bar represents the 95% confidence interval of the equilibrium difference of the two scenarios. d, predicted net SOC change by gradual increase in C input. Total increase in C input is 2880 mg C kg^{-1} soil $month^{-1}$ in the 100 years in both c and d.

After the model evaluation, I used the optimized interactive model to estimate annual C replenishment, priming effect, and net SOC change for all studies with their

respective new C input at the beginning of experiments. The analyses show that new C input indeed induces priming effect, which on average stimulates C loss from old SOC equivalent to 8.4% (7.5%–9.4%, 95% confidence interval) of the added C within one year (Fig. 2.5a). However, 54% to 61% of the added new C is transferred to replenish SOC. The greater magnitude of replenishment than priming leads to a net increase in SOC, equivalent to 45% (40%–49%) of the added new C (Fig. 2.5a). Although the magnitudes of replenishment and priming effect change over time, the conclusion that new C input increases SOC holds (Fig. 2.6). In addition, the replenishment increases with the increase in substrate N:C ratio (Fig. 2.5b). In contrast, a higher priming loss of old SOC occurs when the added substrates have lower N:C ratios (Fig. 2.5b). As a result, the net SOC increase in response to new C input ranges from 63% (high N:C ratio) to 50% (low N:C ratio) and to 22% (without N) of the added new C (Fig. 2.5b).

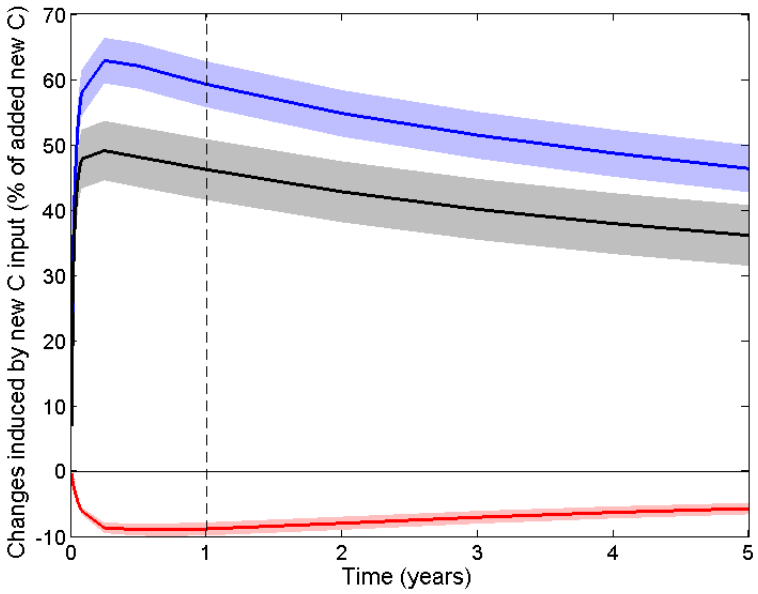

Figure 2.6 Five-year time courses of effects of replenishment (blue) and priming (red) on SOC, and the net SOC change (black) with a one-time new C input at the beginning. Shading areas are 95% confidence intervals. Dashed line means the end of the first year.

In addition, the long-term modeling experiment shows that soil C content at equilibrium in the second scenario is increased by 565–670 mg C kg^{-1} soil, comparing with the first scenario (Fig. 2.5c). Persistent increase in C input in the second scenario leads to gradual SOC accumulation, showing an average increase by 412 mg C kg^{-1} soil (360–464 mg C kg^{-1} soil). The SOC increase induced by gradual C input increase in the third scenario is even greater, ranging from 493 to 549 mg C kg^{-1} soil over the 100 years (Fig. 2.5d).

2.4 Discussion

There may be several reasons for the positive effect of the new C input on SOC storage. First, the added new C may be protected by direct physical and chemical bonding (Jastrow & Miller, 1997, Plaza *et al.*, 2013). In addition, part of the new C is used to increase microbial biomass and the production of metabolic by-products (Cotrufo *et al.*, 2013, Cotrufo *et al.*, 2015). Through the microbial processes, the added C is transferred to stable SOC after microorganisms die (Bird & Torn, 2006, Rubino *et al.*, 2010, Cotrufo *et al.*, 2013, Wieder *et al.*, 2014, Cotrufo *et al.*, 2015). Although the increased microbial growth may promote the decomposition of old SOC for energy and nutrient acquisition (Kuzyakov *et al.*, 2000), the results demonstrate that the amount of C loss resulting from the priming effect is relatively small, compared with the amount of replenished soil C. The long-term modeling experiment confirms that additional new C input promotes SOC storage despite the enhanced old SOC decomposition by the priming effect.

Both the replenishment and priming loss of soil C may be affected by the substrate nitrogen-to-C (N:C) ratio since microbial activity is co-limited by energy and nutrient supplies (Schimel & Weintraub, 2003, Fontaine & Barot, 2005, Hobbie, 2015). The results show that the replenishment increases with the increase in substrate N:C ratio (Fig. 3b). This may be due to more efficient utilization of substrates with high N:C ratios for microbial growth than low N:C substrates, resulting in a higher proportion of substrates transformed to microbial biomass and products (Bird & Torn, 2006, Rubino *et al.*, 2010, Cotrufo *et al.*, 2013, Hobbie, 2015). On the other hand, a higher priming loss of old SOC occurs when the added substrates have lower N:C ratios (Fig. 2.5b), which may be due to the scarcity of N obtained from low N:C substrates. In this case, soil microbes utilize more old soil organic matter for N, resulting in stronger priming effects (Kuzyakov, 2010). As a result, the net SOC increase in response to new C input increases with the substrate N:C ratio. Thus, if atmospheric CO_2 enrichment reduces N:C ratio in plant tissues (de Graaff *et al.*, 2006, Luo *et al.*, 2006, Myers *et al.*, 2014), the rate of SOC increase due to the enhanced substrate input may be suppressed (Sulman *et al.*, 2014, van Groenigen *et al.*, 2014).

Moreover, this study may have potential implications for C cycling models. It has been well agreed that it is necessary to incorporate priming effect into C cycling models (Allison *et al.*, 2010, Wutzler & Reichstein, 2013, Wieder *et al.*, 2014, Guenet *et al.*, 2016, Wang *et al.*, 2016). Although the regular Michaelis-Menten equation is widely used to describe enzyme kinetics with mono-substrate, the model selection in the current study suggests that it may not perform well with mixed, complex SOC. The conventional model with changing parameters and the reverse Michaelis-Menten model

both fit data reasonably well but may have overfitting issues. In the interactive model, though the underlying mechanisms are still to be uncovered, the simple power function of new C pool size represents priming quite well. Thus, incorporating the interactive model into terrestrial C cycling models may improve their performance in simulating soil C dynamics.

In summary, using extensive data sets, I have selected a parsimonious two-pool interactive model. Based on the model, I have revealed the effect of new C addition on SOC storage through two critical processes, replenishment and priming. The analyses highlight that increasing new C inputs increase SOC sequestration due to a higher rate of replenishment versus loss of old C by priming effect. Consequently, increasing C inputs to soils from enhanced plant productivity under elevated CO_2, plant invasion, and vegetation recovery likely result in SOC accumulation in soils over time, potentially mitigating climate change.

Chapter 3: Processes regulating progressive nitrogen limitation under elevated carbon dioxide: A meta-analysis

Abstract: The nitrogen (N) cycle has the potential to regulate climate change through its influence on carbon (C) sequestration. Although extensive research has explored whether or not progressive N limitation (PNL) occurs under CO_2 enrichment, a comprehensive assessment of the processes that regulate PNL is still lacking. Here, I quantitatively synthesized the responses of all major processes and pools in the terrestrial N cycle with meta-analysis of CO_2 experimental data available in the literature. The results showed that CO_2 enrichment significantly increased N sequestration in the plant and litter pools but not in the soil pool, partially supporting one of the basic assumptions in the PNL hypothesis that elevated CO_2 results in more N sequestered in organic pools. However, CO_2 enrichment significantly increased the N influx via biological N fixation and the loss via N_2O emission, but decreased the N efflux via leaching. In addition, no general diminished CO_2 fertilization effect on plant growth was observed over time up to the longest experiment of 13 years. Overall, the analyses suggest that the extra N supply by the increased biological N fixation and decreased leaching may potentially alleviate PNL under elevated CO_2 conditions in spite of the increases in plant N sequestration and N_2O emission. Moreover, the syntheses indicate that CO_2 enrichment increases soil ammonium (NH_4^+) to nitrate (NO_3^-) ratio. The changed NH_4^+/NO_3^- ratio and subsequent biological processes may result in changes in soil microenvironments, above-belowground community structures and associated interactions, which could potentially affect the terrestrial biogeochemical cycles. In addition, the data synthesis suggests that more long-term studies, especially in regions other than temperate ones, are needed for comprehensive assessments of the PNL hypothesis.

3.1 Introduction

Fossil-fuel burning and deforestation have led to substantial increase in atmospheric carbon dioxide (CO_2) concentrations, which could stimulate plant growth (IPCC, 2013). The plant growth stimulated by CO_2 fertilization and the resulting terrestrial carbon (C) storage could partially mitigate the further increase in CO_2 concentrations and associated climate warming (IPCC, 2013). However, this effect may be constrained by the availability of nitrogen (N), an essential element for molecular compounds of amino acids, proteins, ribonucleic acids (RNAs) and deoxyribonucleic acids (DNAs) in organisms (Rastetter *et al.*, 1997, Oren *et al.*, 2001, Luo *et al.*, 2004, Reich *et al.*, 2006, Norby *et al.*, 2010, Reich & Hobbie, 2013). A popular hypothesis of the N constraint to the CO_2 fertilization effect is progressive N limitation (PNL) (Luo *et al.*, 2004).

Progressive N limitation postulates that the stimulation of plant growth by CO_2 enrichment results in more N sequestered in plant, litter and soil organic matter (SOM) so that, the N availability for plant growth progressively declines in soils over time (Luo *et al.*, 2004). The reduced N availability then in turn constrains the further CO_2 fertilization effect on plant growth over longer time scales. However, whether and to what extent PNL occurs depends on the balance of N demand and supply (Luo *et al.*, 2004, Finzi *et al.*, 2006, Walker *et al.*, 2015). If the N supply meets the N demand, PNL may not occur. Otherwise, PNL may lead to a diminished CO_2 fertilization effect on plant growth over time. Some of the site-level studies support (Reich *et al.*, 2006, Norby *et al.*, 2010), while the others refute the PNL hypothesis (Finzi *et al.*, 2006, Moore *et al.*, 2006). To date, no general pattern of PNL across ecosystems has yet been revealed.

Since the key determining PNL occurrence is that whether N supply meets N demand (Luo *et al.*, 2004), it is important to understand how N supply changes under elevated CO_2. The change in the N supply for plant growth under elevated CO_2 is determined by the responses of multiple N cycling processes, including biological N fixation, mineralization, nitrification, denitrification, and leaching (Chapin III *et al.*, 2011). In addition, the responses of these processes to CO_2 enrichment may be influenced by external N addition, such as N deposition and fertilization (Reay *et al.*, 2008). Thus, synthesizing the responses of processes that regulate PNL to CO_2 enrichment may help reveal the general pattern of PNL in terrestrial ecosystems.

In the current study, the main objective was to synthesize data published in the literature on the N limitation to plant growth under enriched CO_2 conditions. The data synthesis was designed to answer two questions: (i) How do the major processes in the terrestrial N cycle respond to CO_2 enrichment? (ii) Does the CO_2 fertilization effect on plant growth diminish over time? To answer these questions, two sets of data from the literature were collected. With the first dataset, I quantitatively examined the effects of CO_2 enrichment on all the major processes and pools in the N cycle using meta-analysis. These processes and pools included N sequestered in organic components (i.e., plant tissues, litter and soil organic matter (SOM)), biological N fixation, net mineralization, nitrification, denitrification, leaching, and total inorganic N (TIN), ammonium (NH_4^+) and nitrate (NO_3^-) contents in soils. I separated the first dataset according to the experimental durations to explore the responses of the N processes to short- vs. long-term CO_2 treatments. In addition, the responses of the N processes to CO_2 enrichment were compared between without and with N addition conditions. The

second dataset was compiled for the plant growth in decadal free air CO_2 enrichment (FACE) experiments. With the dataset, I explored whether the CO_2 fertilization effect on plant growth diminishes or not over time.

3.2 Materials and Methods

3.2.1 Data collection.

For the first dataset, a comprehensive literature search with the terms of "CO_2 enrichment (or CO_2 increase)", "nitrogen" and "terrestrial" was conducted using the online search connection *Web of Science* in Endnote. Then, papers meeting the following two criteria were selected to do the further analyses: (i) including both control and CO_2 enrichment treatments, where the ambient and elevated CO_2 concentrations were around the current and predicted atmospheric CO_2 concentrations by the Intergovernmental Panel on Climate Change (IPCC, 2013), respectively (Fig. 3.1); (ii) including or from which I could calculate at least one of the major N pools or processes: soil TIN content, soil NH_4^+ content, soil NO_3^- content, aboveground plant N pool (APNP), belowground plant N pool (BPNP), total plant N pool (TPNP), litter N pool (LNP), soil N pool (SNP), N fixation, nodule mass and/or number, net mineralization, nitrification, denitrification, and inorganic N leaching. Overall, there were 175 papers included in the first dataset. For each paper, means, variations (standard deviation (*SD*), standard error (*SE*) or confidence intreval (*CI*)) and sample sizes of the variables in both control and CO_2 enrichment treatments were collected.

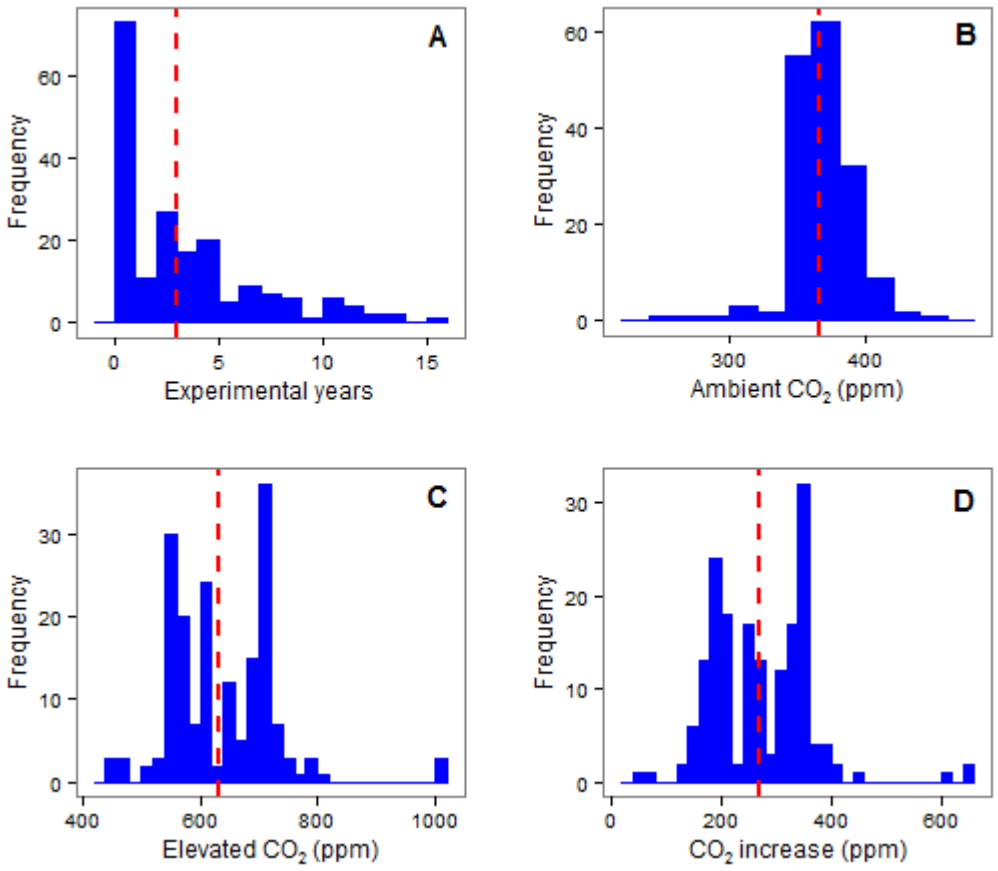

Figure 3.1. Distributions of the experimental duration (A) and the CO_2 concentrations under ambient (B) and elevated (C) treatments and their difference (D) for the 175 collected studies. Red dashed lines represent the mean values.

For those studies that provided *SE* or *CI*, *SD* was computed by

$$SD = SE\sqrt{n} \qquad \text{Eq. (1)}$$

$$\text{or } SD = (CI_u - CI_l)\sqrt{n}/2u_P \qquad \text{Eq. (2)}$$

where n is the sample size, CI_u and CI_l are the upper and lower limits of *CI*, and u_p is the significant level and equal to 1.96 and 1.645 when α = 0.05 and 0.10, respectively. In some studies, if tissue N concentration and biomass were reported, I multiplied the two parts as N pools. When both APNP and BPNP were provided (or calculated), the two

were added together to represent the TPNP. When data from multiple soil layers were provided, they were summed if they were area-based (i.e., m^{-2} land), or averaged if they were weight-based (i.e., g^{-1} soil). In studies where the respective contents of NH_4^+ and NO_3^- were reported, the TIN was calculated by adding the two together. For all the variables, if more than one result were reported during the experiment period, they were averaged by

$$M = \sum_{i=1}^{j} \frac{M_i}{j} \qquad \text{Eq. (3)}$$

with standard deviation

$$SD = \sqrt{\frac{\sum_{i=1}^{j} SD_i^2 (n_i - 1) n_i}{\left(\sum_{i=1}^{j} n_i - 1\right) \sum_{i=1}^{j} n_i}} \qquad \text{Eq. (4)}$$

where j is the number of results, M_i, SD_i and n_i are the mean, SD and sample size of the ith sampling data, respectively (Liang *et al.*, 2013). If additional treatments applied (e.g., N addition), they were treated as independent studies.

Because treatment time and N addition may affect the responses of the N processes to CO_2 enrichment, the dataset was divided into different categories: (i) short-term ($\leq$ 3 years) vs. long-term (> 3 years), and (ii) without N addition vs. with N addition. Moreover, the dataset was also divided into forest, grassland, and cropland to explore possible differences between ecosystem types.

For the second dataset, 15 available time series of plant growth were collected from 7 decadal FACE experiments. The ecosystems included 9 forests, 5 grasslands and 1 desert. Because of the limited data, I included variables that can represent plant growth in one way or another, for example, net primary production (NPP), biomass, and leaf production. These data were collected to reveal whether the effect of CO_2 enrichment

on plant growth diminishes over treatment time as proposed by the PNL hypothesis (Luo *et al.*, 2004). In the 7 studies, the treatment lasted from 7 to 13 years, and at least 6 years' production measurements were reported. For each data, the percentage change in NPP (or biomass or leaf production) by CO_2 enrichment was calculated. Then, a linear regression between the percentage change and the treatment year was conducted. A significantly negative slope indicates that the effect of CO_2 enrichment on the plant production diminishes over time. A non-significant slope was treated as 0. After deriving all the slopes, the frequency distribution of the slopes were fitted by a Gaussian function:

$$y = y0 + ae^{-\frac{(x-\mu)^2}{2\sigma^2}} \qquad \text{Eq. (5)}$$

where x is the mean value of each individual interval, and y is the frequency of each interval. $y0$ is the base frequency. μ and σ are the mean and *SD* of the distribution.

3.2.2 Meta-analysis.

With the first dataset, the effect of CO_2 enrichment for each line of data of the N variables was estimated using the natural logarithm transformed response ratio (*RR*) (Hedges *et al.*, 1999, Liang *et al.*, 2013):

$$\log_e RR = \log_e(X_E/X_C) \qquad \text{Eq. (6)}$$

where X_E and X_C are the variable values under enriched CO_2 and control conditions, respectively. The variation of the log *RR* was

$$V = \left(\frac{SD_C^2}{n_C X_c^2} + \frac{SD_E^2}{n_E X_E^2}\right) \qquad \text{Eq. (7)}$$

where SD_C and SD_E are the standard deviation of X_C and X_E, and n_C and n_E are the sample sizes of X_C and X_E.

Then, the random-effects model was used to calculate the weighted mean. In the random-effects model, the weighted mean was calculated as

$$M_{weighted} = \frac{\sum_{j=1}^{k} W_j^* M_j}{\sum_{j=1}^{k} W_j^*} \qquad \text{Eq. (8)}$$

with the variance as

$$V_{weighted} = \frac{1}{\sum_{j=1}^{k} W_j^*} \qquad \text{Eq. (9)}$$

where k is the number of studies, M_j is the $Ln(RR)$ in study j, and W_j^* is the weighting factor which consists of between- and within-study variances (Rosenberg *et al.*, 2000, Liang *et al.*, 2013). The 95% lower and upper limits ($LL_{weighted}$ and $UL_{weighted}$) for the weighted mean were computed as

$$LL_{weighted} = M_{weighted} - 1.96 \times \sqrt{V_{weighted}} \qquad \text{Eq. (10)}$$

and

$$UL_{weighted} = M_{weighted} + 1.96 \times \sqrt{V_{weighted}} \qquad \text{Eq. (11)}$$

The weighted mean and corresponding 95% bootstrapping *CI* (999 iterations) for each variable and category were calculated in MetaWin 2.1 (details are described in the software handbook by Rosenberg et al., 2000). The results were back-transformed and represented as percentage change by $(RR - 1) \times 100\%$. The response was considered significant if the 95% *CI* did not overlap with zero.

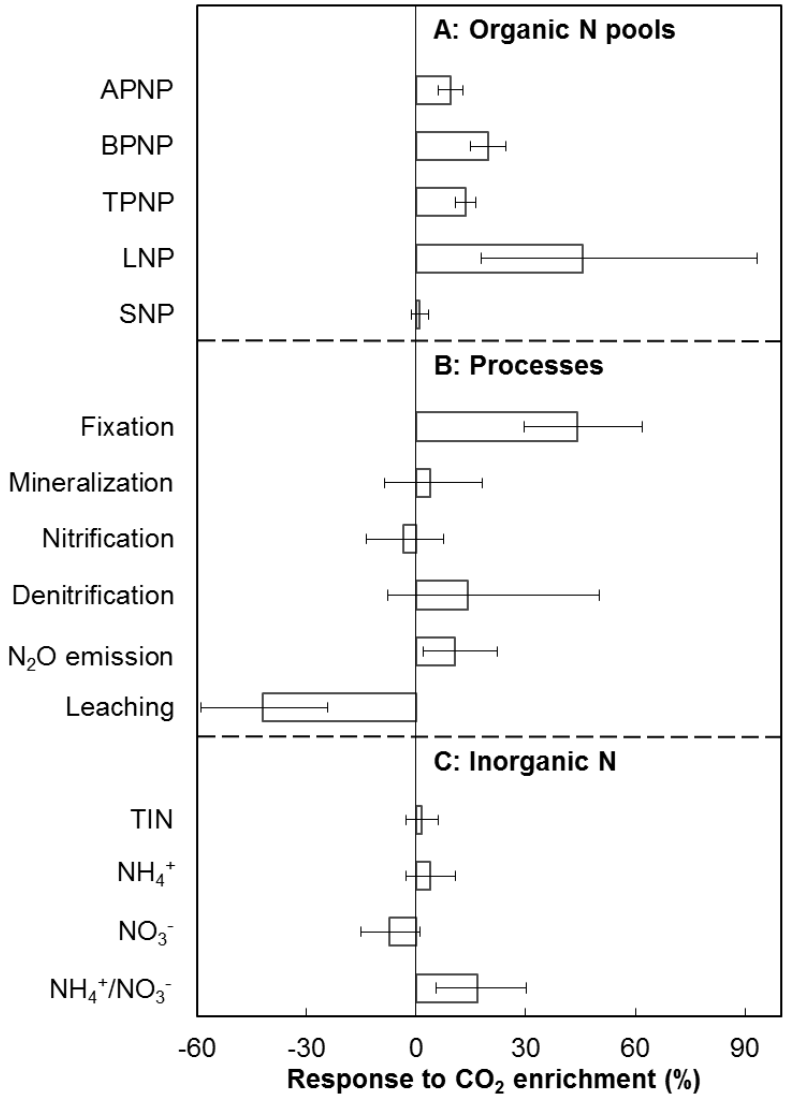

Figure 3.2. Results of a meta-analysis on the responses of nitrogen pools and processes to CO_2 enrichment. In (A), APNP, BPNP, TPNP, LNP, and SNP are the abbreviations for aboveground plant nitrogen pool, belowground plant nitrogen pool, total plant nitrogen pool, litter nitrogen pool, and soil nitrogen pool, respectively. In (C), TIN, NH_4^+ and NO_3^- are total inorganic nitrogen, ammonium, and nitrate in soils, respectively. The error bars represent 95% confidence intervals.

3.3 Results

The meta-analysis of the first dataset showed that CO_2 enrichment significantly increased N sequestered in plants and litter but not in SOM (Fig. 3.2). Whereas CO_2

enrichment had little overall effects on N mineralization, nitrification and denitrification, it significantly increased biological N fixation by 44.3% (with 95% CI from 29.5% to 61.8%). The increased biological N fixation was consistent when using various methods except H_2 evolution (Fig. 3.3). In legume species, CO_2 enrichment significantly increased nodule mass and number (Fig. 3.3B). In addition, CO_2 enrichment increased N_2O emission by 10.7% (with 95% CI from 2.0% to 22.3%), but reduced leaching (i.e., -41.8% with 95% CI from -58.9% to -24.3%) (Fig. 3.2B). Although CO_2 enrichment did not change the total inorganic N availability in soils, it increased the soil NH_4^+/NO_3^- ratio by 16.9% (with 95% CI from 5.4% to 30.2%) (Fig. 3.2C).

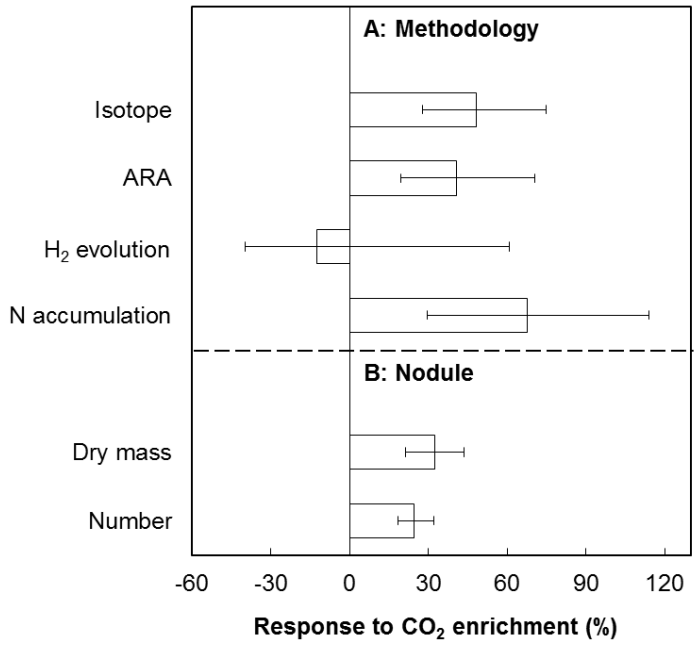

Figure 3.3. Responses of biological N fixation measured by different methods (A) and nodule dry mass and number in legume species (B). ARA: acetylene reduction assay. Mean ± 95% confidence interval.

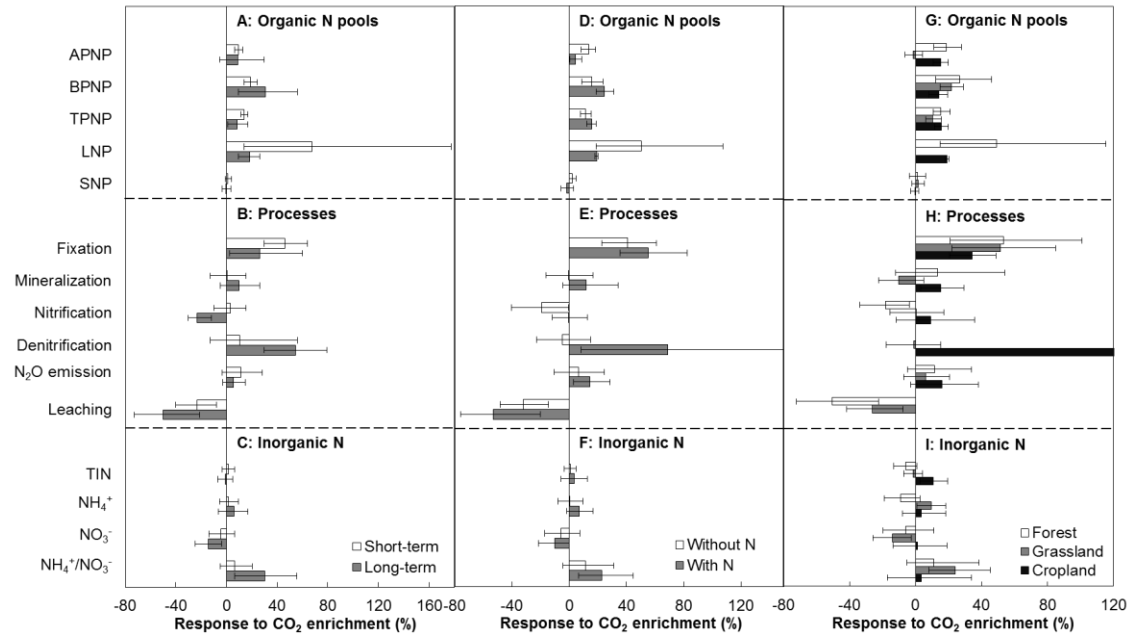

Figure 3.4. Responses of terrestrial nitrogen pools and processes to CO_2 enrichment (Mean ± 95% confidence interval) as regulated by experimental durations (A – C; short-term: ≤ 3 years vs. long-term: > 3 years), nitrogen addition (D – F), and ecosystem types (G – I). Please see Figure 1 for abbreviations.

Treatment time had no effect on most of the variables (overlapped 95% CIs for short- and long-term treatments) except nitrification, which was not changed by short-term treatment, but was significantly reduced (-23.4% with 95% CI from -30.4% to -12.1%) by long-term CO_2 enrichment (Fig. 3.4B). In addition, it seemed that the responses of the NH_4^+/NO_3^- ratio was strengthened over time, representing a neutral response to short-term CO_2 enrichment, but significantly positive and negative responses to long-term CO_2 enrichment (Fig. 3.4C). The effects of CO_2 enrichment were influenced by N addition (Fig. 3.4D – F). For example, nitrification was significantly reduced by CO_2 enrichment without N addition by 19.3% (with 95% CI from -40.5% to -0.65%), but was not changed with N addition. Denitrification and N_2O emission responded to CO_2 enrichment neutrally without N addition, but significantly positively with N addition

(Fig. 3.4E). Additionally, the responses of some variables to CO_2 enrichment were dependent on ecosystem type (Fig. 3.4G – I). APNP responded to CO_2 enrichment positively in forests and croplands, but neutrally in grasslands (Fig. 3.4G). Net mineralization had no response to CO_2 enrichment in forests or grasslands, while it was significantly increased in croplands (Fig. 3.4H). Moreover, the change in the TIN was neutral in forests, grassland, but positive, in croplands, respectively (Fig. 3.4I). In addition, a positive response of the NH_4^+/NO_3^- ratio was only observed in grasslands (Fig. 3.4I).

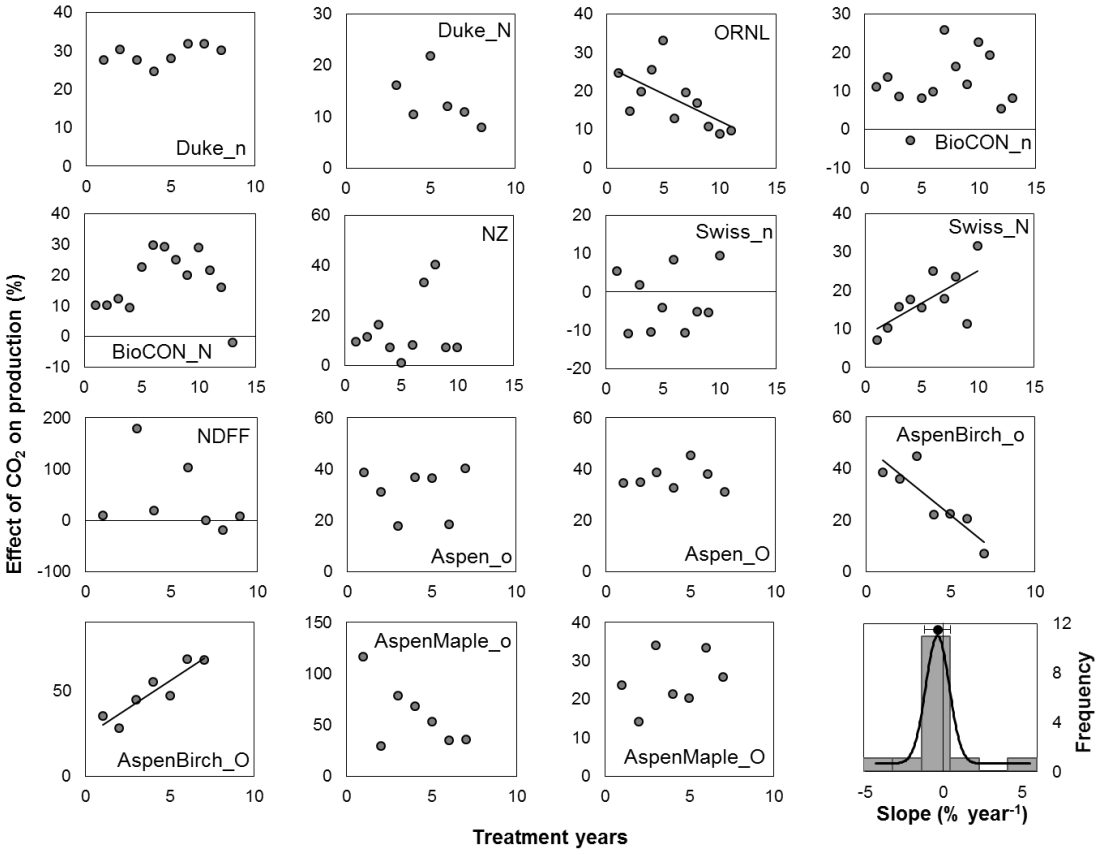

Figure 3.5. Time courses of CO_2 effects on ecosystem NPP (or biomass or leaf production) in decadal-long FACE experiments. Please see Table 1 for details of experiments, references and statistical results. Only statistically significant ($P < 0.05$) regression lines are shown. The panel at the right-low corner shows the distribution of the slopes (-0.37% year^{-1} with 95% CI from -1.84% year^{-1} to 1.09% year^{-1}).

The results from the second dataset showed that CO_2 enrichment significantly increased plant growth in most of the decadal FACE experiments (Fig. 3.5). In addition, the CO_2 fertilization effect on plant growth did not over treatment time change in 11 experiments ($P > 0.05$), decreased in 2 experiments (slope < 0, $P < 0.05$), and increased in 2 experiments (slope > 0, $P < 0.05$), respectively (Table 3.1, Fig. 3.5). Overall, the slope of the response of the plant growth vs. treatment time was not significantly different from 0 (i.e., -0.37% $year^{-1}$ with 95% CI from -1.84% $year^{-1}$ to 1.09% $year^{-1}$; Fig. 3.5).

Table 3.1. Results on the effect of CO_2 enrichment on ecosystem NPP (or biomass or leaf production) in decadal-long free air CO_2 enrichment (FACE) experiments over treatment time.

Experiment	Ecosystem type	Treatment years	Variable	Slope^	R^2	P
Duke_n	Forest	8	NPP	0.50	0.25	0.21
Duke_N	Forest	8	NPP	-1.39	0.27	0.29
ORNL	Forest	11	NPP	-1.42	0.38	**0.04**
BioCON_n*	Grassland	13	Biomass	0.42	0.05	0.48
BioCON_N*	Grassland	13	Biomass	0.23	0.01	0.76
NZ	Grassland	10	Biomass	0.95	0.05	0.53
Swiss_n*	Grassland	10	Biomass	0.30	0.01	0.75
Swiss_N*	Grassland	10	Biomass	1.66	0.47	**0.03**
NDFF	Desert	9	Biomass	-9.54	0.15	0.40
Aspen_o*	Forest	7	Leaf production	-0.07	0.00	0.97
Aspen_O*	Forest	7	Leaf production	0.09	0.00	0.93
AspenBirch_o*	Forest	7	Leaf production	-5.27	0.77	**0.01**
AspenBirch_O*	Forest	7	Leaf production	6.48	0.82	**0.00**
AspenMaple_o*	Forest	7	Leaf production	-9.16	0.40	0.13
AspenMaple_O*	Forest	7	Leaf production	1.11	0.11	0.46

^The values of the slope, R^2 and P in the linear regression in **Fig. 3.5** are shown.
*The lower and upper n (i.e., n and N) mean without and with N addition, respectively. The lower and upper o (i.e., o and O) mean without and with O_3 treatment, respectively.

3.4 Discussion

In this study, I carried out two syntheses on the responses of the terrestrial N cycle and plant growth to CO_2 enrichment to test whether PNL generally occurs across ecosystems.

3.4.1 PNL alleviation.

According to the PNL hypothesis, a prerequisite for PNL occurrence is that more N is sequestered in plant, litter and SOM (Luo *et al.*, 2004). The results showed that elevated CO_2 significantly increased N retention in plant tissues and litter, which is consistent with previous meta-analyses (de Graaff *et al.*, 2006, Luo *et al.*, 2006). Thus, there seems to be evidence for some basic assumptions of the PNL hypothesis. However, the results from the second dataset did not show a general diminished CO_2 fertilization effect on plant growth on the decadal scale, which disagrees with the expectation of the PNL hypothesis, suggesting that N supply under elevated CO_2 may meet the N demand. In this study, I have identified two processes that increase N supply under elevated CO_2, i.e., biological N fixation and leaching.

CO_2 enrichment significantly enhanced the N influx to terrestrial ecosystems through biological N fixation, which reduces dinitrogen (N_2) to NH_4^+ (Fig. 3.2B). The enhanced biological N fixation may have resulted from the stimulated activities of symbiotic (Fig. 3.3B) and free-living heterotrophic N-fixing bacteria (Hoque *et al.*, 2001). In addition, the competition between N_2-fixing and non-N_2-fixing species may have contributed to enhance the biological N fixation at the ecosystem level (Poorter & Navas, 2003, Batterman *et al.*, 2013).

In addition, the N efflux via leaching was reduced under elevated CO_2 conditions (Fig. 3.2B). This could be attributed to the decrease in NO_3^-, which is the primary N form in leaching (Chapin III *et al.*, 2011), and the increased root growth which may immobilize more inorganic N in soils (Luo *et al.*, 2006, Iversen, 2010). In contrast, gaseous N loss through N_2O emission increased under elevated CO_2, although this increase was only observed when additional N was applied.

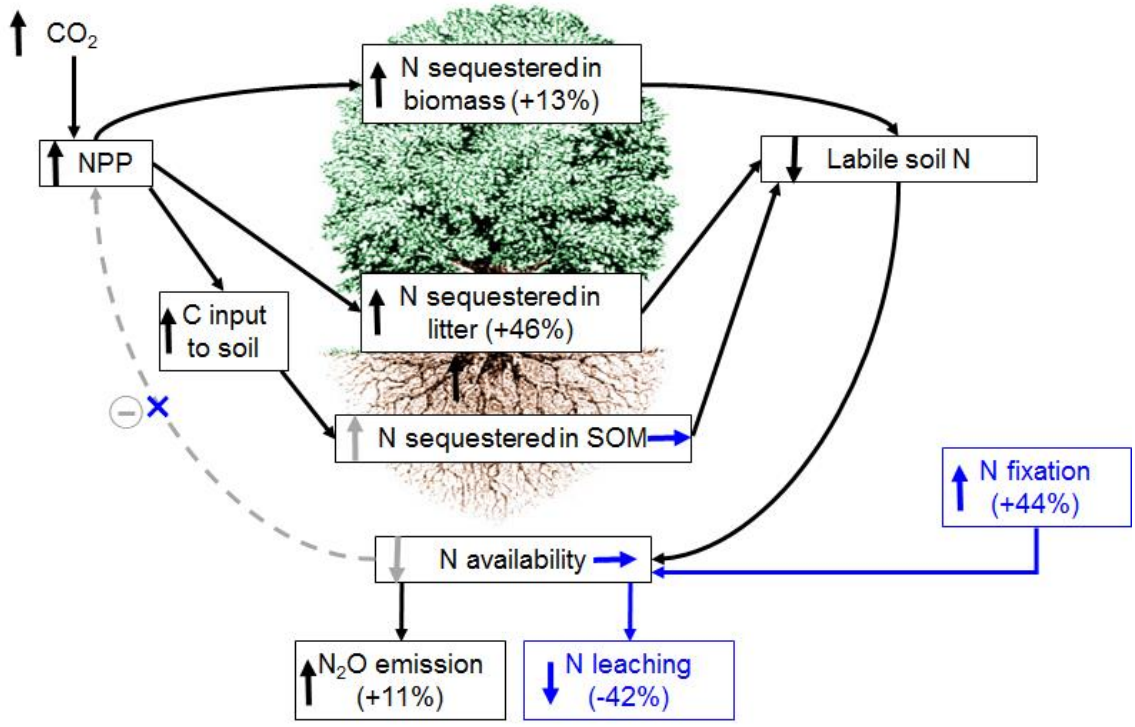

Figure 3.6. Mechanisms that alleviate PNL. PNL hypothesis posits that the stimulated plant growth by CO_2 enrichment leads to more N sequestered in long-lived plant tissues, litter and soil organic matter (SOM) so that, the N availability for plant growth progressively declines over time, and plant growth is downregulated (grey symbols). The current synthesis indicates that the basis of PNL occurrence partially exists (i.e., more N sequestered in plant tissues and litter; black symbols). Despite of the increases in plant N sequestration and N_2O emission, stimulated biological N fixation and reduced N leaching can replenish the N availability, potentially alleviating PNL (blue boxes and arrows). Upward, downward, and horizontal arrows mean increase, decrease, and no change, respectively.

The net effect of the responses of N processes to CO_2 enrichment resulted in higher N retention in ecosystems, especially within plant tissues and litter. Because the product of biological N fixation (i.e., NH_4^+) and the primary form for N leaching loss (i.e., NO_3^-) can be directly used by plants, the effects of CO_2 enrichment on the two processes directly increase the N availability for plant growth, potentially alleviating PNL (Fig. 3.6). The increased N in plant tissues can be re-used by plants via resorption (Norby *et al.*, 2000, Norby *et al.*, 2001), and consequently reduce the N demand from soils. This may be another mechanism that alleviates PNL (Walker *et al.*, 2015). Therefore, the increased N availability from increased N fixation and reduced N leaching could potentially support net accumulation of organic matter in terrestrial ecosystems (Rastetter *et al.*, 1997, Luo & Reynolds, 1999).

Since biological N fixation provides at least 30% of the N requirement across natural biomes (Asner *et al.*, 2001, Galloway *et al.*, 2004), the results suggest that the positive response of biological N fixation to CO_2 enrichment plays an important role in alleviating PNL. The PNL hypothesis was proposed to characterize long-term dynamics of C-N coupling in response to rising atmospheric CO_2 concentration. Thus, it is critical to understand the long-term response of biological N fixation to elevated CO_2. In this paper, I have synthesized 12 studies that lasted 4 – 7 years and binned them in a long-term category (> 3 years). On average, in those long-term studies, CO_2 enrichment increased biological N fixation by 26.2%. The increased biological N fixation is supported by evidence at gene level from long-term experiments. For example, Tu *et al.* (2015) found that the abundance of *nif*H gene amplicons, which is a widely used marker for analyzing biological N fixation, was significantly enhanced by 12 years of CO_2

enrichment in a grassland (BioCON). However, the synthesis showed a relatively wide 95% confidence interval from 2.54% to 59.8%. The wide range can be partially attributed to the relatively small number of studies. In addition, most studies incorporated in the current synthesis were conducted in temperate regions. Thus, longer-term studies, as well as studies in other regions (e.g., boreal and tropical) are critically needed to reveal more general patterns in the future.

In this study, it is suggested that the general trend of the N cycle changes under elevated CO_2 converges towards increased soil N supply for plant growth, which in theory could alleviate PNL. However, the PNL alleviation potential may vary across different ecosystems due to asymmetric distributions of biological N fixation (Cleveland *et al.*, 1999). In addition, PNL alleviation may also be influenced by other factors. While a diminished CO_2 fertilization effect on plant growth was not observed in most of the long-term experiments, it occurred in two sites (i.e., ORNL and Aspen-Birch) (Fig. 3.5). Plant growth is usually influenced by multiple environmental factors (e.g., nutrients, water, light, ozone). The undiminished CO_2 fertilization effect in most studies indicates that resource limitation (including N) was not aggravated, suggesting that no PNL occurred in these sites. However, in the ORNL and Aspen-Birch (without O_3 treatment) experiments, the diminished CO_2 fertilization effect on plant growth was potentially driven by limitation of N, or other resources, or their combined effect. For example, reduced N availability has been identified as one of the primary factors that lead to the diminished CO_2 fertilization effect on NPP in the ORNL FACE experiment (Norby *et al.*, 2010). In the Aspen-Birch community, however, the deceleration of leaf area increases due to canopy closure was responsible for the diminished CO_2

fertilization effect on plant growth without O_3 addition (Talhelm *et al.*, 2012). With O_3 addition, O_3 significantly reduced the canopy development, resulting in a relatively open canopy during the experiment period. In addition, the negative effect of O_3 addition increased over time, leading to the apparent increase in the CO_2 fertilization effect (Fig. 3.5) (Talhelm *et al.*, 2012).

3.4.2 Dependence of the responses of N cycling processes upon methodology, treatment duration, N addition and ecosystem types.

Experimental methodology may potentially influence findings. Cabrerizo *et al.* (2001) found that CO_2 enrichment increased the nitrogenase activity measured by acetylene reduction assay (ARA), but not the specific N fixation measured by the H_2 evolution method. In the studies synthesized here, four methods were used to estimate biological N fixation, including isotope, ARA, H_2 evolution and N accumulation. Among them, ARA and H_2 evolution measure nitrogenase activity (Hunt & Layzell, 1993) whereas isotope and N accumulation methods directly measure biological N fixation. All but the H_2 evolution method showed a significantly positive response to CO_2 enrichment (Fig. 3.3A). The insignificant response shown by the H_2 evolution method was likely because of the small study numbers (i.e., 3). In addition, the biological N fixation measured by ARA, isotope and N accumulation showed similar response magnitudes (Fig. 3.3A), suggesting consistency among the three methods. However, further assessment on the H_2 evolution method is needed.

The responses of some N cycling processes that affect N availability are dependent on treatment duration, N addition, and/or ecosystem types (Fig. 3.4). N mineralization,

in addition to biological N fixation, is a major source of available N in soils. The meta-analysis showed no change in the net N mineralization in response to CO_2 enrichment, which is consistent with the results by de Graaff et al. (2006). However, the response of net mineralization was dependent upon ecosystem types, showing no change in forests and grasslands, but significant increases in croplands (Fig. 3.4H). There may be two reasons for the stimulated net mineralization in croplands. First, N fertilization, which is commonly practiced in croplands, can increase the substrate quantity and quality for mineralization (Barrios *et al.*, 1996, Booth *et al.*, 2005, Chapin III *et al.*, 2011, Lu *et al.*, 2011, Reich & Hobbie, 2013). Second, tillage can alter soil conditions (e.g., increasing O_2 content), which can potentially favor the N mineralization under enriched CO_2 (Wienhold & Halvorson, 1999, Bardgett & Wardle, 2010). These findings suggest that CO_2 enrichment can stimulate the N transfer from organic to inorganic forms in managed croplands.

Unlike leaching, the response of nitrification was dependent upon treatment duration (Fig. 3.4). Nitrification was not changed by short-term treatment, but was significantly reduced by long-term CO_2 enrichment (Fig. 3.4). One possible reason for the reduced nitrification with long-term CO_2 enrichment is the cumulative effect of hydrological changes. CO_2 enrichment is assumed to reduce stomatal conductance and, consequently, water loss via plant transpiration, leading to an increase in soil water content (Niklaus *et al.*, 1998, Tricker *et al.*, 2009, van Groenigen *et al.*, 2011, Keenan *et al.*, 2013). A synthesis by van Groenigen et al. (2011) shows that CO_2 enrichment increases soil water content by 2.6% −10.6%. Increased soil water content may result in less oxygen (O_2) concentration in soils, which could potentially constrain nitrification.

In addition, the response of gaseous N loss was dependent on N addition (Fig. 3.4). The reduced nitrification was only observed under conditions without N addition (Fig. 3.4E). With N addition, no response of nitrification to CO_2 enrichment was observed (Fig. 3.4E). Additionally, the response of denitrification to CO_2 enrichment shifted from neutral, without N addition, to significantly positive with N addition (Fig. 3.4E). One possible reason is that N addition provides more N substrate for nitrifying and denitrifying bacteria (Keller *et al.*, 1988, Stehfest & Bouwman, 2006, Russow *et al.*, 2008). The strengthening trends of both nitrification and denitrification led to a shift of the response of N_2O emission to CO_2 enrichment from neutral without N addition to significantly positive with N addition (Fig. 3.4E). The results indicate that CO_2 enrichment significantly increases gaseous N loss when additional N is applied. This is consistent with a previous synthesis (van Groenigen *et al.*, 2011). Increased N_2O emissions can partially offset the mitigation of climate change by the stimulated plant CO_2 assimilation as the warming potential of N_2O is 296 times that of CO_2. However, a recent modeling study by Zaehle *et al.* (2011) found an opposite result showing that CO_2 enrichment reduced emissions of N_2O. In their model, elevated CO_2 enhanced plant N sequestration and consequently, decreased the N availability for nitrification and denitrification in soils, which led to the reduced N_2O emissions. However, the synthesis shows that inorganic N does not decrease. Especially with additional N application, enhanced denitrification by CO_2 enrichment results in a greater N_2O emission.

3.4.3 Changes in soil microenvironment, community structures and above-belowground interactions.

The meta-analysis showed that the two major forms of soil available N, NH_4^+ and NO_3^-, responded to long-term CO_2 enrichment in opposing manners (Fig. 3.4C). While the enhanced biological N fixation by CO_2 enrichment tended to increase the NH_4^+ content in soils, the reduced nitrification decreased the NO_3^- content in soils, leading to a significant increase in the NH_4^+/NO_3^- ratio (Fig. 3.4C).

Although the total available N did not change under elevated CO_2, the altered proportion of NH_4^+ over NO_3^- in soils may have long-term effects on soil microenvironment and associated aboveground-belowground linkages that control the C cycle (Bardgett & Wardle, 2010). On the one hand, plants would release more hydrogen ion (H^+) to regulate the charge balance when taking up more NH_4^+. As a result, the increased NH_4^+ absorption could acidify the rhizosphere soil (Thomson *et al.*, 1993, Monsant *et al.*, 2008). The lowered pH could have significant effects on soil microbial communities and their associated ecosystem functions. For example, fungal/bacterial ratio increases with the decrease in pH (de Vries *et al.*, 2006, Rousk *et al.*, 2009). The increased fungal/bacterial ratio may result in lower N mineralization because of the higher C/N ratio of fungi and the lower turnover rates of fungal-feeding fauna (de Vries *et al.*, 2006, Rousk & Bååth, 2007). In other words, the increased fungal/bacterial ratio may slow down the N turnover from organic to inorganic forms. On the other hand, the increased NH_4^+/NO_3^- ratio may increase the N use efficiency because it is more energetically expensive for plants to utilize NO_3^- than NH_4^+ (Odum & Barrett, 2005, Lambers *et al.*, 2008, Chapin III *et al.*, 2011). In addition, since the preferences for plant

absorption of different forms of N are different (Odum & Barrett, 2005, Chapin III *et al.*, 2011), the increased NH_4^+/NO_3^- ratio may benefit some plant species while depress others, and consequently alter the community structures over time. These diverse changes in soil microenvironment and microbial and plant community compositions could further affect the terrestrial C cycle on long temporal scales, on which more studies are needed.

3.4.4 Summary.

This chapter synthesizes data in the literature on the effects of CO_2 enrichment on the terrestrial N cycle to improve the understanding of the N limitation to plant growth under elevated CO_2. The results indicate that elevated CO_2 stimulates N influx via biological N fixation but reduces N loss via leaching, leading to increased N supply for plant growth. The additional N supply via the enhanced biological N fixation and the reduced leaching may partially meet the increased N demand under elevated CO_2, potentially alleviating PNL. In addition, the analysis indicates that increased N_2O emissions may partially offset the mitigation of climate change by stimulated plant CO_2 assimilation. Moreover, changes in soil microenvironments, ecosystem communities and above-belowground interactions induced by the different responses of NH_4^+ and NO_3^- to CO_2 enrichment may have long-term effects on the terrestrial biogeochemical cycles and climate change.

Chapter 4: Methods for estimating temperature sensitivity of soil organic matter based on incubation data: A comparative evaluation

Abstract: Although the temperature sensitivity (Q_{10}) of soil organic matter (SOM) decomposition has been widely studied, the estimate substantially depends on the methods used with specific assumptions. Here I compared several commonly used methods (i.e., one-pool (1P) model, two-discrete-pool (2P) model, three-discrete-pool (3P) model, and time-for-substrate (T4S) Q_{10} method) plus a new and more process-oriented approach for estimating Q_{10} of SOM decomposition from laboratory incubation data to evaluate the influences of the different methods and assumptions on Q_{10} estimation. The process-oriented approach is a three-transfer-pool (3PX) model that resembles the decomposition sub-model commonly used in Earth system models. The temperature sensitivity and other parameters in the models were estimated from the cumulative CO_2 emission using the Bayesian Markov Chain Monte Carlo (MCMC) technique. The estimated Q_{10}s generally increased with the soil recalcitrance, but decreased with the incubation temperature increase. The results indicated that the 1P model did not adequately simulate the dynamics of SOM decomposition and thus was not adequate for the Q_{10} estimation. All the multi-pool models fitted the soil incubation data well. The Akaike information criterion (*AIC*) analysis suggested that the 2P model is the most parsimonious. As the incubation progressed, Q_{10} estimated by the 3PX model was smaller than those by the 2P and 3P models because the continuous C transfers from the slow and passive pools to the active pool were included in the 3PX model. Although the T4S method could estimate the Q_{10} of labile carbon appropriately, the analyses showed that it overestimated that of recalcitrant SOM. The similar structure of 3PX model with the decomposition sub-model of Earth system models

provides a possible approach, via the data assimilation techniques, to incorporate results from numerous incubation experiments into Earth system models.

4.1 Introduction

Soil organic matter (SOM) is the largest carbon (C) pool in terrestrial ecosystems (Schlesinger, 1995). As a biochemical process, the decomposition of SOM is sensitive to increased temperature (Luo *et al.*, 2001, Fang *et al.*, 2005, Davidson & Janssens, 2006), and consequently has critical impacts on global C cycle and climate change (Cox *et al.*, 2000, Schlesinger & Andrews, 2000). However, SOM consists of many components with different kinetic properties (Davidson & Janssens, 2006), leading to large uncertainty in predicted soil C storage under future climate change (Friedlingstein *et al.*, 2006). Therefore, there is an increasing concern on how temperature sensitivity (expressed as Q_{10}, which measures the change in decay rates for a 10 K warming) depends on the SOM compounds and C qualities (Fang *et al.*, 2005, Conant *et al.*, 2008, Xu *et al.*, 2012). However, the Q_{10} estimation substantially relies on the methods used, which usually have their respective assumptions, leading to contradictory conclusions (Liski *et al.*, 1999, Fang *et al.*, 2005, Rey & Jarvis, 2006, Conant *et al.*, 2008). To better understand the warming impacts on SOM decomposition, it is important to evaluate these methods and the underlying assumptions.

The direct calculation at specific incubation time has been used to estimate the Q_{10} of SOM decomposition based on incubation data using an equation $\left(\frac{R_2}{R_1}\right)^{\frac{10}{T_2-T_1}}$, where T_1 and T_2 are the incubation temperatures, and R_1 and R_2 are the CO_2 emission rates at T_1 and T_2, respectively (Rey & Jarvis, 2006). The estimate is usually an apparent Q_{10} and

likely underestimates the temperature sensitivity after the initial incubation stage because greater decomposition results in less substrate at high than low temperatures at the same point of incubation time. To resolve this issue, a method that estimates the apparent Q_{10} by comparing the times for respiring a given amount of C at different temperatures (called the time-for-substrate Q_{10}) has been developed (Rey & Jarvis, 2006, Conant *et al.*, 2008). One important assumption of this method is that a given amount of respired CO_2 is from similar fractions of SOM when the substrates are at the same level at different temperatures (Conant *et al.*, 2008).

In addition, first-order kinetic models have also been used to estimate the Q_{10} (Kätterer *et al.*, 1998, Rey & Jarvis, 2006). In these models, the soil is usually treated as one or several discrete fractions (or pools) based on the turnover times (Kätterer *et al.*, 1998, Rey & Jarvis, 2006). Through these models, the intrinsic Q_{10} (defined as the temperature sensitivity of individual C pools with similar turnover time) for each pool can be derived (Rey & Jarvis, 2006). Generally, the multi-pool models fit the incubation data very well (Kätterer *et al.*, 1998, Rey & Jarvis, 2006). However, these models do not include C transfers across pools which occur in natural ecosystems (Rovira & Vallejo, 2002, Cheng *et al.*, 2007). On the other hand, although three conceptual pools with C transfers among them have been widely used to describe SOM dynamics in Earth system models (Parton *et al.*, 1987, Jenkinson, 1990, Luo *et al.*, 2003), the three-transfer-pool model has never been used, to my knowledge, to estimate temperature sensitivity of SOM decomposition from soil incubation data. Moreover, although a large amount of experimental studies have been conducted and have improved our understanding of the temperature sensitivity of SOM decomposition, the Q_{10} is usually

set to be one single value (usually around 2) in Earth system models. It is imperative to find ways to use results from numerous incubation experiments to improve these models.

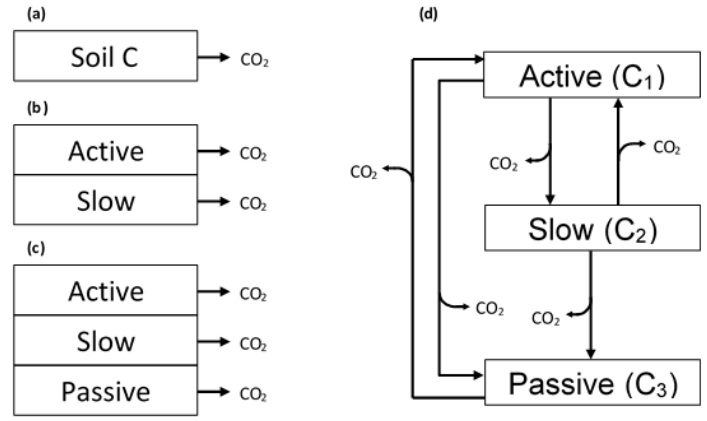

Figure 4.1. Model structures of one-pool (a), two-discrete-pool (b), three-discrete-pool (c), and three-transfer-pool (d) models.

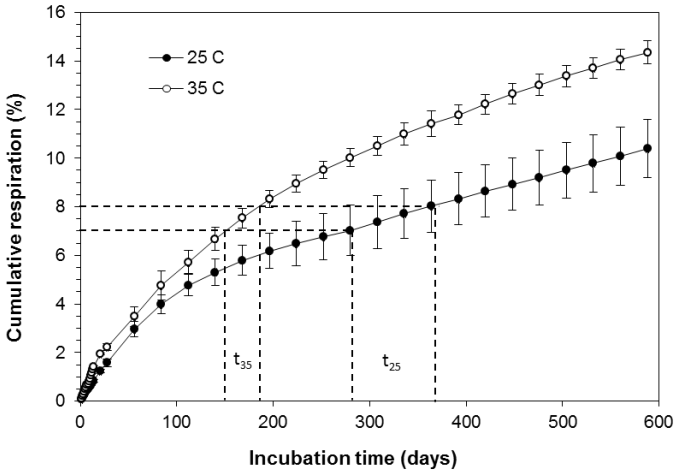

Figure 4.2. An example of the calculation of the time-for-substrate Q_{10} at 25 °C which is determined by comparing the times required to decompose a given amount of carbon at specific substrate levels at different incubation temperatures ($Q_{10} = t_{25}/t_{35}$)

In this study, I developed a new three-transfer-pool (3PX) model to resemble the model structure of soil carbon dynamics in Earth system models for estimating Q_{10} of

SOM decomposition. Then I compared four widely used methods: one-pool (1P) model (Fig. 4.1a), two-discrete-pool (2P) model (Fig. 4.1b), three-discrete-pool (3P) model (Fig. 4.1c), and time-for-substrate (T4S) (Fig. 4.2) with the 3PX model (Fig. 4.1d) for Q_{10} estimation using the same data set from a laboratory soil incubation experiment. Parameters of these models were estimated using the Bayesian Markov Chain Monte Carlo (MCMC) technique, which has recently been used to improve parameterization of ecological models (Xu *et al.*, 2006, Gaucherel *et al.*, 2008, Luo *et al.*, 2011, Ahrens *et al.*, 2014). In these models, the intrinsic Q_{10} for each pool was estimated directly through fitting the CO_2 emission data and the apparent Q_{10} was calculated from the estimated intrinsic Q_{10}, pool size and decay rate of each pool. The T4S method estimates temperature sensitivity by comparing the times for decomposing a given amount of C at different temperatures (Fig. 4.2) (Conant *et al.*, 2008, Xu *et al.*, 2010, Haddix *et al.*, 2011).

4.2 Materials and Methods

4.2.1 Soil incubation data.

The data used here were from a published paper by Haddix *et al*. (2011). The soil incubation data collected from a native grassland in Indian Head, Saskatchewan, Canada (50.533°N, 103.517°W). The mean annual temperature and precipitation are 2 °C and 421 mm, respectively. Information about soil sampling and incubation was described in detail in Haddix *et al*. (2011). Briefly, samples were collected from three separated locations that were several meters apart (field replicate n = 3). Surface litter and aboveground vegetation were cleared away before sampling and soil from 0 to 20

cm was collected. In the laboratory, rocks, surface litter and root materials were removed. The soil was homogenized and passed a 2-mm sieve before incubation. Then the soil samples were incubated at 15, 25, and 35 °C for 588 days (laboratory replicate *n* = 4). CO_2 emission rates were measured daily during the first 2 weeks of incubation, weekly for the next 2 weeks, and every 4 weeks thereafter. Overall, there were 36 sampling times over the 588-day incubation period. Data at all the 15, 25 and 35 °C were used in this study to evaluate various methods as described below.

4.2.2 Model description.

Generally, first-order discrete-pool models have similar structure described in Eq. 1 (Stanford & Smith, 1972, Andrén & Paustian, 1987, Kätterer *et al.*, 1998, Rey & Jarvis, 2006, Li *et al.*, 2013, Schädel *et al.*, 2013):

$$C_{cum} = \sum_{i=1}^{n} f_i C_{tot}(1 - e^{-k_i t}) \qquad (1)$$

where C_{cum} is the cumulative CO_2-C emission at time t (mg C g^{-1} soil), C_{tot} is the initial soil C content (mg C g^{-1} soil), f_i and k_i are the initial fraction and decay rate of the ith pool. The sum of f_is is 1. The only difference of these models is the number of pools (Fig. 4.1a, b, c). It is generally assumed that the initial fractions of pools are not affected by incubation temperature (Rey & Jarvis, 2006). Hence, I fitted each of the models with the data at all the three temperatures simultaneously using the data assimilation method described below, and the f_is were set to be independent of incubation temperature.

In addition to the discrete-pool models described above, a three-pool model with transfers among soil pools was developed. The basic concept was derived from the

CENTURY and TECO model (Parton *et al.*, 1987, Luo *et al.*, 2003). In the model, SOM dynamics are represented by the following first-order differential equation:

$$\frac{dC(t)}{dt} = AKC(t) \qquad (2)$$

where *A* and *K* are matrices given by

$$A = \begin{pmatrix} -1 & f_{1,2} & f_{1,3} \\ f_{2,1} & -1 & 0 \\ f_{3,1} & f_{3,2} & -1 \end{pmatrix}$$

$$K = diag(k) = \begin{pmatrix} k_1 & 0 & 0 \\ 0 & k_2 & 0 \\ 0 & 0 & k_3 \end{pmatrix}$$

and $C(t) = (C_1(t)\ C_2(t)\ C_3(t))^T$ is a 3 × 1 vector describing soil C pool sizes (Fig. 4.1d).

Matrix *A* is C transfers between individual C pools as described by the arrows in Fig. 4.1d. The elements ($f_{i,j}$) are C transfer coefficients, representing the fractions of the C entering *i*th (row) pool from *j*th (column) pool. *K* is a 3 × 3 diagonal matrix representing decay rates (the amounts of C per unit mass leaving each of the pools per day). As in the above models, those parameters in the 3PX model were also estimated using the data assimilation approach below.

4.2.3 Data assimilation.

We used probabilistic inversion approach described in Xu *et al.* (2006) and Weng and Luo (2011) to estimate parameters in those models from the soil incubation data. The approach is based on Bayes' theorem:

$$P(\theta|Z) \propto P(Z|\theta)P(\theta) \qquad (3)$$

with which the posterior probability density function (PDF) $P(\theta|Z)$ of model parameters (θ) can be obtained from the prior knowledge of parameters represented by a prior PDF

$P(\theta)$ and the information in the soil incubation data represented by a likelihood function $P(Z|\theta)$. The prior PDF were specified as the uniform distributions over specific parameter ranges. The likelihood function $P(Z|\theta)$ was calculated with the assumption that errors between observed and modeled values were independent from each other and followed a multivariate Gaussian distribution with a zero mean:

$$P(Z|\theta) \propto exp\left\{-\sum_{i=1}^{3}\sum_{t\in obs(Z_i)}\frac{[Z_i(t)-X_i(t)]^2}{2\sigma_i^2(t)}\right\} \qquad (4)$$

where $Z_i(t)$ and $X_i(t)$ are the observed and modeled cumulative respiration values, and $\sigma_i(t)$ is the standard deviation of measurements.

The probabilistic inversion was carried on using the Metropolis-Hastings (M-H) algorithm, which is a Markov Chain Monte Carlo (MCMC) technique (Metropolis *et al.*, 1953, Hastings, 1970), to construct posterior PDFs of parameters. Briefly, the M-H algorithm repeats two steps: a proposing step and a moving step (Xu *et al.*, 2006). In the proposing step, a new point θ^{new} is generated based on the previously accepted point θ^{old} with a proposal distribution $P(\theta^{new}|\theta^{old})$:

$$\theta^{new} = \theta^{old} + d(\theta_{max} - \theta_{min})/D \qquad (5)$$

where θ_{max} and θ_{min} are the maximum and minimum values in the prior range of the given parameter, d is a random variable between -0.5 and 0.5 with a uniform distribution, and D is used to control the proposing step size and was set to 10 in the current study. In the moving step, the new point θ^{new} is tested against the Metropolis criterion (Xu *et al.*, 2006) to examine if it should be accepted or rejected. Because the initial accepted samples are in the burn-in period (Gelman & Rubin, 1992), the first half of accepted samples were discarded and only the rest were used to generate posterior

PDFs. The M-H algorithm was formally run 5 replicates and 500,000 times for each replicate for statistical analysis of the parameters.

It is guaranteed for the Markov chain generated by the M-H algorithm to converge to a unique stationary distribution. In the current study, the convergence of the sampling chains was tested by the Gelman-Rubin (*G-R*) diagnostic method to ensure that the within-run variation (W_i, Eq. 6) is roughly equal to the between-run variation (B_i, Eq. 7) (Gelman & Rubin, 1992).

$$W_i = \frac{1}{K}\sum_{k=1}^{K} {\sigma_k}^2 \qquad (6)$$

$$B_i = \frac{N}{K-1}\sum_{k=1}^{K}\left(\overline{p}^{\cdot,k} - \overline{p}^{\cdot,\cdot}\right)^2 \qquad (7)$$

where K is the number of replicates, N is the number of accepted iterations after burn-in period, $\overline{p}^{\cdot,k}$ and σ_k are the mean and standard deviation of the specific parameter in the kth replicate, and $\overline{p}^{\cdot,\cdot}$ is the mean of the specific parameter over the five replicates. When the Markov chain reaches convergence, the GR_i (Eq. 8) is equal to one.

$$GR_i = \sqrt{\frac{W_i(N-1)/N + B_i/N}{W_i}} \qquad (8)$$

In this study, *GR*s of all the parameters of all the models were approximately one (Table 4.1).

Table 4.1. Gelman-Rubin statistics of parameters in the one-pool (1P), two-discrete-pool (2P), three-discrete-pool (3P) and three-transfer-pool (3PX) models

	G-R statistics			
Parameters*	1P	2P	3P	3PX
f_1	-	1.0	1.0	1.0
f_2	-	-	1.0	1.0
k_1	1.0	1.0	1.0	1.0
k_2	-	1.0	1.0	1.0
k_3	-	-	1.0	1.0
Q_{10a}_15	1.0	1.0	1.0	1.0
Q_{10s}_15	-	1.0	1.0	1.0
Q_{10p}_15	-	-	1.0	1.0
Q_{10a}_25	1.0	1.0	1.0	1.0
Q_{10s}_25	-	1.0	1.0	1.0
Q_{10p}_25	-	-	1.0	1.0
$f_{2,1}$	-	-	-	1.0
$f_{3,1}$	-	-	-	1.0
$f_{1,2}$	-	-	-	1.0
$f_{3,2}$	-	-	-	1.0
$f_{1,3}$	-	-	-	1.0

*f_1 and f_2 are the initial fractions of active and slow pools; k_1, k_2 and k_3 are the decay rates of individual pools at 25 °C; Q_{10a}_15, Q_{10s}_15 and Q_{10p}_15 are the temperature sensitivities at 15 °C of active, slow and passive pool respectively; Q_{10a}_25, Q_{10s}_25 and Q_{10p}_25 are the temperature sensitivities at 25 °C of active, slow and passive pool respectively; $f_{2,1}$ and $f_{3,1}$ are the fractions of C entering, respectively, the slow and passive pools from the fast pool; $f_{1,2}$ and $f_{3,2}$ are the fractions of C entering, respectively, the fast and passive pools from the slow pool; $f_{1,3}$ is the fraction of C entering the fast pools from the passive pool in the 3PX model

4.2.4 Q_{10} calculations.

In this study, I estimated three types of temperature sensitivity (Q_{10}): Q_{10} of bulk soil, intrinsic Q_{10} for each of the SOM pools, and apparent Q_{10} at different times of soil incubation. Bulk soil Q_{10} at 15 °C was estimated by dividing CO_2 emission rate at 25 °C by the rate at 15 °C at the first incubation day with the assumption that soil compounds and microbial community were the same at the two temperatures. Similarly, the bulk soil Q_{10} at 25 °C was estimated by dividing CO_2 emission rate at 35 °C by the rate at 25 °C at the first incubation day.

Intrinsic Q_{10} of the *i*th pool was estimated using Eq. 9:

$$Q_{10}^{i} = \left(\frac{k_i(T_2)}{k_i(T_1)}\right)^{\frac{10}{T_2 - T_1}} \qquad (9)$$

where T_1 and T_2 are the incubation temperatures, $k_i(T_1)$ and $k_i(T_2)$ are the inherent decay rates of the *i*th pool at the incubation temperatures. In the current study, T_1 and T_2 are 15 and 25 ºC for the Q_{10} calculation at 15 °C, and are 25 and 35 ºC for the Q_{10} calculation at 25 °C. Consequently the intrinsic Q_{10} was calculated by $k_i(25)/k_i(15)$ and $k_i(35)/k_i(25)$ at 15 and 25 °C, respectively.

Apparent Q_{10} is dependent on the intrinsic Q_{10} and the size of each C pool in the soil. It was calculated using soil CO_2-C emission rate at T_2 divided by that at T_1 at specific substrate levels and fractions of SOM pools:

$$Q_{10}^{a} = \frac{\sum_{i=1}^{n} R_i(T_2)}{\sum_{i=1}^{n} R_i(T_1)} = \frac{\sum_{i=1}^{n}\left[k_i(T_2) \times C_i \times f_{c,i}\right]}{\sum_{i=1}^{n}\left[k_i(T_1) \times C_i \times f_{c,i}\right]} \qquad (10)$$

where k_i is the inherent decay rate of the *i*th pool at T_1 and T_2, C_i is the C content (pool size) of the *i*th pool, $f_{c,i}$ is the transfer coefficient from the *i*th pool to CO_2. $f_{c,i}$ is 1 in the discrete-pool models (i.e., all C comes from the *i*th pool becomes CO_2 as assumed), and is the difference between 1 and transfer coefficients from *i*th pool to the other two pools in the 3PX model (e.g., $f_{c,1} = 1 - f_{2,1} - f_{3,1}$). T_1 and T_2 are 15 and 25 ºC for the Q_{10} calculation at 15 °C, and are 25 and 35 ºC for the Q_{10} calculation at 25 °C.

Besides, T4S Q_{10} is comparing the times for decomposing a given amount of soil C at different temperatures (Fig. 4.2):

$$Q_{10} = t_{T_1}/t_{T_2} \qquad (11)$$

where t_{T_1} and t_{T_2} are the times required at T_1 and T_2, respectively. The Q_{10} values for labile and recalcitrant SOM were determined using times taken to respire the first and last 0.5% of initial soil C, respectively. T_1 and T_2 are 15 and 25 °C for the Q_{10} calculation at 15 °C, and are 25 and 35 °C for the Q_{10} calculation at 25 °C.

4.2.5 Akaike information criterion (AIC).

The goodness of fit relative to the number of model parameters was evaluated by *AIC* (Akaike, 1974, Burnham & Anderson, 2004):

$$AIC = a \ln\left(\frac{\sum(\hat{\epsilon}_i)^2}{n}\right) + 2b \qquad (12)$$

where a is the number of data points, $\hat{\epsilon}_i$ is the estimated residual of each data point, and b is the total number of estimated model parameters. The model with a smaller *AIC* value is more parsimonious (Saffron *et al.*, 2006).

4.3 Results

The estimated Q_{10}s from all the methods were greater at 15 °C than that at 25 °C (Table 4.2). The multi-pool models fitted the incubation data better than the single-pool model (Table 4.2; Fig. 4.3). Although all the multi-pool models described SOM dynamics adequately, the estimated parameters were different (Table 4.2). The estimated initial active pool size was greater in the 3PX model than that in the 2P and 3P models. Additionally, the decay rate of the slow pool was smaller in the 2P model than those in the 3P and 3PX models. The 1P model can only generate one Q_{10} at each of the temperatures of 15 and 25 °C. In the multi-pool models, the Q_{10} increased with

Table 4.2 Maximum likelihood estimates (MLEs) of parameters, P values, R^2 values and Akaike information criterion (AIC) values in the one-pool (1P), two-discrete-pool (2P), three-discrete-pool (3P) and three-transfer-pool (3PX) models simulated to the same soil incubation data. Please see Table S2 for the values of transfer coefficients in the 3PX model.

Model	Initial pool size (%)			Decay rate at 25 °C			Q_{10} at 15 °C			Q_{10} at 25 °C					
	Active	Slow	passive	Active (10^{-3})	Slow (10^{-4})	Passive (10^{-5})	Active	Slow	Passive	Active	Slow	passive	*P*	R^2	*AIC*
1P	-	-	-	0.22	-	-	1.64	-	-	1.43	-	-	< 0.001	0.955	-80.1
2P	5.76	-	-	8.68	0.74	-	2.06	4.52	-	1.25	2.11	-	< 0.001	0.999	-260.5
3P	4.65	14.53	-	9.75	3.79	1.37	2.12	3.07	3.53	1.22	1.76	2.67	< 0.001	0.999	-256.2
3PX	10.65	19.90	-	8.84	2.57	1.38	2.35	3.33	3.62	1.26	2.00	2.87	< 0.001	0.999	-241.3

SOM recalcitrance. Although the fit of all the multi-pool models were highly significant (all $P < 0.001$ and $R^2 > 0.99$), the 2P model had the lowest *AIC* value followed by the 3P model. The *AIC* value of the 3PX was larger than both of these but smaller than that of the 1P model (Table 4.2).

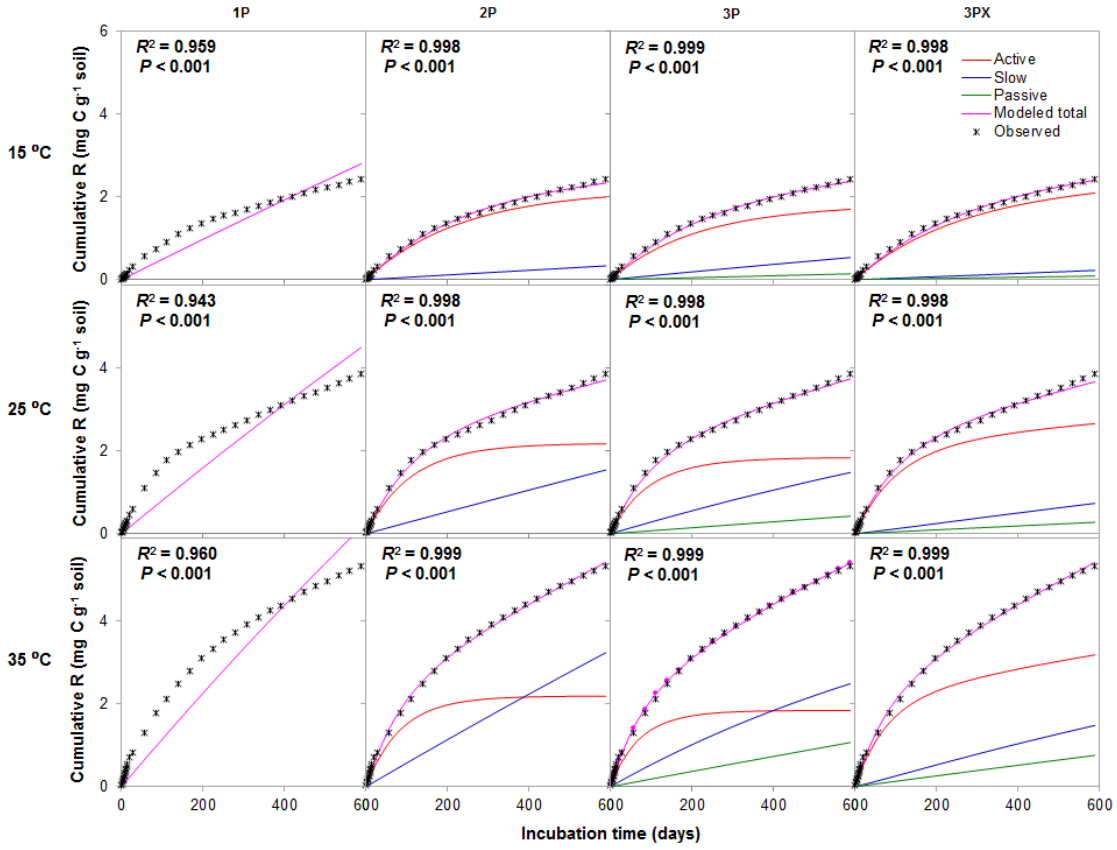

Figure 4.3. Observed and modeled cumulative CO_2 releases (R) from individual and total pools at all the three incubation temperatures (i.e., 15, 25, and 35 °C) in the one-pool (1P), two-discrete-pool (2P), three-discrete-pool (3P) and three-transfer-pool (3PX) models.

During the incubation period, the active pool size declined rapidly (Fig. 4.4). In all the multi-pool models, the remaining active C was more at higher than that at lower temperatures when the same amount of C was respired, especially in the late incubation period (Fig. 4.4). In addition, the modeled active pool size was smaller in the 2P and 3P

models than that in the 3PX model. In the meantime, the contribution of the active pool to CO_2 emission rate reduced quickly with the incubation progress, while the contributions of the slow and passive pools increased (Fig. 4.5). The modeled contributions of the active pool to CO_2 emission at all the incubation temperatures were greater in the 3PX model than those in the 2P and 3P models. Correspondingly, the modeled contributions of the slow and passive pools were smaller in the 3PX model over the incubation period (Fig. 4.5).

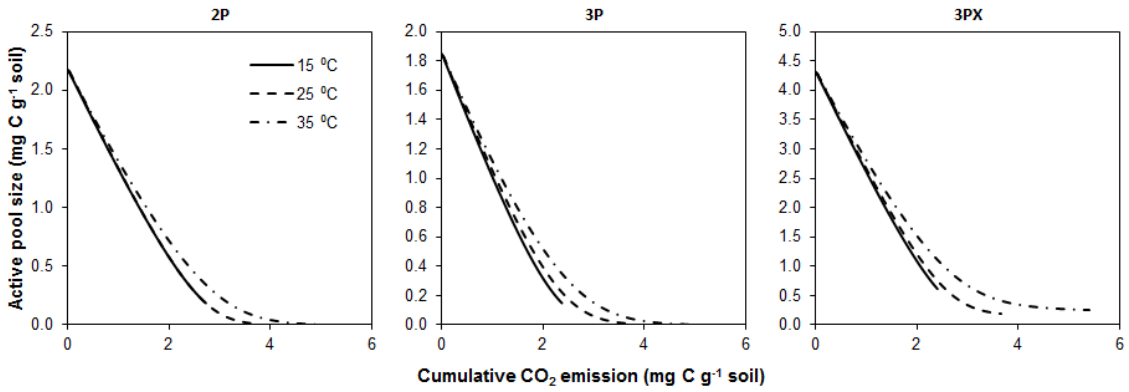

Figure 4.4. Simulated dynamics of active pool size against cumulative CO_2 emission at all the three incubation temperatures in the two-discrete-pool (2P), three-discrete-pool (3P) and three-transfer-pool (3PX) models.

Although the temperature sensitivity generally increased with the SOM recalcitrance (Table 4.1), the estimates were dependent on the methods used (Fig. 4.6). It seemed that the estimated Q_{10} of bulk soil from all the methods was within the 95% confidence range of the direct calculation at the first incubation day at 15 °C (Fig. 4.6a), while only the T4S method estimated the Q_{10} of bulk soil at 25 °C appropriately (Fig. 4.6c). In addition, the difference of the estimated Q_{10}s among these methods changed with the incubation progress (Fig. 4.6b, d). The only Q_{10} value estimated from the 1P model cannot represent the dynamics of temperature sensitivity with the change in SOM

compounds. The discrete-pool models generated higher apparent Q_{10} than the 3PX model at both 15 and 25 °C when the active pool size diminished as the SOM decomposition progressed (Fig. 4.6b, d). The estimated apparent Q_{10} of the recalcitrant SOM by the T4S calculation was significantly greater than those by all the models at the end of the incubation at 25 °C (Fig. 4.6d). In addition, the apparent Q_{10} decreased with the increased contribution of the active pool to CO_2 emission rate, and increased with the increase in the contributions of the slow and passive pools to CO_2 emission rate (Fig. 4.7).

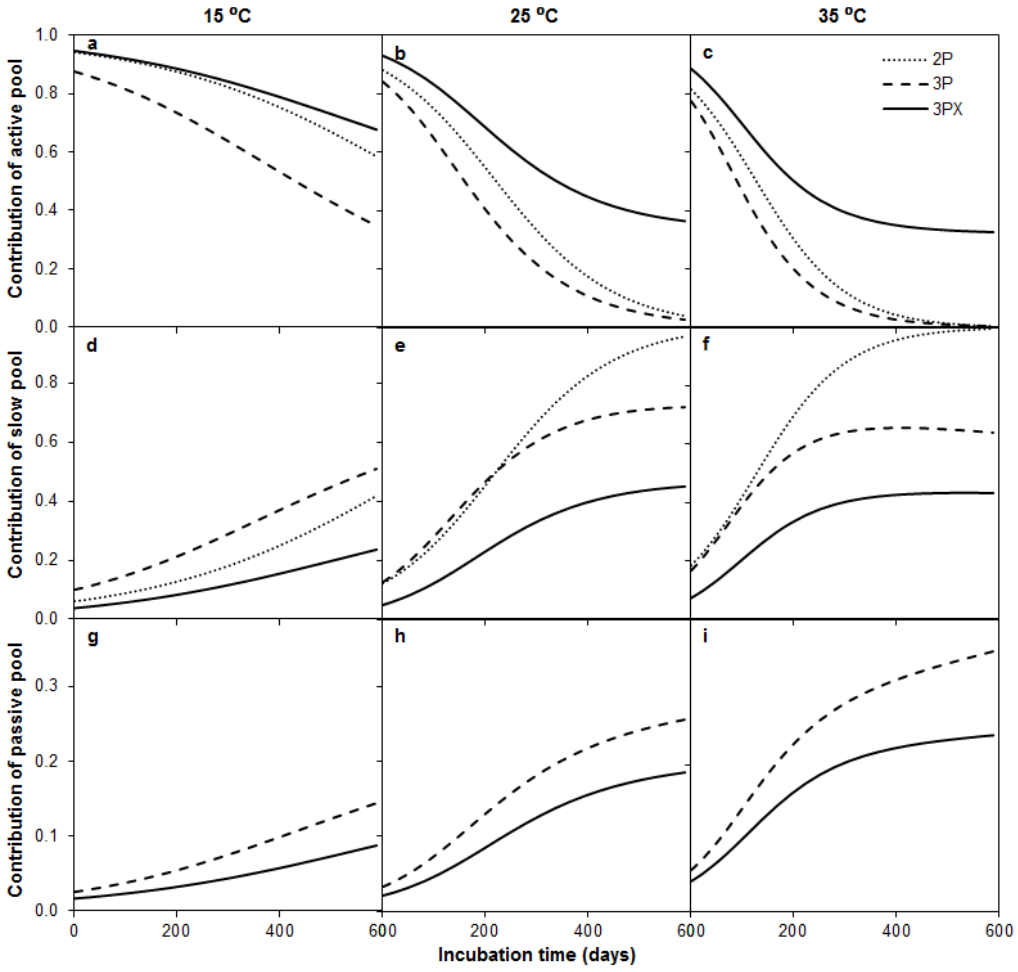

Figure 4.5. Simulated contributions of individual pools to CO_2 emission rate at all the three incubation temperatures in the two-discrete-pool (2P), three-discrete-pool (3P) and three-transfer-pool (3PX) models.

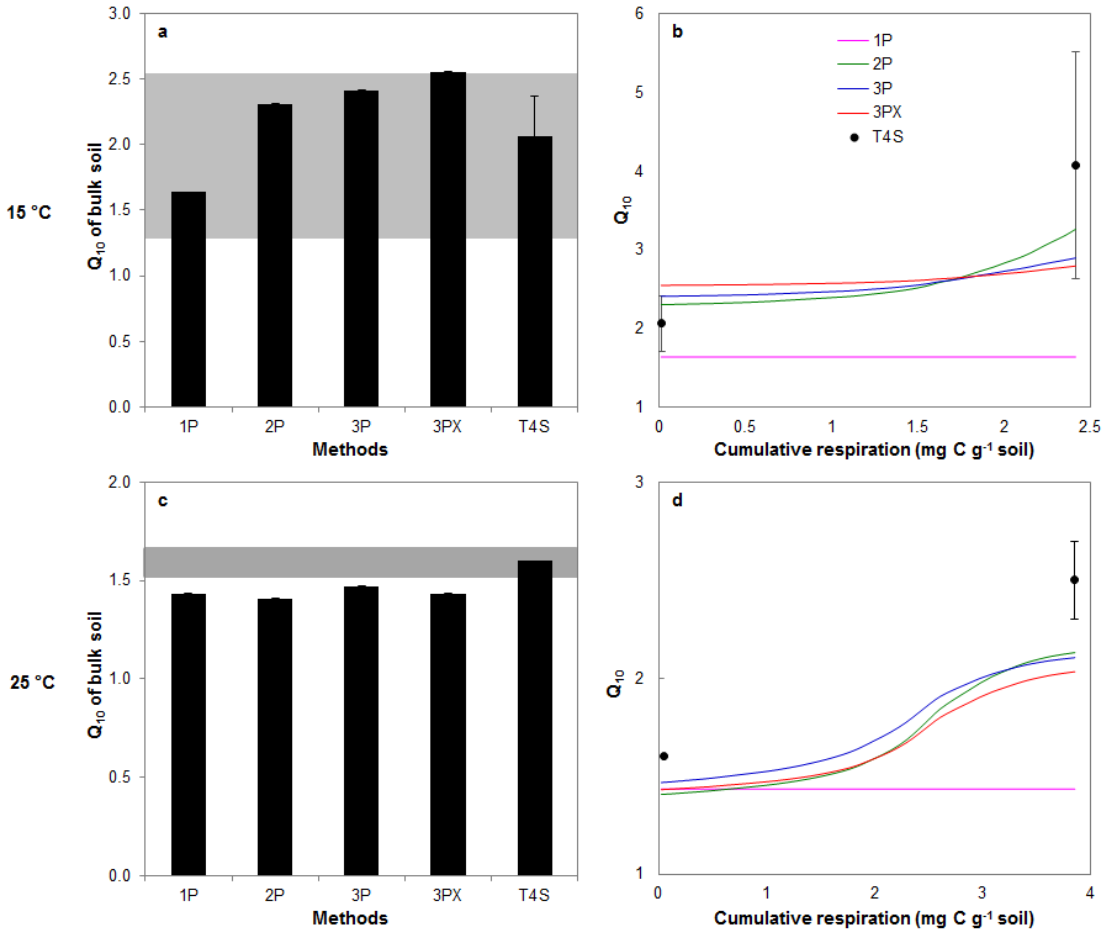

Figure 4.6. Estimated Q_{10}s from the one-pool (1P), two-discrete-pool (2P), three-discrete-pool (3P) and three-transfer-pool (3PX) models, and the time-for-substrate calculation (T4S). Panel (a) and (c) show the estimated Q_{10}s of bulk soil from different methods (mean ± 95% CI). The gray areas are the 95% confidence ranges of Q_{10} from direct calculation at the first incubation day at 15 (a) and 25 °C (c), respectively. Panel (b) and (d) show the dynamics of estimated apparent Q_{10}s with SOM respiration.

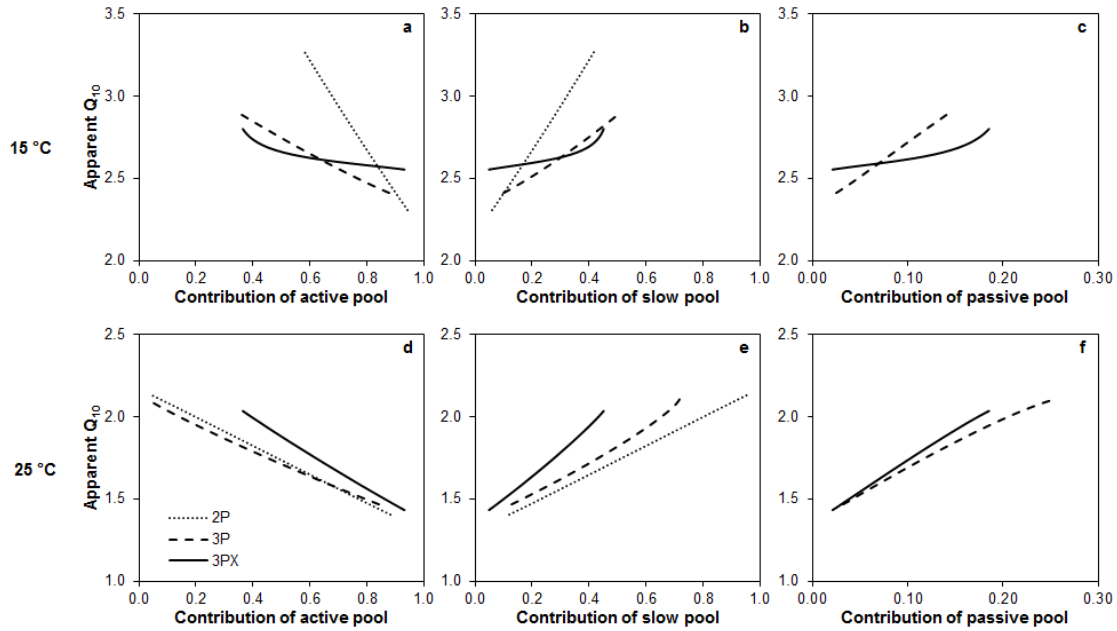

Figure 4.7. Relationships of the modeled apparent Q_{10} against the modeled contributions of active (a), slow (b) and passive (c) pools to the instantaneous CO_2 emission rate in the two-discrete-pool (2P), three-discrete-pool (3P) and three-transfer-pool (3PX) models.

4.4 Discussion

4.4.1 Comparison of the models.

Generally, the estimated Q_{10} increased with SOM recalcitrance and decreased with the increase in the incubation temperature, which is in accord with the Arrhenius equation and many previous studies (Knorr *et al.*, 2005, Davidson & Janssens, 2006, Conant *et al.*, 2008, Haddix *et al.*, 2011, Xu *et al.*, 2012). However, the estimations substantially rely on the methods used and their respective assumptions. The 1P model assumes the soil as a single C pool (Stanford & Smith, 1972, Kätterer *et al.*, 1998, Rey & Jarvis, 2006). Compared with the multi-pool models, it does not fit the data well enough (Kätterer *et al.*, 1998, Rey & Jarvis, 2006). In addition, it cannot represent the dynamics of temperature sensitivity with the changes in SOM compounds. Therefore, the 1P model is not adequate for describing the dynamics of SOM decomposition in

general and estimating the temperature sensitivity in particular. All the 2P, 3P and 3PX models fitted the incubation data adequately ($R^2 > 0.99$, $P < 0.001$), but the modeled decay rates of the slow pool in the 2P model were smaller than those in the 3P and 3PX models. It is mainly because the slow pool in the 2P model conceptually amounts to the sum of slow and passive pools in the three-pool models.

In this study, the Bayesian MCMC technique provided the distributions of estimated parameters for each model. In the four models, the goodness of the parameter constraint decreased with the increase in the parameter number. In the 1P model, although the parameters were constrained perfectly, the *AIC* analysis demonstrated that it is the worst model. In the other three models, the *AIC* analysis indicated that the 2P model is the most parsimonious model, followed by the 3P model. The 3PX model seems to have an overfitting issue when it is used to simulate the CO_2-C emission data alone. However, in the 3PX model, the transfers from slow and passive pools can alleviate the rapid consumption of active pool, leading to greater active pool size and its contribution to CO_2 emission rate than that in the discrete-pool models. Because the apparent Q_{10} decreased with the increased contribution of the active SOM to CO_2 emission rate (Fig. 4.7), the estimated apparent Q_{10}s in the 2P and 3P models were higher than that in the 3PX model after the early incubation period.

4.4.2 Correlations between parameters.

Strong correlations between some parameters were observed in all the four models (Table 4.3). In these models, the values of k at 25 °C and the corresponding Q_{10} at 25 °C of the active pool are usually negatively correlated, meaning when the decay rate at

the 25 °C incubation temperature is high, low Q_{10} values are needed to match the data at the 35 °C incubation temperature. In contrast, the values of k at 25 °C and the corresponding Q_{10} at 15 °C of the active pool are usually positively correlated, meaning when the decay rate at the 25 °C incubation temperature is high, high Q_{10} values are needed to match the data at the 15 °C incubation temperature. In the multi-pool models, the high initial fraction of the labile pool is accompanied by the low decay rate, mainly because the two parameters are constrained by the information of CO_2 emission from the labile pool synchronously. As a result, there is a trade-off between them. In the 3PX model, the positive correlation between f_1 and $f_{2,1}$ means when more C is allocated to labile pool, more proportion of the labile pool would transfer to the slow pool.

The strong correlations between parameters partly indicate that the models are overparameterized with the available data (Braakhekke *et al.*, 2013). However, the inherent correlations of parameters due to the model structures may be another important reason. For example, the only existed three parameters in the simplest 1P model are the decay rate (k) and Q_{10}s at 15 and 25 °C. The Q_{10}s themselves, measure the responses of the decay rate to temperature. As a result, they are highly correlated with each other (Table 4.3).

Table 4.3 Correlations of the posterior parameter distributions for the one-pool (1P), two-discrete-pool (2P), three-discrete-pool (3P) and three-transfer-pool (3PX) models

Model		Parameter correlations																	
1P	k_1	1.00																	
	Q_{10s}_15	0.66	1.00																
	Q_{10s}_25	-0.93	-0.61	1.00															
		k_1	Q_{10s}_15	Q_{10s}_25															
2P	f_1	1.00																	
	k_1	-0.66	1.00																
	k_2	-0.85	0.39	1.00															
	Q_{10a}_15	-0.17	0.69	-0.02	1.00														
	Q_{10s}_15	0.53	-0.38	-0.39	-0.50	1.00													
	Q_{10a}_25	0.01	-0.65	0.21	-0.67	0.05	1.00												
	Q_{10s}_25	0.58	-0.13	-0.90	0.16	0.21	-0.34	1.00											
		f_1	k_1	k_2	Q_{10a}_15	Q_{10s}_15	Q_{10a}_25	Q_{10s}_25											
3P	f_1	1.00																	
	f_2	0.02	1.00																
	k_1	-0.70	-0.01	1.00															
	k_2	-0.62	-0.60	0.37	1.00														
	k_3	0.22	-0.32	-0.11	-0.12	1.00													
	Q_{10a}_15	0.07	0.02	0.44	-0.12	0.08	1.00												
	Q_{10s}_15	0.31	0.08	-0.29	-0.18	0.00	-0.34	1.00											
	Q_{10p}_15	0.16	-0.08	-0.12	-0.04	0.09	-0.11	-0.14	1.00										
	Q_{10a}_25	-0.12	0.10	-0.41	0.04	-0.05	-0.53	0.04	-0.04	1.00									
	Q_{10s}_25	0.15	-0.07	-0.07	-0.11	0.00	0.04	-0.09	0.03	-0.19	1.00								
	Q_{10p}_25	0.25	0.06	-0.14	-0.12	-0.21	0.04	0.13	0.00	-0.01	-0.49	1.00							
		f_1	f_2	k_1	k_2	k_3	Q_{10a}_15	Q_{10s}_15	Q_{10p}_15	Q_{10a}_25	Q_{10s}_25	Q_{10p}_25							
3PX	f_1	1.00																	
	f_2	-0.14	1.00																
	k_1	-0.45	0.08	1.00															
	k_2	-0.20	-0.58	0.27	1.00														
	k_3	0.00	-0.12	-0.04	-0.24	1.00													
	$f_{2,1}$	0.78	-0.04	-0.01	0.05	-0.03	1.00												
	$f_{3,1}$	0.09	-0.15	0.00	0.11	-0.07	0.08	1.00											
	$f_{1,2}$	0.10	0.04	-0.07	0.12	0.03	-0.04	-0.07	1.00										
	$f_{3,2}$	0.02	0.03	-0.03	0.00	-0.01	0.00	0.04	-0.02	1.00									
	$f_{1,3}$	-0.01	0.01	0.05	0.11	-0.06	0.01	0.02	0.04	0.05	1.00								
	Q_{10a}_15	0.04	-0.08	0.46	-0.06	0.02	0.00	0.01	0.05	-0.01	0.03	1.00							
	Q_{10s}_15	0.04	0.06	-0.07	-0.03	-0.01	0.01	-0.01	0.00	0.03	-0.01	-0.34	1.00						
	Q_{10p}_15	0.05	-0.03	-0.05	0.00	0.08	0.02	0.00	0.04	0.02	-0.07	-0.16	-0.04	1.00					
	Q_{10a}_25	-0.02	0.12	-0.49	0.07	-0.01	0.00	-0.02	0.07	0.00	0.02	-0.63	0.02	0.01	1.00				
	Q_{10s}_25	0.25	-0.20	-0.13	-0.08	-0.15	0.06	0.08	0.05	-0.01	0.01	0.14	-0.05	-0.03	-0.20	1.00			
	Q_{10p}_25	0.08	0.06	-0.10	-0.17	-0.11	-0.05	-0.06	0.06	0.00	0.04	0.05	0.00	-0.02	-0.08	-0.42	1.00		
		f_1	f_2	k_1	k_2	k_3	$f_{2,1}$	$f_{3,1}$	$f_{1,2}$	$f_{3,2}$	$f_{1,3}$	Q_{10a}_15	Q_{10s}_15	Q_{10p}_15	Q_{10a}_25	Q_{10s}_25	Q_{10p}_25		

4.4.3 Estimated Q10 from the T4S method.

The T4S Q_{10} calculation assumes that the respired CO_2 is from similar SOM fractions at different temperatures at the same substrate levels (Conant *et al.*, 2008). However, the current and many previous studies have indicated that the recalcitrant SOM is more temperature sensitive (Knorr *et al.*, 2005, Craine *et al.*, 2010, Karhu *et al.*, 2010, Xu *et al.*, 2012). As a result, when the same amount of SOM is decomposed, the proportion of emitted CO_2 from the slow and passive pools would be more at high than that at lower temperatures. The results in the current study confirmed that the active pool size increased with the increased incubation temperature when the same amount of CO_2 was respired in all the multi-pool models (Fig. 4.4). Because the decay rate of the active pool is much greater than that of the slow and passive pools, the CO_2 emission rate at the higher temperatures should be greater than assumed by the method. In other words, the time for respiring a given amount of C was less than assumed. Moreover, the difference between the active pools at different temperatures increased with SOM decomposition (Fig. 4.4), indicating that the assumption of this method causes little bias for short-term incubation, but it would lead to overestimation of Q_{10} of the recalcitrant SOM decomposition when applying to long-term incubation experiments. This is supported by the results that the estimated Q_{10} of recalcitrant SOM from the T4S method was significantly greater than that from the other methods (Fig. 4.6d).

4.4.4 Potential implication of 3PX model.

Multi-discrete-pool models assume soil C can be divided into several discrete pools (Andrén & Paustian, 1987, Kätterer *et al.*, 1998, Rey & Jarvis, 2006, Li *et al.*, 2013,

Schädel *et al.*, 2013). However, in natural ecosystems there are likely C transfers among soil SOM pools (Rovira & Vallejo, 2002, Cheng *et al.*, 2007) and the transfers are included in Earth system models (Parton *et al.*, 1987, Jenkinson, 1990, Luo *et al.*, 2003). Although the discrete-pool models can fit the soil incubation data well, the estimated Q_{10} and other parameters with those models could not be directly used to improve Earth system models. The 3PX model, on the other hand, represents different soil pools and transfers among the pools to resemble ecosystem carbon cycle models. Thus, the 3PX model can facilitate knowledge transfer from soil incubation studies to Earth system modeling.

Although the structures of the terrestrial decomposition sub-model may be different in different Earth system models, the 3PX-type model and data assimilation techniques could provide an effective approach to incorporate the incubation data into these large-scale models with minor adjustment of the model structure. For example, the 3PX model in the current study corresponds to the CENTURY and TECO model (Parton *et al.*, 1987, Luo *et al.*, 2003). Instead of the traditional way that giving the parameters specific values, the 3PX model can provide constrained values and the uncertainties from experimental data. However, because there is little information for the C transfers in the data with CO_2 emission alone, none of the five parameters relative to the C transfers are well constrained. Therefore, data relative to the C transfers should be gathered together with CO_2 emission and used for the estimates of these parameters. For example, isotope measurements have recently been used to constrain the transfer coefficient from the active to slow pool (Ahrens *et al.*, 2014).

4.4.5 Summary.

The results in this study indicate that temperature sensitivity estimated from soil incubation data strongly depends on the methods used. The 1P model is not adequate for Q_{10} estimate. The 2P model is the most parsimonious one and can fit data well with all parameters commendably constrained. The 3P model can estimate the C release and its temperature sensitivity of the passive SOM with a minor decrease in the model parsimony. The estimated Q_{10} of the soil with less labile C from the 3PX model is smaller than that from the 2P and 3P models due to considering the transfers among pools. The T4S method is effective to estimate Q_{10} of the labile SOM, but would overestimate that of the recalcitrant SOM. The 3PX model structure offers a possible approach to facilitate the transfer of knowledge learned from soil incubation data into Earth system models.

Chapter 5: Acclimation of soil carbon dioxide loss to warming in Alaskan tundra

Abstract: Climate warming can result in physical (e.g., temperature rise and permafrost thaw) and biological (e.g., microbial community and activity) changes in permafrost regions. While it is well agreed that physical changes can accelerate C releases to the atmosphere by increasing thermodynamic reaction rates and the accessibility of soil organic C (SOC) to decomposers, how biological changes impact permafrost soil C loss is still unclear. Here, combining a process-based model and a unique field experiment through data assimilation, this study shows that warming reduced the base turnover rate of SOC, which is the representation of unresolved microbial community and activity on the resolved scale. The reduced base turnover rate of SOC suggests that microbial decomposers acclimate to warming in Alaskan tundra. Although warming still accelerates SOC loss, the acclimation counterbalances the SOC loss acceleration by 62%. Our study suggests that it is critical to incorporate changes in biological properties (as parameters) to improve the model performance in predicting C dynamics and its feedback to climate change.

5.1 Introduction

Arctic ecosystems in the Northern Hemisphere have experienced, and are projected to continue to experience faster climate warming than other regions (IPCC, 2013). Soil organic carbon (SOC) in arctic ecosystems is huge in magnitude and has long been protected due to low temperatures. As climate gets warmer, SOC in these ecosystems can become vulnerable to rising temperatures and could potentially lose a large amount of carbon (C) to the atmosphere, acting as an important C source in this century (Schuur *et al.*, 2009, Koven *et al.*, 2011, MacDougall *et al.*, 2012, Schuur *et al.*, 2015, Hicks

Pries *et al.*, 2016). However, the magnitude of the C source is still uncertain due to poor understanding of mechanisms that control soil C balance in the frontier ecosystems (McGuire *et al.*, 2012, Koven *et al.*, 2013).

Under climate warming, several aspects may influence soil C balance in arctic ecosystems. First, temperature increase itself can directly stimulate soil C release due to the thermal kinetic behavior of microbial-mediated processes (Davidson & Janssens, 2006, Liang *et al.*, 2015, Bracho *et al.*, 2016). Second, permafrost thaw can increase SOC accessibility for decomposers by lifting temperature and moisture constraints (i.e., thawing permafrost and increasing soil drainage), potentially resulting in more C release from arctic ecosystems to the atmosphere (Schuur *et al.*, 2009, Koven *et al.*, 2011, Hicks Pries *et al.*, 2016). The two aspects are both direct effects of physical changes on soil C balance in arctic ecosystems. In addition, a third aspect, biological changes, may be also important to determine soil C changes. For example, warming and permafrost thaw can change microbial community composition and activity (Manzoni *et al.*, 2012, Hultman *et al.*, 2015, Xue *et al.*, 2016), which may further affect CO_2 emissions to the atmosphere.

While the direct effects of physical changes have been paid more and more attention during the past years (e.g., Zhuang *et al.*, 2006, Koven *et al.*, 2011, MacDougall *et al.*, 2012), few studies have been conducted to quantitatively examine how and to what extent possible changes in biological properties contribute to soil C changes in arctic ecosystems. In Earth system models (ESMs), biological properties, as parameters (e.g., base turnover rates of C pools), are usually set constant. Thus, changes in biological properties are rarely considered in ESMs, which may result in inaccurate predictions of

soil C changes in arctic ecosystems and its feedback to climate change (Koven *et al.*, 2013, Schuur *et al.*, 2015).

In this study, I quantitatively estimated the contributions of changes in physical forcings and biological properties to soil C changes in an arctic tundra by integrating data from a unique long-term field manipulative experiment and a process-based model. I tested the following hypothesis that soil microbial community can acclimate to warming, and consequently partially counterbalance the accelerated SOC loss.

5.2 Materials and Methods

A model-data assimilation, combining a 5-year old field experiment and Terrestrial ECOsystem (TECO) model, was conducted.

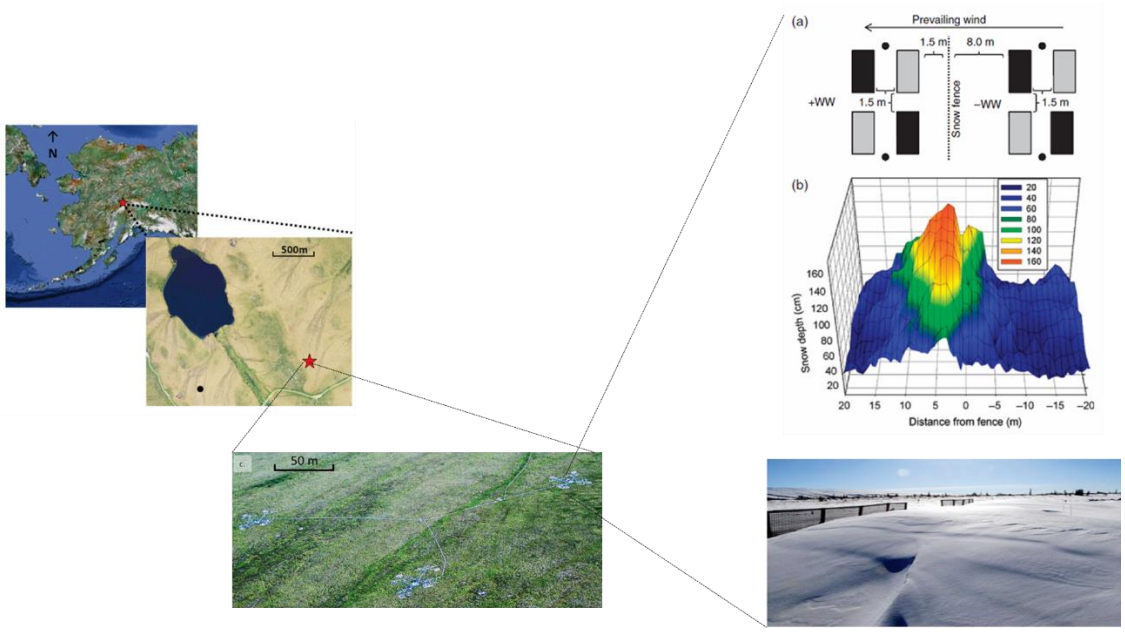

Figure 5.1 Site information and experimental design and treatment.

5.2.1 Experimental design and observations.

A warming experiment, the Carbon in Permafrost Experimental Heating Research (CiPEHR) project, was established at a moist acidic tundra in the region of Eight Mile Lake (EML), Alaska, USA (63°52'59"N, 149°13'32"W) (Fig. 5.1). Site information, experimental design and field observations are described in detail in Natali *et al.* (2011), Natali *et al.* (2012), Natali *et al.* (2014). Briefly, the site is within the area of discontinuous permafrost, with active layer depth about 50 cm. Mean annual temperature and precipitation are -1.0 °C and 378 mm, respectively. The lowest and highest mean monthly temperatures are -16 °C in December and 15 °C in July.

In the experiment, soil was warmed by using snow fences that drift snow to accumulate in winter. There were six replicate fences in three blocks. The excess snow, as well as the snow fences, were removed from the warming plots before snowmelt in early spring to ensure comparable melt out dates and moisture conditions across treatments. The experimental treatment started in September 2008, and continued every winter from then on. Throughout the growing seasons (May – September) from 2009 to 2013, gross primary production (GPP), ecosystem respiration (ER), net ecosystem CO_2 exchange (NEE), and soil moisture were automatically monitored (Natali *et al.*, 2011). Soil temperatures at 5 cm, 10 cm, 20 cm, and 40 cm were monitored across the experimental period (Natali *et al.*, 2011). In addition, thaw depth during growing seasons were measured twice a week (Natali *et al.*, 2011). Aboveground biomass was measured using a nondestructive point-frame method every year (Natali *et al.*, 2012). Belowground biomass down to 35 cm was measured by sampling soil cores in 2011. In 2009, 2010, 2011, and 2013, soils were sampled for SOC, bulk density, ash weight

measurements. SOC profile was corrected using bulk density and ash weight to eliminate the influence of soil compaction due to warming.

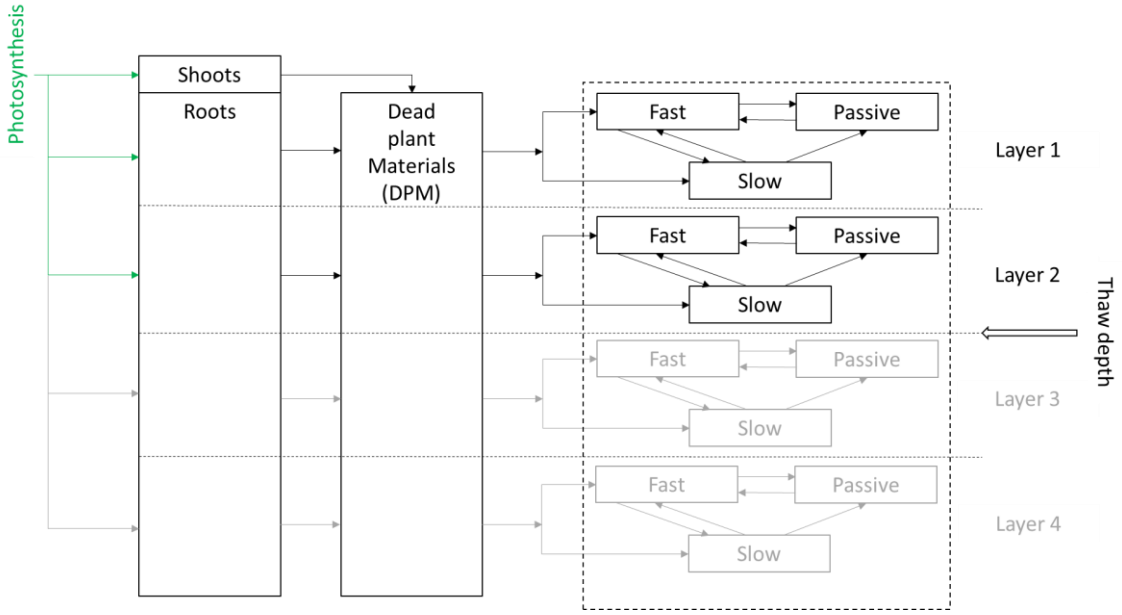

Figure 5.2 Schematic diagram of model used in this study. The proportion of roots, belowground litter and SOC is dependent upon thaw depth.

5.2.2 Model.

Terrestrial ECOsystem (TECO) model was used in this study (Fig. 5.2). TECO model is a daily process-based model. To mimic the dependences of soil C availability and root activity on thaw depth in the permafrost site, daily thaw depth was gap-filled. A linear function (i.e., $y = ax + b$) between thaw depth and cumulative air temperature was used for the daily gap-filling. In growing seasons, positive cumulative air temperature was used to fill the increasing thaw depth. At the end of growing seasons, negative cumulative air temperature was used to fill the decreasing thaw depth. At the beginning of each growing season, when air temperatures in 7 continuous days were greater than 0 °C, the first day of the days was marked as the beginning day (DOB). At

the end of each growing season, when air temperatures in 7 continuous days were below 0 °C, the day before the first day of the days was marked as the ending day (DOE). During DOB and DOE, positive cumulative air temperature was calculated. During (DOE + 1) and (DOB – 1) in the next year, negative cumulative air temperature was calculated. Parameters *a* and *b* were determined by fitting the observed thaw depth during growing seasons using a Markov Chain Monte Carlo (MCMC) technique (Liang *et al.*, 2015). The values of *a* and *b* were 3.58×10^{-4} and 0.035 in ambient, and 3.65×10^{-4} and 0.056 in warming, respectively. The same parameters were used for simulating decreasing thaw depth after DOEs. A minimum thaw depth of 0.5 cm was set to represent soil C availability in winters.

Gross primary production (GPP) was simulated by

$$GPP(t) = PAR(t) \times FAPAR(t) \times \varepsilon \times \tau(t)$$

where PAR is photosynthetic active radiation, which is derived from a weather station located approximately 100 m from the experiment. FAPAR is the fraction of absorbed PAR by plants, which is Moderate Resolution Imaging Spectroradiometer (MODIS) Normalized Difference Vegetation Index (NDVI) in the grid cell which the experiment site is in. Due to warming effect on plant growth, a factor 1.068 was applied to FAPAR in warming based on NDVI measurements *in situ* (Natali *et al.*, 2012). ε is light use efficiency, which was determined by data assimilation described in next section. τ is environmental scaler.

Carbon dynamics within the ecosystem was modeled by

$$\frac{dX(t)}{dt} = B \times GPP(t) + \delta \times A \times K \times X(t)$$

where $X(t)$ is a 15 × 1 vector describing C pool sizes (i.e., two plant pools, one litter pool, 4 soil layers with 3 soil pools in each layer) at time t. $B = [b_{shoot}\ b_{root}\ 0\ 0\ 0\ 0\ 0\ 0\ 0\ 0\ 0\ 0\ 0\ 0\ 0]^T$ is a vector describing GPP allocations to the C pools. GPP only directly allocates to shoots (b_{shoot}), roots (b_{root}) and autotrophic respiration. To derive better parameter estimations, measured GPP are used when they are available. A is a square matrix representing C transfers between individual C pools (black arrows in Fig. 5.2). All the diagonal elements in the matrix A are -1. K is a diagonal matrix representing turnover rates of pools (the amounts of C per unit mass leaving each of the pools per time step). δ is environmental scaler. In the model, C dynamic is dependent on thaw depth (Fig. 5.2). Only pools above the thaw depth are involved at each time step. The vertical distributions of root and soil C are described in the following section.

5.2.3 Data assimilation for parameter constraints.

In this study, constrained initial pool sizes by data assimilation, instead of prescribed with the equilibrium assumption, are used. In transient systems, data assimilation can provide more reasonable initial conditions for model compared to prescription (Carvalhais *et al.*, 2008, Williams *et al.*, 2009). Thus, 6 parameters, which are the initial pool sizes of shoots, roots, litter, fast soil, slow soil, and passive soil pools, are included in the ambient treatment. The constrained initial pools in the ambient are also used in the warming treatment, assuming that no significant difference exists in the ambient and warming before treatment started.

Besides, 16 parameters are to be constrained in the ambient and warming treatments, respectively. These parameters include (1) light use efficiency (ε) in the GPP model; GPP allocations to (2) shoots (b_{shoot}) and (3) roots (b_{root}) in the vector *B*; turnover rates of (4) shoots (k_{shoot}), (5) roots (k_{root}), (6) litter (k_{litter}), (7) fast soil C (k_{fast}), (8) show soil C (k_{slow}), and (9) passive soil C ($k_{passive}$) in matrix *K*; C transfer coefficient from (10) litter to fast soil C ($a_{fast,litter}$),(11) from litter to slow soil C ($a_{slow,litter}$),(12) from fast soil C to slow soil C ($a_{slow,fast}$),(13) from fast soil C to passive soil C ($a_{passive,fast}$),(14) from slow soil C to fast soil C ($a_{fast,slow}$),(15) from slow soil C to passive soil C ($a_{passive,slow}$),(16) from passive soil C to fast soil C ($a_{fast,passive}$).

A probabilistic inversion approach is used to constrain model parameters (Xu *et al.*, 2006, Liang *et al.*, 2015). The approach is based on Bayes' theorem:

$$P(\theta|Z) \propto P(Z|\theta)P(\theta),$$

where $P(\theta)$ is prior probability density function (PDF). $P(Z|\theta)$ is a likelihood function with the assumption that the model error follows a multivariate Gaussian distribution. $P(\theta|Z)$ is the posterior PDF, which is constrained by using adaptive Metropolis (AM) algorithm, a Markov Chain Monte Carlo (MCMC) technique (Haario *et al.*, 2001, Hararuk *et al.*, 2014). In the AM algorithm, the proposal distribution at each iteration is estimated depending on the past iterations by setting a covariance matrix

$$C_i = \begin{cases} C_0 & i \leq i_0, \\ s_d cov(\theta_0, \dots, \theta_{i-1}) & i > i_0, \end{cases}$$

where s_d is a parameter calculated based on dimension *d* (i.e., $s_d = 2.38/\sqrt{d}$, and *d* = 22 in this study) (Gelman *et al.*, 1996, Hararuk *et al.*, 2014). An arbitrary initial

covariance C_0 is required in the AM algorithm when iteration is not greater than i_0 (i_0 = 4000 in this study). C_0 is constructed by a test run in which the new parameter is selected by a random move from the previous one within a uniform distributed range (Xu *et al.*, 2006, Hararuk *et al.*, 2014, Liang *et al.*, 2015). The AM algorithm is run repeatedly for 50, 000 iterations to derive the posterior PDF. At each iteration, a set of parameters (θ^{new}) is proposed based on the accepted parameters in the previous iteration (θ^{old}) and C_i. Then the acceptance probability is calculated by

$$\alpha = min\left\{1, \frac{P(Z|\theta^{new})P(\theta^{new})}{P(Z|\theta^{old})P(\theta^{old})}\right\}.$$

The acceptance probability is compared with a random number u between 0 and 1. If $\alpha > u$, the new set of parameters θ^{new} is accepted. Otherwise, θ^{new} is set to θ^{old}. To test the convergence of the Markov chain, five parallel runs are conducted. After discarding the first half of the accepted simulations in each run, Gelman-Rubin diagnostic method is employed to test the convergence to stationary distributions (Gelman & Rubin, 1992). The posterior parameter distributions are converged.

5.2.4 Modeling experiment.

With all the accepted parameter sets, the model was run in three scenarios. The first scenario is physical forcings (i.e., temperature, thaw depth, and etc) in the ambient with parameter sets constrained by data in the ambient. The second scenario is physical forcings in the warming treatment with parameter sets constrained by data in the ambient. The third scenario is physical forcings in the warming treatment with parameter sets constrained by data in the warming treatment. By comparing the three

scenarios, we can explore how biological changes (i.e., parameters) influence the C dynamic in the permafrost site.

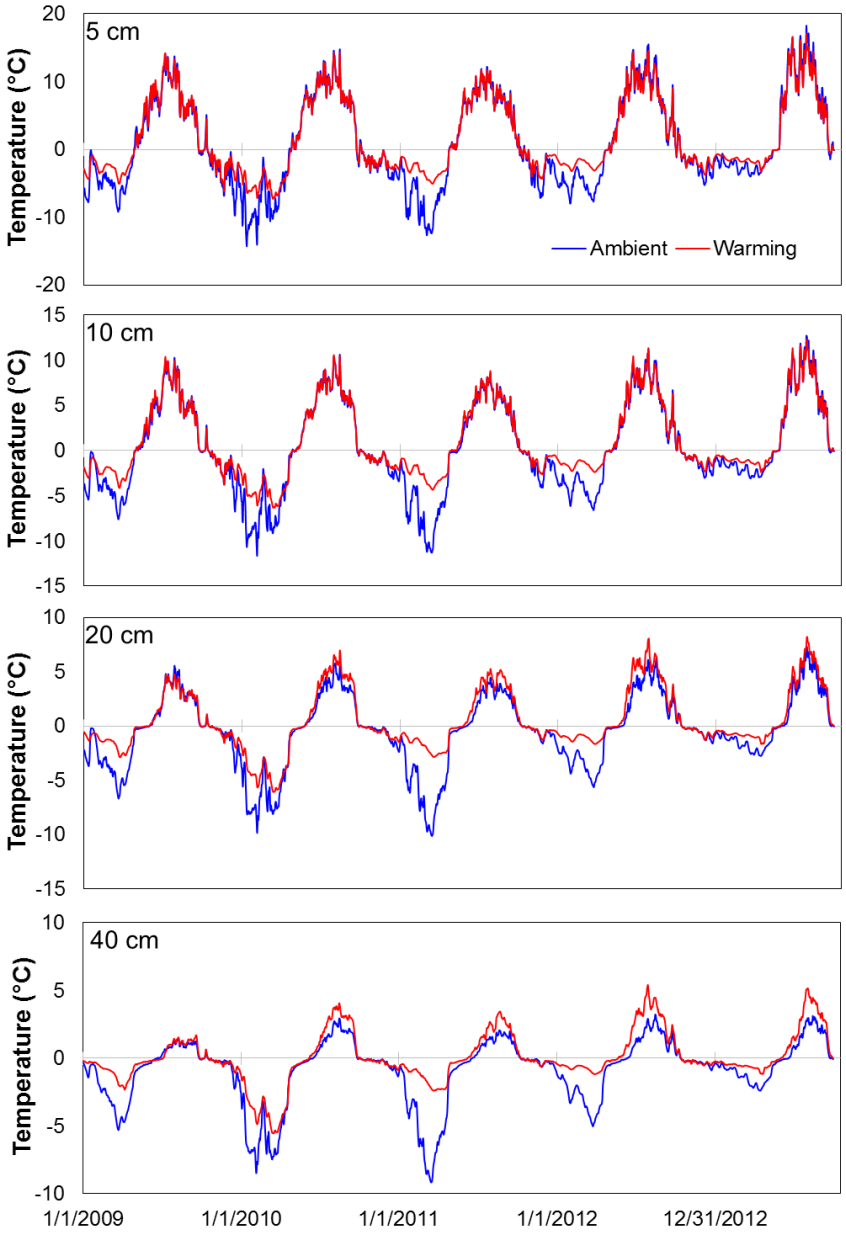

Figure 5.3 Effect of warming treatment on soil temperatures during the experimental period. Warming increases temperatures at top layers in winters, and that at lower layers across the experimental period.

5.3 Results

The experimental treatment increased temperatures at top layers in winters, and increased temperatures at lower layers across the experimental period (Fig. 5.3). Warming significantly increased thaw depth during growing seasons (Fig. 5.4). In addition, the gap-filled daily thaw depth matched observation quite well (Fig. 5.4), allowing me to conduct further analyses. With the gap-filled thaw depth and measured bulk density and ash profile, the amount of active soil was calculated across the experimental period for both the ambient and warming treatments (Fig. 5.5). Warming significantly increased the amount of active soil during growing seasons (Fig. 5.5).

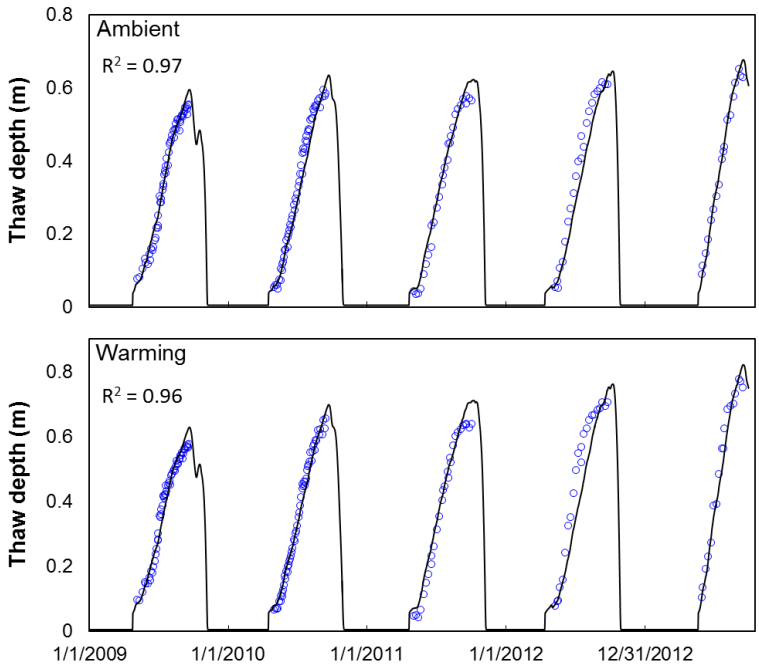

Figure 5.4 Measured (blue dots) and gap-filled (black lines) thaw depth in the ambient (upper panel) and warming (lower panel) treatments.

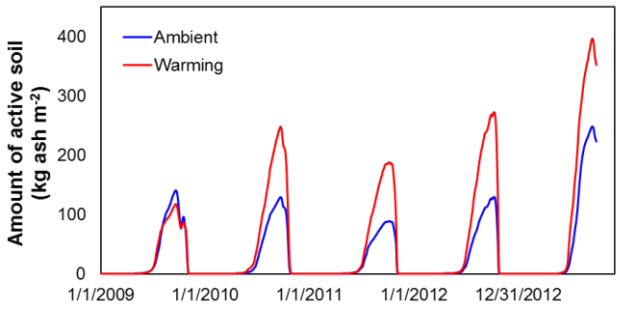

Figure 5.5 Amount of active soil during the experimental period. Warming significantly increases the amount of active soil.

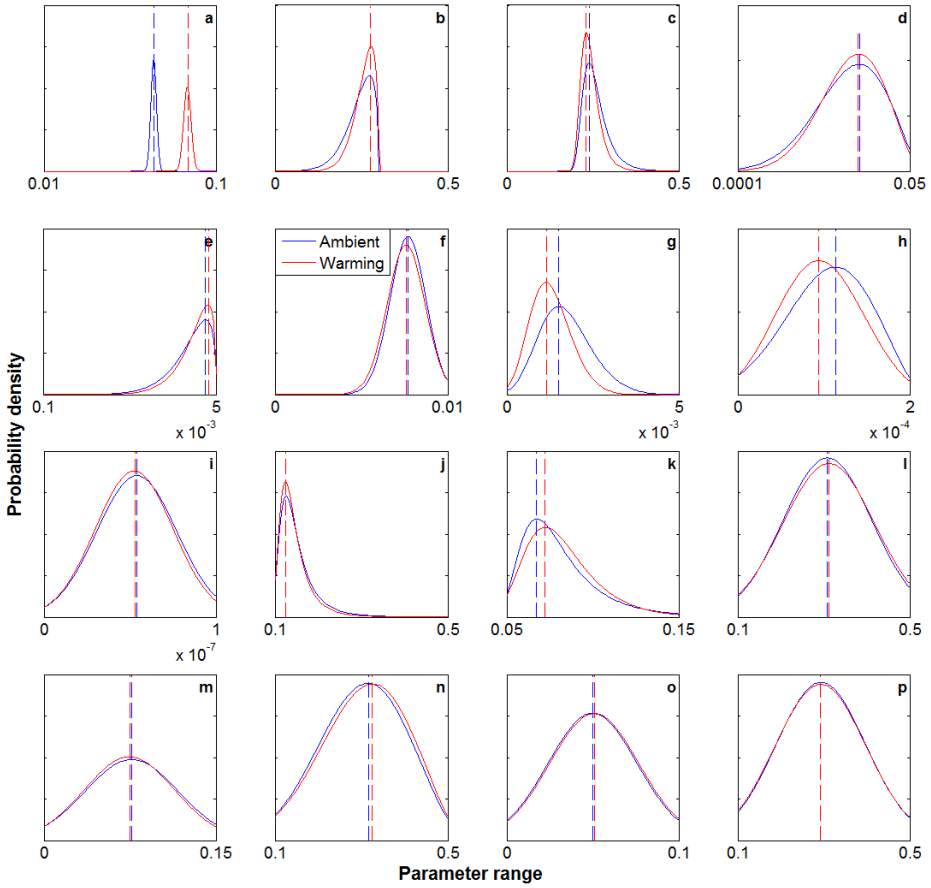

Figure 5.6 Parameter distributions from data-model integration. a, photosynthetic light use efficiency; b, c, GPP allocations to above- and below-ground biomass; d – i, base turnover rates of shoots, roots, litter, fast SOC, slow SOC, and passive SOC, respectively; j, k, C transfer coefficient from litter to fast and slow SOC; l, m, C transfer coefficient from fast to slow and passive SOC; n, o, C transfer coefficient from slow to fast and passive SOC; p, C transfer coefficient from passive to fast SOC.

Warming significantly changed biological properties of both vegetation and soil (Fig. 5.6). Specifically, warming increased photosynthetic light use efficiency (Fig. 5.6a), and slightly decreased GPP allocation to roots (Fig. 5.6c). In addition, warming changed the base turnover rates of C pools (Fig. 5.6d – i). Warming significantly reduced the base turnover rates of fast and slow SOC pools, whereas the effect on litter and passive SOC was minor. Moreover, warming slighted increased C use efficiency of slow SOC pool (Fig. 5.7).

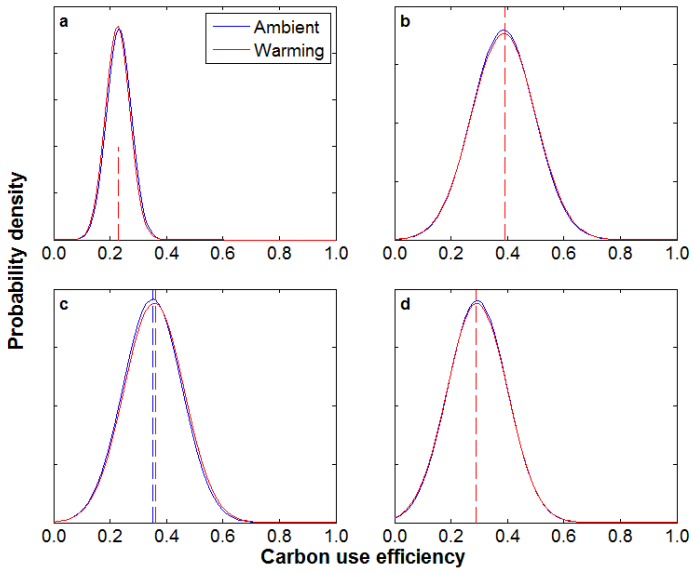

Figure 5.7 Distributions of C use efficiency of litter (a), fast SOC (b), slow SOC (c), and passive SOC (d).

The changed biological properties had significant effect on SOC loss (Fig. 5.8). On average, SOC loss during the experimental period was 96 and 170 g C m^{-2} in the ambient and warming, respectively (Fig. 5.8a, b). However, if the biological changes were not considered, the SOC loss would be 290 g C m^{-2} (Fig. 5.8c). In other words, biological changes alleviate the SOC loss acceleration by 62% (Fig. 5.8d).

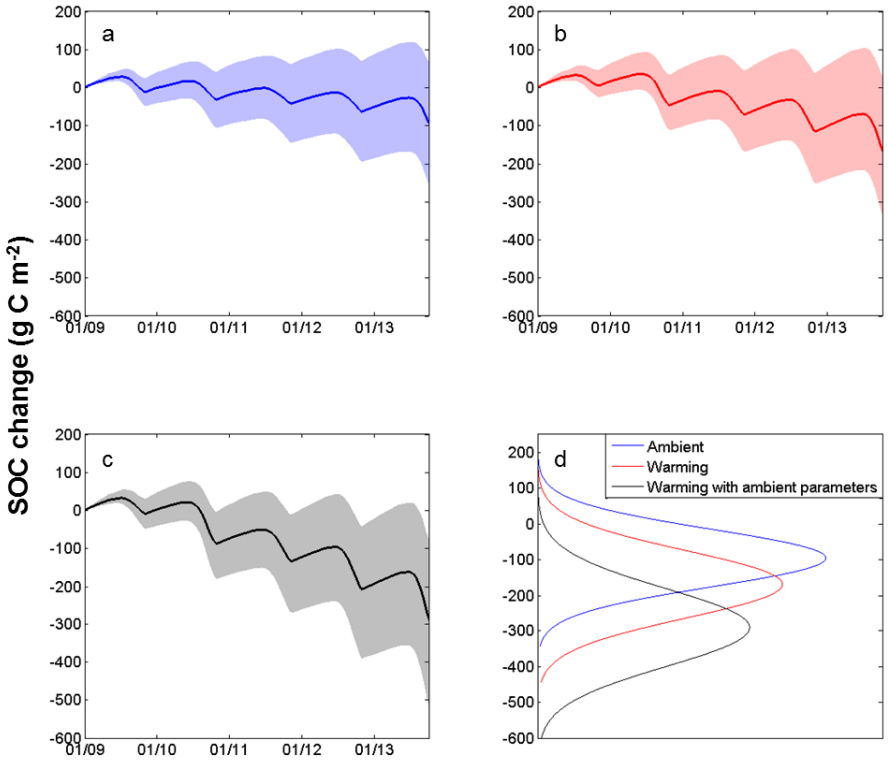

Figure 5.8 SOC change over time (a – c) and the total SOC loss during the experimental period (d). a, ambient environmental factors + ambient parameters; b, warming environmental factors + warming parameters; c, warming environmental factors + ambient parameters.

5.4 Discussion

5.4.1 Acceleration of SOC loss by warming.

In this study, the warming treatment significantly increased thaw depth and the amount of active soil during growing seasons, leading to more SOC accessible to decomposers. In addition, the warming treatment also directly increased soil temperature across the soil profile. The increased SOC accessibility and temperature can directly accelerate SOC loss in Alaskan tundra.

In addition to the physical changes (e.g., temperature increase and permafrost thaw), warming also significantly changed biological properties in the Alaskan tundra. This study shows that warming increases photosynthetic light use efficiency. The enhanced light use efficiency could be attributed to increased canopy nitrogen content and released temperature limitation (Hirose & Bazzaz, 1998, Kergoat *et al.*, 2008, Natali *et al.*, 2011). Because warming increases soil nitrogen mineralization rate and permafrost thaw provides more available nitrogen, plants can acquire more nitrogen for growth, leading to the increase in canopy nitrogen content. As a critical element in plant photosynthetic process, the increase in canopy nitrogen content is able to enhance the light use efficiency. In addition, increased temperature itself can promote plant physiological activities. As a result, warming significantly increases photosynthetic C assimilation in the study site (Natali *et al.*, 2012).

Even though the increased photosynthetic C assimilation can partially offset the accelerated SOC decomposition, warming still leads to net SOC loss. The soil C dynamic in the permafrost regions is different from that in other regions. In other regions, warming treatment may accelerate the loss of relatively labile SOC in early stage (Kirschbaum, 2004, Hartley *et al.*, 2007). As a result, the reduced labile SOC may constrain the further acceleration of SOC loss by warming, resulting in similar soil respiration between control and warming treatment in later years (Kirschbaum, 2004, Hartley *et al.*, 2007). In the permafrost regions, however, temperature-protected SOC in permafrost layers becomes active due to permafrost thaw. Thus, although warming accelerated the loss of SOC, there is actually more substrate for microbial decomposers.

Therefore, it is unlikely that substrate availability will limit the decomposition of SOC in the permafrost regions. Permafrost will still be an important C source in the future.

5.4.2 Acclimation of SOC decomposition to warming.

The temperature increase and permafrost thaw may alter microbial community composition and activity (Manzoni *et al.*, 2012, Hultman *et al.*, 2015, Xue *et al.*, 2016), which may further affect CO_2 emissions to the atmosphere. This study shows that warming significantly decreases the base turnover rates of fast and slow SOC pools, suggesting that the microbial community may have acclimated to warming. There may be two reasons for the acclimation. The first one is the physiological adjustments of microbial decomposers under warming (Luo *et al.*, 2001, Bradford *et al.*, 2008, Allison *et al.*, 2010). Warming reduces the conformational flexibility of enzymes due to the increased selective force of temperature (Hochachka & Somero, 2002, Bradford *et al.*, 2008), leading to the reduced base turnover rates of SOC pools. Second, changes in soil microbial community composition may also contribute to the acclimation (Zogg *et al.*, 1997, Hochachka & Somero, 2002, Bradford *et al.*, 2008). Previous studies in the same site indicates that warming has significantly changed microbial community composition (Penton *et al.*, 2013, Xue *et al.*, 2016). The changed community may alter decomposition activity and shift the optimum temperature, resulting in the acclimation (Hochachka & Somero, 2002, Bradford *et al.*, 2008, Hall *et al.*, 2008).

The acclimation observed in this study is consistent with my hypothesis. In addition, acclimation has also been found in other ecosystems (Luo *et al.*, 2001, Hochachka & Somero, 2002, Bradford *et al.*, 2008), suggesting that acclimation may be a common

phenomenon across ecosystems. The acclimation of SOC decomposition to warming can partially counterbalance the acceleration of SOC loss by temperature increase and permafrost thaw. In this study, I calculated the SOC loss in a scenario that does not take the acclimation in to consideration. Results show that acclimation reduced the acceleration of SOC loss by 62%, suggesting that the C source in the permafrost regions may not as large as by current ESMs. In these ESMs, parameters, which are calibrated by historical data, are usually set constant. However, because parameters are the representations of multiple unresolved processes on the resolved scale (e.g., soil C turnover rate is a parameter that includes impacts of diverse microbial composition, accessibility determined by extra enzyme activity and structural protections, and other factors), they are changeable once the unresolved processes respond to environmental change over time (Bauer *et al.*, 2015). Thus, it is less reasonable to set parameters constant, especially in the context of rapid global change. Specifically, since acclimation is a common phenomenon, with constant C turnover parameters, ESMs may overestimate SOC loss. This study illustrates that integrating field experiments and model is efficient to quantify changes in parameters (i.e., unresolved biological properties) in models, and consequently improve model performance.

5.4.3 Summary.

Warming significantly increases soil temperature and permafrost thaw, leading to significant acceleration of SOC loss in the Alaskan tundra. On the other hand, the data-model integration shows that soil microbial community acclimates to warming. The acclimation partially counterbalances the acceleration of SOC loss by temperature

increase and permafrost thaw. It is also suggested that the current generation of ESMs, with constant parameters, may overestimate the permafrost soil C loss. Long-term experiments and data-model integration are needed to update biology-related parameters to improve model performance.

Chapter 6: Conclusions and Perspectives

6.1 Conclusions

In this dissertation, I studied the responses of soil carbon (C) and related biogeochemical processes to increased CO_2 concentrations and temperature. In Chapter 2, I revealed the effect of new C addition on soil organic C (SOC) storage through two critical processes, replenishment and priming. The analyses highlight that increasing new C inputs increase SOC sequestration due to a higher rate of replenishment than loss of old C by priming effect. Consequently, increasing C inputs to soils from enhanced plant productivity under elevated CO_2, plant invasion, and vegetation recovery likely result in SOC accumulation in soils over time, potentially mitigating climate change.

In Chapter 3, I synthesized effects of CO_2 enrichment on the terrestrial nitrogen (N) cycle and the N limitation to plant growth under elevated CO_2. The results indicate that elevated CO_2 stimulates N influx via biological N fixation but reduces N loss via leaching, leading to increased N supply for plant growth. The additional N supply via the enhanced biological N fixation and the reduced leaching may partially meet the increased N demand under elevated CO_2, potentially alleviating PNL. In addition, the analysis indicates that increased N_2O emissions may partially offset the mitigation of climate change by stimulated plant CO_2 assimilation. Moreover, changes in soil microenvironments, ecosystem communities and above-belowground interactions induced by the different responses of NH_4^+ and NO_3^- to CO_2 enrichment may have long-term effects on the terrestrial biogeochemical cycles and climate change.

In Chapter 4, I conclude that temperature sensitivity estimated from soil incubation data strongly depends on the methods used. The 1P model is not adequate for Q_{10} estimate. The 2P model is the most parsimonious one and can fit data well with all

parameters commendably constrained. The 3P model can estimate the C release and its temperature sensitivity of the passive SOC with a minor decrease in the model parsimony. The estimated Q_{10} of the soil with less labile C from the 3PX model is smaller than that from the 2P and 3P models due to considering the transfers among pools. The T4S method is effective to estimate Q_{10} of the labile C, but would overestimate that of the recalcitrant C. The 3PX model structure offers a possible approach to facilitate the transfer of knowledge learned from soil incubation data into Earth system models.

In Chapter 5, I studied how warming affects soil C storage in Alaskan tundra, through integrating a process-based model with a long-term field experiment. Results show that warming enhances soil temperature and permafrost thaw, which further accelerate SOC loss in the Alaskan tundra. however, results also shows that soil microbial community acclimates to warming, partially counterbalancing the acceleration of SOC loss. In addition, the changed parameters by warming suggest that the current generation of Earth system models (ESMs), which usually have constant parameters, may overestimate the SOC loss in permafrost regions.

6.2 Perspectives

How ecosystems respond to global change will significantly influence their functions and services. Research in the area has lasted for decades, during which a large amount of data have been collected from observations and experiments. This dissertation demonstrates that synthesizing existing data can provide general patterns of ecosystem responses to global change. Meanwhile, models have also been developed to simulate

and predict the responses and feedback of ecosystems to global change. However, data collection and model development are relatively independent. Although both of them alone have advanced our understanding of ecosystem structures, functions, and services in the context of global change, this dissertation indicates that integrating data and model can provide more insights. In addition, data are helpful for model development. On the other way around, modeling studies are helpful for experimental and observational designs. Thus, further data-model integration studies are needed. Specifically, when models are developed, they should be parameterized and tested using different types of data.

Chapter 3 indicates that though CO_2 enrichment does not affect total soil inorganic N much, the ratio of ammonium to nitrate is increased. It is needed to study how the changed ratio of ammonium to nitrate may affect soil microenvironments, ecosystem communities and above-belowground interactions, and consequently possibly terrestrial biogeochemical cycles and climate change on long-term time scales.

In Chapter 4, the methods for estimating temperature sensitivity I evaluated are based on laboratory incubation data. In laboratory incubation experiments, environmental factors (e.g., temperature and moisture) are well controlled, which is not the case in the field. In addition, soil incubated in laboratory is usually disturbed. The estimated temperature sensitivity with laboratory incubation data may not be directly used in the field. Thus, field incubation with undisturbed soil is needed in the future.

The analyses in Chapter 5 indicate soil microbial decomposers acclimate to warming in the Alaskan tundra. Further studies are needed to quantify the dependence of acclimation magnitude upon warming intensity. In addition, model parameters, which is

the representation of multiple unresolved processes on the resolved scale, are changeable once the unresolved processes respond to environmental change. Thus, setting parameters constant in ESMs may resulting in inaccurate predictions. Integrating model and data is needed to improve model performance.

In addition, results in Chapter 4 demonstrate that the decomposition of SOC increases by warming, whereas SOC increases by increased C input as indicated in Chapter 2. This suggests that different global change factors may affect SOC in different ways. Thus, future research is needed to explore the integrated effect of global change factors.

References

Ahrens B, Reichstein M, Borken W, Muhr J, Trumbore SE, Wutzler T (2014) Bayesian calibration of a soil organic carbon model using $\Delta^{14}C$ measurements of soil organic carbon and heterotrophic respiration as joint constraints. Biogeosciences, **11**, 2147-2168.

Akaike H (1974) A new look at the statistical model identification. Automatic Control, IEEE Transactions on, **19**, 716-723.

Allison SD, Wallenstein MD, Bradford MA (2010) Soil-carbon response to warming dependent on microbial physiology. Nature Geoscience, **3**, 336-340.

Andrén O, Kätterer T (1997) ICBM: The introductory carbon balance model for exploration of soil carbon balances. Ecological Applications, **7**, 1226-1236.

Andrén O, Paustian K (1987) Barley Straw Decomposition in the Field - a Comparison of Models. Ecology, **68**, 1190-1200.

Asner GP, Townsend AR, Riley WJ, Matson PA, Neff JC, Cleveland CC (2001) Physical and biogeochemical controls over terrestrial ecosystem responses to nitrogen deposition. Biogeochemistry, **54**, 1-39.

Bardgett RD, Wardle DA (2010) *Aboveground-belowground linkages: biotic interactions, ecosystem processes, and global change*, Oxford University Press.

Barrios E, Buresh RJ, Sprent JI (1996) Nitrogen mineralization in density fractions of soil organic matter from maize and legume cropping systems. Soil Biology & Biochemistry, **28**, 1459-1465.

Batterman SA, Hedin LO, van Breugel M, Ransijn J, Craven DJ, Hall JS (2013) Key role of symbiotic dinitrogen fixation in tropical forest secondary succession. Nature, **502**, 224-227.

Bauer P, Thorpe A, Brunet G (2015) The quiet revolution of numerical weather prediction. Nature, **525**, 47-55.

Bell JM, Smith JL, Bailey VL, Bolton H (2003) Priming effect and C storage in semi-arid no-till spring crop rotations. Biology and Fertility of Soils, **37**, 237-244.

Bird JA, Torn MS (2006) Fine roots vs. needles: a comparison of ^{13}C and ^{15}N dynamics in a ponderosa pine forest soil. Biogeochemistry, **79**, 361-382.

Blagodatskaya E, Yuyukina T, Blagodatsky S, Kuzyakov Y (2011) Three-source-partitioning of microbial biomass and of CO2 efflux from soil to evaluate mechanisms of priming effects. Soil Biology & Biochemistry, **43**, 778-786.

Booth MS, Stark JM, Rastetter E (2005) Controls on nitrogen cycling in terrestrial ecosystems: A synthetic analysis of literature data. Ecological Monographs, **75**, 139-157.

Borenstein M, Hedges LV, Higgins JPT, Rothstein HR (2009) *Introduction to Meta-Analysis*, Chichester, UK, John Wiley & Sons, Ltd.

Braakhekke MC, Wutzler T, Beer C *et al.* (2013) Modeling the vertical soil organic matter profile using Bayesian parameter estimation. Biogeosciences, **10**, 399-420.

Bracho R, Natali S, Pegoraro E *et al.* (2016) Temperature sensitivity of organic matter decomposition of permafrost-region soils during laboratory incubations. Soil Biology and Biochemistry, **97**, 1-14.

Bradford MA, Davies CA, Frey SD *et al.* (2008) Thermal adaptation of soil microbial respiration to elevated temperature. Ecology Letters, **11**, 1316-1327.

Burnham KP, Anderson DR (2002) *Model selection and multimodel inference: a practical information-theoretic approach*, New York, Springer.

Burnham KP, Anderson DR (2004) Multimodel Inference: Understanding AIC and BIC in Model Selection. Sociological Methods & Research, **33**, 261-304.

Cabrerizo PM, Gonzalez EM, Aparicio-Tejo PM, Arrese-Igor C (2001) Continuous CO_2 enrichment leads to increased nodule biomass, carbon availability to nodules and activity of carbon-metabolising enzymes but does not enhance specific nitrogen fixation in pea. Physiologia Plantarum, **113**, 33-40.

Carvalhais N, Reichstein M, Seixas J *et al.* (2008) Implications of the carbon cycle steady state assumption for biogeochemical modeling performance and inverse parameter retrieval. Global Biogeochemical Cycles, **22**, DOI: 10.1029/2007GB003033.

Chapin III FS, Matson PA, Vitousek P (2011) *Principles of terrestrial ecosystem ecology*, Springer.

Cheng L, Leavitt SW, Kimball BA *et al.* (2007) Dynamics of labile and recalcitrant soil carbon pools in a sorghum free-air CO_2 enrichment (FACE) agroecosystem. Soil Biology and Biochemistry, **39**, 2250-2263.

Cheng WX, Parton WJ, Gonzalez-Meler MA *et al.* (2014) Synthesis and modeling perspectives of rhizosphere priming. New Phytologist, **201**, 31-44.

Chotte JL, Ladd JN, Amato M (1998) Sites of microbial assimilation, and turnover of soluble and particulate ^{14}C-labelled substrates decomposing in a clay soil. Soil Biology & Biochemistry, **30**, 205-218.

Cleveland CC, Townsend AR, Schimel DS *et al.* (1999) Global patterns of terrestrial biological nitrogen (N-2) fixation in natural ecosystems. Global Biogeochemical Cycles, **13**, 623-645.

Conant RT, Drijber RA, Haddix ML *et al.* (2008) Sensitivity of organic matter decomposition to warming varies with its quality. Global Change Biology, **14**, 868-877.

Cotrufo MF, Soong JL, Horton AJ, Campbell EE, Haddix ML, Wall DH, Parton WJ (2015) Formation of soil organic matter via biochemical and physical pathways of litter mass loss. Nature Geosci, **8**, 776-779.

Cotrufo MF, Wallenstein MD, Boot CM, Denef K, Paul E (2013) The Microbial Efficiency-Matrix Stabilization (MEMS) framework integrates plant litter decomposition with soil organic matter stabilization: do labile plant inputs form stable soil organic matter? Global Change Biology, **19**, 988-995.

Cox PM, Betts RA, Jones CD, Spall SA, Totterdell IJ (2000) Acceleration of global warming due to carbon-cycle feedbacks in a coupled climate model. Nature, **408**, 184-187.

Craine JM, Fierer N, McLauchlan KK (2010) Widespread coupling between the rate and temperature sensitivity of organic matter decay. Nature Geoscience, **3**, 854-857.

Davidson EA, Janssens IA (2006) Temperature sensitivity of soil carbon decomposition and feedbacks to climate change. Nature, **440**, 165-173.

de Graaff MA, van Groenigen KJ, Six J, Hungate B, van Kessel C (2006) Interactions between plant growth and soil nutrient cycling under elevated CO_2: a meta-analysis. Global Change Biology, **12**, 2077-2091.

de Vries FT, Hoffland E, van Eekeren N, Brussaard L, Bloem J (2006) Fungal/bacterial ratios in grasslands with contrasting nitrogen management. Soil Biology & Biochemistry, **38**, 2092-2103.

Dijkstra FA, Cheng WX (2007) Interactions between soil and tree roots accelerate long-term soil carbon decomposition. Ecology Letters, **10**, 1046-1053.

Fang CM, Smith P, Moncrieff JB, Smith JU (2005) Similar response of labile and resistant soil organic matter pools to changes in temperature. Nature, **433**, 57-59.

Field CB, Behrenfeld MJ, Randerson JT, Falkowski P (1998) Primary Production of the Biosphere: Integrating Terrestrial and Oceanic Components. Science, **281**, 237-240.

Finzi AC, Moore DJP, DeLucia EH *et al.* (2006) Progressive nitrogen limitation of ecosystem processes under elevated CO_2 in a warm-temperate forest. Ecology, **87**, 15-25.

Fontaine S, Bardoux G, Abbadie L, Mariotti A (2004a) Carbon input to soil may decrease soil carbon content. Ecology Letters, **7**, 314-320.

Fontaine S, Bardoux G, Benest D, Verdier B, Mariotti A, Abbadie L (2004b) Mechanisms of the priming effect in a savannah soil amended with cellulose. Soil Science Society of America Journal, **68**, 125-131.

Fontaine S, Barot S (2005) Size and functional diversity of microbe populations control plant persistence and long-term soil carbon accumulation. Ecology Letters, **8**, 1075-1087.

Fontaine S, Barot S, Barre P, Bdioui N, Mary B, Rumpel C (2007) Stability of organic carbon in deep soil layers controlled by fresh carbon supply. Nature, **450**, 277-U210.

Friedlingstein P, Cox P, Betts R *et al.* (2006) Climate-carbon cycle feedback analysis: Results from the (CMIP)-M-4 model intercomparison. Journal of Climate, **19**, 3337-3353.

Galloway JN, Dentener FJ, Capone DG *et al.* (2004) Nitrogen cycles: past, present, and future. Biogeochemistry, **70**, 153-226.

Gaucherel C, Campillo F, Misson L, Guiot J, Boreux JJ (2008) Parameterization of a process-based tree-growth model: Comparison of optimization, MCMC and Particle Filtering algorithms. Environmental Modelling & Software, **23**, 1280-1288.

Gelman A, Roberts G, Gilks W (1996) Efficient metropolis jumping hules. Bayesian statistics, **5**, 599-607.

Gelman A, Rubin DB (1992) Inference from Iterative Simulation Using Multiple Sequences. Statistical Science, **7**, 457-472.

Guenet B, Juarez S, Bardoux G, Abbadie L, Chenu C (2012) Evidence that stable C is as vulnerable to priming effect as is more labile C in soil. Soil Biology & Biochemistry, **52**, 43-48.

Guenet B, Leloup J, Raynaud X, Bardoux G, Abbadie L (2010a) Negative priming effect on mineralization in a soil free of vegetation for 80 years. European Journal of Soil Science, **61**, 384-391.

Guenet B, Moyano FE, Peylin P, Ciais P, Janssens IA (2016) Towards a representation of priming on soil carbon decomposition in the global land biosphere model ORCHIDEE (version 1.9.5.2). Geosci. Model Dev., **9**, 841-855.

Guenet B, Neill C, Bardoux G, Abbadie L (2010b) Is there a linear relationship between priming effect intensity and the amount of organic matter input? Applied Soil Ecology, **46**, 436-442.

Haario H, Saksman E, Tamminen J (2001) An Adaptive Metropolis Algorithm. Bernoulli, **7**, 223-242.

Haddix ML, Plante AF, Conant RT *et al.* (2011) The Role of Soil Characteristics on Temperature Sensitivity of Soil Organic Matter. Soil Science Society of America Journal, **75**, 56-68.

Hall EK, Neuhauser C, Cotner JB (2008) Toward a mechanistic understanding of how natural bacterial communities respond to changes in temperature in aquatic ecosystems. Isme Journal, **2**, 471-481.

Hararuk O, Xia J, Luo Y (2014) Evaluation and improvement of a global land model against soil carbon data using a Bayesian Markov chain Monte Carlo method. Journal of Geophysical Research: Biogeosciences, **119**, 403-417.

Hartley IP, Heinemeyer A, Ineson P (2007) Effects of three years of soil warming and shading on the rate of soil respiration: substrate availability and not thermal acclimation mediates observed response. Global Change Biology, **13**, 1761-1770.

Hartley IP, Hopkins DW, Garnett MH, Sommerkorn M, Wookey PA (2008) Soil microbial respiration in arctic soil does not acclimate to temperature. Ecology Letters, **11**, 1092-1100.

Hastings WK (1970) Monte-Carlo Sampling Methods Using Markov Chains and Their Applications. Biometrika, **57**, 97-109.

Hedges LV, Gurevitch J, Curtis PS (1999) The meta-analysis of response ratios in experimental ecology. Ecology, **80**, 1150-1156.

Heimann M, Reichstein M (2008) Terrestrial ecosystem carbon dynamics and climate feedbacks. Nature, **451**, 289-292.

Hicks Pries CE, Schuur EAG, Natali SM, Crummer KG (2016) Old soil carbon losses increase with ecosystem respiration in experimentally thawed tundra. Nature Clim. Change, **6**, 214-218.

Hirose T, Bazzaz FA (1998) Trade-off between light- and nitrogen-use efficiency in canopy photosynthesis. Annals of Botany, **82**, 195-202.

Hobbie SE (2015) Plant species effects on nutrient cycling: revisiting litter feedbacks. Trends in ecology & evolution, **30**, 357-363.

Hochachka PW, Somero GN (2002) *Biochemical Adaptation: Mechanism and Process in Physiological Evolution*, New York, Oxford University Press.

Hoque MM, Inubushi K, Miura S, Kobayashi K, Kim HY, Okada M, Yabashi S (2001) Biological dinitrogen fixation and soil microbial biomass carbon as influenced by free-air carbon dioxide enrichment (FACE) at three levels of nitrogen fertilization in a paddy field. Biology and Fertility of Soils, **34**, 453-459.

Hultman J, Waldrop MP, Mackelprang R *et al.* (2015) Multi-omics of permafrost, active layer and thermokarst bog soil microbiomes. Nature, **521**, 208-212.

Hungate BA, Dukes JS, Shaw MR, Luo YQ, Field CB (2003) Nitrogen and climate change. Science, **302**, 1512-1513.

Hunt S, Layzell DB (1993) Gas-Exchange of Legume Nodules and the Regulation of Nitrogenase Activity. Annual Review of Plant Physiology and Plant Molecular Biology, **44**, 483-511.

IPCC (2013) *Climate Change 2013: The Physical Science Basis. Contribution of Working Group I to the Fifth Assessment Report of the Intergovernmental Panel on Climate Change,* Cambridge, United Kingdom and New York, NY, USA, Cambridge University Press.

Iversen CM (2010) Digging deeper: fine-root responses to rising atmospheric CO_2 concentration in forested ecosystems. New Phytologist, **186**, 346-357.

Iversen CM, Hooker TD, Classen AT, Norby RJ (2011) Net mineralization of N at deeper soil depths as a potential mechanism for sustained forest production under elevated [CO_2]. Global Change Biology, **17**, 1130-1139.

Jastrow J, Miller R (1997) Soil aggregate stabilization and carbon sequestration: feedbacks through organomineral associations. In: *Soil processes and the carbon cycle.* (eds Lal R, Kimble JM, Follett RF, Stewart BA) pp Page.

Jenkinson DS (1990) The Turnover of Organic-Carbon and Nitrogen in Soil. Philosophical Transactions of the Royal Society of London Series B-Biological Sciences, **329**, 361-368.

Jones C, Robertson E, Arora V *et al.* (2013) Twenty-First-Century Compatible CO_2 Emissions and Airborne Fraction Simulated by CMIP5 Earth System Models under Four Representative Concentration Pathways. Journal of Climate, **26**, 4398-4413.

Justes E, Mary B, Meynard JM, Machet JM, Thelierhuche L (1994) Determination of a Critical Nitrogen Dilution Curve for Winter-Wheat Crops. Annals of Botany, **74**, 397-407.

Karhu K, Auffret MD, Dungait JAJ *et al.* (2014) Temperature sensitivity of soil respiration rates enhanced by microbial community response. Nature, **513**, 81-+.

Karhu K, Fritze H, Tuomi M, Vanhala P, Spetz P, Kitunen V, Liski J (2010) Temperature sensitivity of organic matter decomposition in two boreal forest soil profiles. Soil Biology & Biochemistry, **42**, 72-82.

Kätterer T, Reichstein M, Andrén O, Lomander A (1998) Temperature dependence of organic matter decomposition: a critical review using literature data analyzed with different models. Biology and Fertility of Soils, **27**, 258-262.

Keenan TF, Hollinger DY, Bohrer G, Dragoni D, Munger JW, Schmid HP, Richardson AD (2013) Increase in forest water-use efficiency as atmospheric carbon dioxide concentrations rise. Nature, **499**, 324-+.

Keiluweit M, Bougoure JJ, Nico PS, Pett-Ridge J, Weber PK, Kleber M (2015) Mineral protection of soil carbon counteracted by root exudates. Nature Clim. Change, **5**, 588-595.

Keller M, Kaplan WA, Wofsy SC, Dacosta JM (1988) Emissions of N_2O from Tropical Forest Soils: Response to Fertilization with NH_4^+, $NO3^-$, and PO_4^{3-}. Journal of Geophysical Research-Atmospheres, **93**, 1600-1604.

Kergoat L, Lafont S, Arneth A, Le Dantec V, Saugier B (2008) Nitrogen controls plant canopy light-use efficiency in temperate and boreal ecosystems. Journal of Geophysical Research-Biogeosciences, **113**, doi: 10.1029/2007JG000676.

Kirschbaum MUF (2004) Soil respiration under prolonged soil warming: are rate reductions caused by acclimation or substrate loss? Global Change Biology, **10**, 1870-1877.

Knorr W, Prentice IC, House JI, Holland EA (2005) Long-term sensitivity of soil carbon turnover to warming. Nature, **433**, 298-301.

Koven CD, Riley WJ, Stern A (2013) Analysis of Permafrost Thermal Dynamics and Response to Climate Change in the CMIP5 Earth System Models. Journal of Climate, **26**, 1877-1900.

Koven CD, Ringeval B, Friedlingstein P *et al.* (2011) Permafrost carbon-climate feedbacks accelerate global warming. Proceedings of the National Academy of Sciences of the United States of America, **108**, 14769-14774.

Kuzyakov Y (2010) Priming effects: Interactions between living and dead organic matter. Soil Biology & Biochemistry, **42**, 1363-1371.

Kuzyakov Y, Friedel JK, Stahr K (2000) Review of mechanisms and quantification of priming effects. Soil Biology & Biochemistry, **32**, 1485-1498.

Lambers H, Chapin III FS, Pons TL (2008) *Plant Physiological Ecology*, New York, Springer.

Li D, Schädel C, Haddix ML *et al.* (2013) Differential responses of soil organic carbon fractions to warming: Results from an analysis with data assimilation. Soil Biology and Biochemistry, **67**, 24-30.

Li JW, Wang GS, Allison SD, Mayes MA, Luo YQ (2014) Soil carbon sensitivity to temperature and carbon use efficiency compared across microbial-ecosystem models of varying complexity. Biogeochemistry, **119**, 67-84.

Liang J, Xia J, Liu L, Wan S (2013) Global patterns of the responses of leaf-level photosynthesis and respiration in terrestrial plants to experimental warming. Journal of Plant Ecology, **6**, 437-447.

Liang JY, Li DJ, Shi Z *et al.* (2015) Methods for estimating temperature sensitivity of soil organic matter based on incubation data: A comparative evaluation. Soil Biology & Biochemistry, **80**, 127-135.

Liski J, Ilvesniemi H, Makela A, Westman CJ (1999) CO_2 emissions from soil in response to climatic warming are overestimated - The decomposition of old soil organic matter is tolerant of temperature. Ambio, **28**, 171-174.

Löhnis F (1926) Nitrogen availability of green manures. Soil Science, **22**, 253-290.

Lu M, Yang YH, Luo YQ *et al.* (2011) Responses of ecosystem nitrogen cycle to nitrogen addition: a meta-analysis. New Phytologist, **189**, 1040-1050.

Luna-Guido ML, Dendooven L (2001) Simulating the dynamics of glucose and NH_4^+ in alkaline saline soils of the former Lake Texcoco with the Detran model. European Journal of Soil Science, **52**, 269-277.

Luo Y, Ogle K, Tucker C *et al.* (2011) Ecological forecasting and data assimilation in a data-rich era. Ecological Applications, **21**, 1429-1442.

Luo Y, Reynolds JF (1999) Validity of extrapolating field CO_2 experiments to predict carbon sequestration in natural ecosystems. Ecology, **80**, 1568-1583.

Luo Y, Su B, Currie WS *et al.* (2004) Progressive nitrogen limitation of ecosystem responses to rising atmospheric carbon dioxide. Bioscience, **54**, 731-739.

Luo YQ, Ahlstrom A, Allison SD *et al.* (2016) Toward more realistic projections of soil carbon dynamics by Earth system models. Global Biogeochemical Cycles, **30**, 40-56.

Luo YQ, Hui DF, Zhang DQ (2006) Elevated CO_2 stimulates net accumulations of carbon and nitrogen in land ecosystems: A meta-analysis. Ecology, **87**, 53-63.

Luo YQ, Wan SQ, Hui DF, Wallace LL (2001) Acclimatization of soil respiration to warming in a tall grass prairie. Nature, **413**, 622-625.

Luo YQ, White LW, Canadell JG *et al.* (2003) Sustainability of terrestrial carbon sequestration: A case study in Duke Forest with inversion approach. Global Biogeochemical Cycles, **17**.

Luscher A, Hartwig UA, Suter D, Nosberger J (2000) Direct evidence that symbiotic N_2 fixation in fertile grassland is an important trait for a strong response of plants to elevated atmospheric CO_2. Global Change Biology, **6**, 655-662.

MacDougall AH, Avis CA, Weaver AJ (2012) Significant contribution to climate warming from the permafrost carbon feedback. Nature Geoscience, **5**, 719-721.

Magid J, Kjærgaard C, Gorissen A, Kuikman P (1999) Drying and rewetting of a loamy sand soil did not increase the turnover of native organic matter, but retarded the decomposition of added ^{14}C-labelled plant material. Soil Biology and Biochemistry, **31**, 595-602.

Manzoni S, Taylor P, Richter A, Porporato A, Ågren GI (2012) Environmental and stoichiometric controls on microbial carbon-use efficiency in soils. New Phytologist, **196**, 79-91.

McGuire AD, Christensen TR, Hayes D *et al.* (2012) An assessment of the carbon balance of Arctic tundra: comparisons among observations, process models, and atmospheric inversions. Biogeosciences, **9**, 3185-3204.

Metropolis N, Rosenbluth AW, Rosenbluth MN, Teller AH, Teller E (1953) Equation of state calculations by fast computing machines. The journal of chemical physics, **21**, 1087-1092.

Monsant AC, Tang C, Baker AJM (2008) The effect of nitrogen form on rhizosphere soil pH and zinc phytoextraction by Thlaspi caerulescens. Chemosphere, **73**, 635-642.

Moore DJP, Aref S, Ho RM, Pippen JS, Hamilton JG, De Lucia EH (2006) Annual basal area increment and growth duration of Pinus taeda in response to eight years of free-air carbon dioxide enrichment. Global Change Biology, **12**, 1367-1377.

Myers SS, Zanobetti A, Kloog I *et al.* (2014) Increasing CO_2 threatens human nutrition. Nature, **510**, 139-142.

Natali SM, Schuur EAG, Rubin RL (2012) Increased plant productivity in Alaskan tundra as a result of experimental warming of soil and permafrost. Journal of Ecology, **100**, 488-498.

Natali SM, Schuur EAG, Trucco C, Pries CEH, Crummer KG, Lopez AFB (2011) Effects of experimental warming of air, soil and permafrost on carbon balance in Alaskan tundra. Global Change Biology, **17**, 1394-1407.

Natali SM, Schuur EAG, Webb EE, Pries CEH, Crummer KG (2014) Permafrost degradation stimulates carbon loss from experimentally warmed tundra. Ecology, **95**, 602-608.

Niklaus PA, Spinnler D, Korner C (1998) Soil moisture dynamics of calcareous grassland under elevated CO2. Oecologia, **117**, 201-208.

Norby RJ, Cotrufo MF, Ineson P, O'Neill EG, Canadell JG (2001) Elevated CO_2, litter chemistry, and decomposition: a synthesis. Oecologia, **127**, 153-165.

Norby RJ, Long TM, Hartz-Rubin JS, O'Neill EG (2000) Nitrogen resorption in senescing tree leaves in a warmer, CO_2-enriched atmosephere. Plant and Soil, **224**, 15-29.

Norby RJ, Warren JM, Iversen CM, Medlyn BE, McMurtrie RE (2010) CO_2 enhancement of forest productivity constrained by limited nitrogen availability. Proceedings of the National Academy of Sciences of the United States of America, **107**, 19368-19373.

Nottingham AT, Griffiths H, Chamberlain PM, Stott AW, Tanner EVJ (2009) Soil priming by sugar and leaf-litter substrates: A link to microbial groups. Applied Soil Ecology, **42**, 183-190.

Odum EP, Barrett GW (2005) *Fundamentals of Ecology*, Thomson Brooks/Cole.

Oren R, Ellsworth DS, Johnsen KH *et al.* (2001) Soil fertility limits carbon sequestration by forest ecosystems in a CO_2-enriched atmosphere. Nature, **411**, 469-472.

Parton WJ, Schimel DS, Cole CV, Ojima DS (1987) Analysis of Factors Controlling Soil Organic-Matter Levels in Great-Plains Grasslands. Soil Science Society of America Journal, **51**, 1173-1179.

Pascault N, Ranjard L, Kaisermann A *et al.* (2013) Stimulation of Different Functional Groups of Bacteria by Various Plant Residues as a Driver of Soil Priming Effect. Ecosystems, **16**, 810-822.

Penton CR, St Louis D, Cole JR *et al.* (2013) Fungal Diversity in Permafrost and Tallgrass Prairie Soils under Experimental Warming Conditions. Applied and Environmental Microbiology, **79**, 7063-7072.

Perelo LW, Munch JC (2005) Microbial immobilisation and turnover of ^{13}C labelled substrates in two arable soils under field and laboratory conditions. Soil Biology & Biochemistry, **37**, 2263-2272.

Plaza C, Courtier-Murias D, Fernández JM, Polo A, Simpson AJ (2013) Physical, chemical, and biochemical mechanisms of soil organic matter stabilization under conservation tillage systems: A central role for microbes and microbial by-products in C sequestration. Soil Biology and Biochemistry, **57**, 124-134.

Poorter H, Navas ML (2003) Plant growth and competition at elevated CO_2: on winners, losers and functional groups. New Phytologist, **157**, 175-198.

Qiao N, Schaefer D, Blagodatskaya E, Zou XM, Xu XL, Kuzyakov Y (2014) Labile carbon retention compensates for CO_2 released by priming in forest soils. Global Change Biology, **20**, 1943-1954.

Rastetter EB, Agren GI, Shaver GR (1997) Responses of N-limited ecosystems to increased CO_2: A balanced-nutrition, coupled-element-cycles model. Ecological Applications, **7**, 444-460.

Reay DS, Dentener F, Smith P, Grace J, Feely RA (2008) Global nitrogen deposition and carbon sinks. Nature Geoscience, **1**, 430-437.

Reich PB, Hobbie SE (2013) Decade-long soil nitrogen constraint on the CO_2 fertilization of plant biomass. Nature Climate Change, **3**, 278-282.

Reich PB, Hobbie SE, Lee T *et al.* (2006) Nitrogen limitation constrains sustainability of ecosystem response to CO_2. Nature, **440**, 922-925.

Rey A, Jarvis P (2006) Modelling the effect of temperature on carbon mineralization rates across a network of European forest sites (FORCAST). Global Change Biology, **12**, 1894-1908.

Rosenberg MS, Adams DC, Gurevitch J (2000) *MetaWin: statistical software for meta-analysis*, Sinauer Associates Sunderland, Massachusetts, USA.

Rousk J, Bååth E (2007) Fungal biomass production and turnover in soil estimated using the acetate-in-ergosterol technique. Soil Biology & Biochemistry, **39**, 2173-2177.

Rousk J, Brookes PC, Baath E (2009) Contrasting Soil pH Effects on Fungal and Bacterial Growth Suggest Functional Redundancy in Carbon Mineralization. Applied and Environmental Microbiology, **75**, 1589-1596.

Rovira P, Vallejo VR (2002) Labile and recalcitrant pools of carbon and nitrogen in organic matter decomposing at different depths in soil: an acid hydrolysis approach. Geoderma, **107**, 109-141.

Rubino M, Dungait J, Evershed R *et al.* (2010) Carbon input belowground is the major C flux contributing to leaf litter mass loss: Evidences from a ^{13}C labelled-leaf litter experiment. Soil Biology and Biochemistry, **42**, 1009-1016.

Russow R, Spott O, Stange CF (2008) Evaluation of nitrate and ammonium as sources of NO and N_2O emissions from black earth soils (Haplic Chernozem) based on ^{15}N field experiments. Soil Biology & Biochemistry, **40**, 380-391.

Rustad LE (2006) From transient to steady-state response of ecosystems to atmospheric CO_2-enrichment and global climate change: Conceptual challenges and need for an integrated approach. Plant Ecology, **182**, 43-62.

Saffron CM, Park JH, Dale BE, Voice TC (2006) Kinetics of contaminant desorption from soil: Comparison of model formulations using the akaike information criterion. Environmental Science & Technology, **40**, 7662-7667.

Sayer EJ, Heard MS, Grant HK, Marthews TR, Tanner EV (2011) Soil carbon release enhanced by increased tropical forest litterfall. Nature Climate Change, **1**, 304-307.

Schädel C, Luo Y, David Evans R, Fei S, Schaeffer S (2013) Separating soil CO_2 efflux into C-pool-specific decay rates via inverse analysis of soil incubation data. Oecologia, 10.1007/s00442-012-2577-4, 1-12.

Schimel JP, Weintraub MN (2003) The implications of exoenzyme activity on microbial carbon and nitrogen limitation in soil: a theoretical model. Soil Biology & Biochemistry, **35**, 549-563.

Schlesinger WH (1995) An overview of the carbon cycle. In: *Soils and global change.* (eds Lal R, Kimble J, Levine E, Stewart BA) pp Page. Boca Raton, USA, CRC Press.

Schlesinger WH, Andrews JA (2000) Soil respiration and the global carbon cycle. Biogeochemistry, **48**, 7-20.

Schmidt MWI, Torn MS, Abiven S *et al.* (2011) Persistence of soil organic matter as an ecosystem property. Nature, **478**, 49-56.

Schuur EAG, Bockheim J, Canadell JG *et al.* (2008) Vulnerability of permafrost carbon to climate change: Implications for the global carbon cycle. Bioscience, **58**, 701-714.

Schuur EAG, McGuire AD, Schadel C *et al.* (2015) Climate change and the permafrost carbon feedback. Nature, **520**, 171-179.

Schuur EAG, Vogel JG, Crummer KG, Lee H, Sickman JO, Osterkamp TE (2009) The effect of permafrost thaw on old carbon release and net carbon exchange from tundra. Nature, **459**, 556-559.

Schwalm CR, Williams CA, Schaefer K *et al.* (2010) Assimilation exceeds respiration sensitivity to drought: A FLUXNET synthesis. Global Change Biology, **16**, 657-670.

Six J, Conant RT, Paul EA, Paustian K (2002) Stabilization mechanisms of soil organic matter: Implications for C-saturation of soils. Plant and Soil, **241**, 155-176.

Sollins P, Homann P, Caldwell BA (1996) Stabilization and destabilization of soil organic matter: Mechanisms and controls. Geoderma, **74**, 65-105.

Soong JL, Cotrufo MF (2015) Annual burning of a tallgrass prairie inhibits C and N cycling in soil, increasing recalcitrant pyrogenic organic matter storage while reducing N availability. Global Change Biology, **21**, 2321-2333.

Spiegelhalter DJ, Best NG, Carlin BP, Van Der Linde A (2002) Bayesian measures of model complexity and fit. Journal of the Royal Statistical Society: Series B, **64**, 583-639.

Stanford G, Smith SJ (1972) Nitrogen Mineralization Potentials of Soils. Soil Science Society of America Proceedings, **36**, 465-472.

Stehfest E, Bouwman L (2006) N_2O and NO emission from agricultural fields and soils under natural vegetation: summarizing available measurement data and modeling of global annual emissions. Nutrient Cycling in Agroecosystems, **74**, 207-228.

Sulman BN, Phillips RP, Oishi AC, Shevliakova E, Pacala SW (2014) Microbe-driven turnover offsets mineral-mediated storage of soil carbon under elevated CO2. Nature Climate Change, **4**, 1099-1102.

Talhelm AF, Pregitzer KS, Giardina CP (2012) Long-Term Leaf Production Response to Elevated Atmospheric Carbon Dioxide and Tropospheric Ozone. Ecosystems, **15**, 71-82.

Thomson CJ, Marschner H, Romheld V (1993) Effect of Nitrogen-Fertilizer Form on pH of the Bulk Soil and Rhizosphere, and on the Growth, Phosphorus, and Micronutrient Uptake of Bean. Journal of Plant Nutrition, **16**, 493-506.

Thornton PE, Doney SC, Lindsay K *et al.* (2009) Carbon-nitrogen interactions regulate climate-carbon cycle feedbacks: results from an atmosphere-ocean general circulation model. Biogeosciences, **6**, 2099-2120.

Tricker PJ, Pecchiari M, Bunn SM, Vaccari FP, Peressotti A, Miglietta F, Taylor G (2009) Water use of a bioenergy plantation increases in a future high CO_2 world. Biomass & Bioenergy, **33**, 200-208.

Tu Q, Zhou X, He Z *et al.* (2015) The Diversity and Co-occurrence Patterns of N2-Fixing Communities in a CO2-Enriched Grassland Ecosystem. Microbial Ecology, 1-12.

van Groenigen KJ, Osenberg CW, Hungate BA (2011) Increased soil emissions of potent greenhouse gases under increased atmospheric CO2. Nature, **475**, 214-U121.

van Groenigen KJ, Qi X, Osenberg CW, Luo YQ, Hungate BA (2014) Faster Decomposition Under Increased Atmospheric CO_2 Limits Soil Carbon Storage. Science, **344**, 508-509.

Walker AP, Zaehle S, Medlyn BE *et al.* (2015) Predicting long-term carbon sequestration in response to CO_2 enrichment: How and why do current ecosystem models differ? Global Biogeochemical Cycles, **29**, 476-495.

Wang QK, Wang SL, He TX, Liu L, Wu JB (2014a) Response of organic carbon mineralization and microbial community to leaf litter and nutrient additions in subtropical forest soils. Soil Biology & Biochemistry, **71**, 13-20.

Wang QK, Wang YP, Wang SL, He TX, Liu L (2014b) Fresh carbon and nitrogen inputs alter organic carbon mineralization and microbial community in forest deep soil layers. Soil Biology & Biochemistry, **72**, 145-151.

Wang YP, Chen BC, Wieder WR *et al.* (2014c) Oscillatory behavior of two nonlinear microbial models of soil carbon decomposition. Biogeosciences, **11**, 1817-1831.

Wang YP, Jiang J, Chen-Charpentier B *et al.* (2016) Responses of two nonlinear microbial models to warming and increased carbon input. Biogeosciences, **13**, 887-902.

Weng E, Luo Y (2011) Relative information contributions of model vs. data to short- and long-term forecasts of forest carbon dynamics. Ecological Applications, **21**, 1490-1505.

Wieder WR, Bonan GB, Allison SD (2013) Global soil carbon projections are improved by modelling microbial processes. Nature Climate Change, **3**, 909-912.

Wieder WR, Grandy AS, Kallenbach CM, Bonan GB (2014) Integrating microbial physiology and physio-chemical principles in soils with the MIcrobial-MIneral Carbon Stabilization (MIMICS) model. Biogeosciences, **11**, 3899-3917.

Wienhold BJ, Halvorson AD (1999) Nitrogen mineralization responses to cropping, tillage, and nitrogen rate in the Northern Great Plains. Soil Science Society of America Journal, **63**, 192-196.

Williams M, Richardson A, Reichstein M *et al.* (2009) Improving land surface models with FLUXNET data. Biogeosciences, **6**, 1341-1359.

Wu J, Brookes PC, Jenkinson DS (1993) Formation and Destruction of Microbial Biomass during the Decomposition of Glucose and Ryegrass in Soil. Soil Biology & Biochemistry, **25**, 1435-1441.

Wutzler T, Reichstein M (2013) Priming and substrate quality interactions in soil organic matter models. Biogeosciences, **10**, 2089-2103.

Xu T, White L, Hui D, Luo Y (2006) Probabilistic inversion of a terrestrial ecosystem model: Analysis of uncertainty in parameter estimation and model prediction. Global Biogeochemical Cycles, **20**, GB2007.

Xu X, Luo YQ, Zhou JZ (2012) Carbon quality and the temperature sensitivity of soil organic carbon decomposition in a tallgrass prairie. Soil Biology & Biochemistry, **50**, 142-148.

Xu X, Zhou Y, Ruan HH, Luo YQ, Wang JS (2010) Temperature sensitivity increases with soil organic carbon recalcitrance along an elevational gradient in the Wuyi Mountains, China. Soil Biology & Biochemistry, **42**, 1811-1815.

Xue K, M. Yuan M, J. Shi Z *et al.* (2016) Tundra soil carbon is vulnerable to rapid microbial decomposition under climate warming. Nature Climate Change, doi:10.1038/nclimate2940.

Zaehle S, Ciais P, Friend AD, Prieur V (2011) Carbon benefits of anthropogenic reactive nitrogen offset by nitrous oxide emissions. Nature Geoscience, **4**, 601-605.

Zhuang QL, Melillo JM, Sarofim MC *et al.* (2006) CO_2 and CH_4 exchanges between land ecosystems and the atmosphere in northern high latitudes over the 21st century. Geophysical Research Letters, **33**, doi:10.1029/2006GL026972.

Zimov SA, Schuur EAG, Chapin FS (2006) Permafrost and the global carbon budget. Science, **312**, 1612-1613.

Zogg GP, Zak DR, Ringelberg DB, MacDonald NW, Pregitzer KS, White DC (1997) Compositional and functional shifts in microbial communities due to soil warming. Soil Science Society of America Journal, **61**, 475-481.